Ministry of Science and Higher Education of the Republic of Kazakhstan

Kazakh National Research Technical University named after Satbayev K.I.

(Satbayev University)

UDC 622.32 Manuscript Copyright

SAGYNDIKOV MARAT SERIKOVICH

Systematic Approach Investigation for Improving Polymer Flood Technology at the Kalamkas field

8D07202 – Petroleum Engineering

A thesis submitted on the Requirements for the Degree of Doctor of Philosophy (Ph.D.) in Petroleum Engineering

Scientific Advisors:

Sarkyt Elekenovich Kudaibergenov,
Doctor of Chemical Sciences, Professor

Evgeni Kiponievich Ogay,
Doctor of Technical Sciences, Professor

Randall Scott Seright,
Ph.D., Adjunct Professor at New Mexico Tech

Almaty, 2022

CONTENT

NOMENCLATURE

ASP = alkaline surfactant polymer;
ATBS = Acrylamide-Tertiary-Butyl Sulfonate;
bbl = barrel;
BHP = bottom-hole pressure, bar;
C_i = concentration of polymer solution injected, unit fraction;
cp = centipoise (dynamic viscosity unit);
C_p = concentration of polymer in the produced sample, unit fraction;
DI = depletion intensity, fraction;
D_{sample} = formation sample depth, cm;
EOR = enhanced oil recovery;
ESP = electrical submersible pumps;
FDP = field development project;
ft/d = feet per day;
f_w = fractional water curve or watercut, fraction;
h = perforation thickness, m;
Hoil = oil formation height, m;
HPAM = partially hydrolyzed polyacrylamide;
IAPV = inaccessible pore volume'
IFT = interfacial tension, mN/m;
ILT = injection logging test;
IOP = incremental oil production for 5 years, thousand tonnes;
IPR = inflow performance relationship;
IRR = internal rate of return, %;
JSC = joint stock company;
K layer = formation layering or compartmentalization index, dim.;
k_{ro} = relative permeability by oil, fraction;
k_{rw} = relative permeability by water, fraction;
LLP = limited liability partnership;
M = bulk mass of the core, g;
md = millidarcy (rock permeability unit);
MD = measured depth;
MW = molecular weight, Daltons;
NPV = net present value, million KZT;
NTG = net-to-gross, fraction;
NVP = N-Vinyl-Pyrrolidone;
ø = porosity, unit fraction;
OOIP = original oil in place;
OPEX = operational expenditure;
P = polymer;
PAM = polyacrylamide;
PCP = progressing-cavity pump;
PF = polymer flood;

PI = profitability index, dim.;
PLT = production logging test;
ppb = parts per billion;
ppm = parts per million;
psi = pounds per square inch;
PSU = polymer slicing unit;
PV = pore volume, %;
PVT = pressure volume temperature;
R = retention, $\mu g/g$;
RF = recovery factor, fraction;
RF = resistance factor, dim.;
RoK = Republic of Kazakhstan;
RRF = residual resistance factor, dim.;
SAGD = steam assisted gravity drainage;
SCAL = special core analysis;
S_{or} = residual oil saturation, unit fraction;
SE = sweep efficiency;
SP = surfactant polymer;
STOIIP = stock tank oil initially in place;
S_w = water saturation, fraction;
S_{wc} = connate water saturation, unit fraction;
TAN = total acid number, mg KOH/g;
TDS = total dissolved solids, ppm;
TSS = total suspended solids, ppm;
UL = ultra low;
USA = United States of America;
USD = United States Dollars;
V pi = productivity indexes variation, dim.;
V_{casing} = volume between tubing end and perforation bottom, m^3;
V_f = volume back-produced from formation, m^3;
V_p = back-produced volume, m^3;
V_{tubing} = tubing inner volume, m^3;
w = fracture width, m;
W = weight of polymer injected;
WCT = watercut, fraction;
Y = weight of fluid produced and analyzed, g.

INTRODUCTION

General overview. Only 3-5% of global oil production can be attributed to enhanced oil recovery (EOR) [1]. This fraction is expected to grow, even for reservoirs with harsh conditions that do not allow for efficient oil production [2]. There are commonly several directions of EOR [3]: gas (CO_2, N_2, hydrocarbon, immiscible), thermal (steam, hot water, in-situ combustion, SAGD), chemical (polymer (P), surfactant polymer (SP), alkaline surfactant polymer (ASP) floods) and others (microbiological). Gas injection is used as an agent for a pressure maintenance system, and usually starts near the beginning of the field production (secondary recovery). Also, a central aspect is the availability of a gas source. For example, most EOR gas projects in the USA, Canada, and China are neighboring huge CO_2 reservoirs/fields [4; 5]. Some operators inject gas for utilization purposes and mask it as an EOR technique [6; 7; 8]. Thermal EOR is generally effectively applicable for heavy oil fields, where viscosity ranges from 100-10 000 cp or even higher. But implementation of thermal methods is mainly limited by heat losses [9; 10; 11]. Heat losses can occur due to the initial reservoir condition (high thermal conductivity of the upper and/or lower impermeable layers, reservoir depth), development stage (high formation water saturation near injection wells), and infrastructure (well construction type, completion, tubing). Also, another critical issue is the obtainability of the freshwater source. In contrast, chemical EOR does not have the limitations mentioned above. Hence it has been widely used in sandstone fields, especially at the late development stage. Furthermore, polymer flooding (PF) is often the most feasible chemical EOR technology. Especially, polymer flooding has prominance, where ASP/SP flooding is not profitable and causes serious on-site problems (scaling, uptime decrease, injectivity issue, hard-to-break emulsions) [12; 13; 14; 15]. The principle of polymer flooding is to increase the viscosity of injected water and thereby develop a more favorable mobility ratio between displacing water and oil in place [16]. This approach reduces or avoids water fingering caused by geological heterogeneity [17].

The relevance of the work. The majority of giant oil fields in Kazakhstan are entering or already in the brownfield development stage, and the Kalamkas oilfield is one of them. The field was discovered in 1976 and developed commercially since 1979 according to the Field Development Project – FDP [18]. Oil and gas reservoirs were established in Jurassic deposits. Reservoirs mainly consist of sandstones deposited in deltaic, fluvial, and shallow marine environments. The reservoirs' main geological and physical features are highly-layered heterogeneity and unfavorable mobility ratio (>7) in reservoir conditions. The permeability ranges from 0.055 to 1.273 Darcy. The oil viscosity is at least 16 cp at reservoir temperature (38-43°C). These factors explain non-uniform depletion and relatively low recovery factor for the Kalamkas oilfield. To date, the water cut is significantly higher than expected considering the depletion of recoverable reserves.

To improve hydrocarbon production and enhance oil recovery, a polymer flood pilot design started in 2011. The design of the injected polymer viscosity was based

on the optimum economic output (i.e., net present value) according to reservoir modeling and feasibility studies, and on concepts presented in literature sources [19; 20]. Pilot projects were conducted since September 2014. As a result, pilots showed no injectivity loss; polymer injection unit up-time high; sweep efficiency increased (based on injection and production logging tests); water-cut decreased to 10%; and oil production rates doubled. The estimated incremental recovery factor over waterflood was 9% [21].

Although polymer flooding worldwide has been applied ~60 years, and it still requires further investigation to provide improvements. Thus, this dissertation describes a systematic approach investigation for improving polymer flood technology at the Kalamkas field. The systematic approach investigation includes the combination of data analysis, laboratory studies, field observations, numerical & analytical modeling, and feasibility studies.

Research Objectives. The objective of this dissertation was to investigate polymer flood at the Kalamkas field to develop a systematic approach for improving technology. Therefore, the research scope of this dissertation was focused on the following aspects:

1. A comprehensive literature review of recent worldwide polymer EOR projects focusing on the Kalamkas field polymer flood aspects.
2. Assess polyacrylamide solution chemical and mechanical stability during a polymer flood in the Kalamkas field.
3. Develop a novel method for the field assessment of polymer degradation during a polymer flood of an oil reservoir.
4. Experimental and numerical studies of the Kalamkas polymer flood technology. Examine the oil recovery at various simulation scenarios.
5. The Kalamkas polymer flood projects feasibility studies and choose most rational scenario for full field deployment.

Novelty. The novelty in this work resides in field demonstration of the correctness of previous conceptual ideas—(1) that the vertical HPAM injection wells contained fractures that were necessary for polymer injection, (2) that the fractures substantially reduced mechanical degradation, and (3) that injected polymer solutions were quickly stripped of dissolved oxygen (thereby promoting oxidative stability). These demonstrations have value in countering arguments by others [26; 27; 28; 29] that polymer injectivity into vertical wells could be acceptable without fractures. To our knowledge, this is the first published report demonstrating that backflowed HPAM samples from an injection well showed no detectable dissolved oxygen. Also, to our knowledge, this is the first published report demonstrating that backflowed samples from an injection well showed no HPAM mechanical (or oxidative) degradation. Finally, we developed an unconventional approach to model a polymer flood that can be used to optimize technology at the Kalamkas field.

Defending hypotheses:
1. Vertical HPAM injection wells contained fractures that were necessary for polymer injection. And these fractures substantially reduced polymer mechanical degradation.

2. Injected polymer solutions were quickly stripped of dissolved oxygen, thereby promoting oxidative (or chemical) stability.
3. At Kalamkas conditions, residual resistance factor (RRF) is not significantly different from unity, i.e., post chase water injection will not benefit oil recovery. Therefore, polymer injection should be underway as far as net present value (NPV) is positive.
4. Polymer flood at oil price volatility is a long-term project that extends the field's economically feasible lifetime and enhances oil recovery.

Practical value. A developed novel method for the field assessment of polymer degradation can be used to understand in-situ polymer EOR mechanisms better. Provided mitigation plan to eliminate chemical degradation that can save 25% of OPEX at the Kalamkas field conditions, thereby improving project economics. In addition, a novel approach to model polymer flood can be used to optimize polymer injection parameters, thereby improving technology efficiency.

Personal contribution. The dissertation's author contribution consists of the literature review, geological & reservoir dynamics data analysis, laboratory studies, field observations, and numerical & analytical modeling. The research results presented in the dissertation were obtained by the author personally or with his direct participation. Finally, the author formulated conclusions and recommendations.

Approbation. The main results of the dissertation were reported and discussed at the following conferences and workshops: International Scientific Conference "Satbayev Readings – 2020" and "Satbayev Readings – 2021" (Kazakhstan, Almaty, April 2020 and April 2021); SPE Virtual Improved Oil Recovery Conference (USA, Tulsa, April 2022); Workshop organized by GazPromNeft "Chemical Enhanced Oil Recovery: challenges and prospects" (Russia, Kazan, June 2022); International Scientific Conference titled "Prospects for the use of chemical methods for enhanced oil recovery (cEOR) at a late stage of development" (Kazakhstan, Astana, September 2022).

Publications. The main hypotheses of the dissertation have been published in 7 articles, which include 1 – in the Scientific Journal cited in the Scopus base (Q1, 94 percentile), 2 – in the Scientific Journals listed in the recommended by the Committee for Quality Assurance in the Sphere of Education and Science of the Ministry of Science and Higher Education RoK, 3 – International Conferences, 1 – Patent for the utility model (KazPatent):

1. **Sagyndikov**, M., Seright, R.S., Kudaibergenov, S., and Ogay, E. 2022. Field Demonstration of the Impact of Fractures on Hydolyzed Polyacrilamide Injectivity, Propagation and Degradation. SPE Journal 27 (02): 999-1016. SPE-208611-PA. https://doi:10.2118/208611-PA
2. **Sagyndikov**, M., Kushekov, R.M., Seright, R.S. 2022. Review of Important Aspects and Performances of Polymer Flooding versus ASP Flooding. Bulletin of the Karaganda University Chemistry Series 107 (3): 35-55. https://doi.org/10.31489/2022Ch3/3-22-13
3. **Sagyndikov**, M., Salimgarayev, I., Ogay, E., Seright, R.S., Kudaibergenov, S. 2022. Assessing polyacrylamide solution chemical stability during a polymer

flood in the Kalamkas field, Western Kazakhstan. Bulletin of the Karaganda University Chemistry Series 105 (1): 99-112. https://doi.org/10.31489/2022Ch1/99-112

4. **Sagyndikov**, M., Seright, R.S., Tuyakov, N. 2022. An unconventional approach to model a polymer flood in the Kalamkas oilfield. Paper presented at the SPE Virtual Improved Oil Recovery Conference to be held 25-29 April 2022. SPE-209355-MS. https://doi.org/10.2118/209355-MS

5. **Sagyndikov**, M., Imanbayev, B., Salimgarayev, I., Baipakov, S. 2022. Method for the field assessment of polymer degradation during a polymer flood of oil reservoir. Patent for Utility Model №7054, National Institute Of Intellectual Property RoK (in Russian) – APPENDIX A.

6. **Sagyndikov**, M., Ogay, E., Kudaibergenov, S. 2021. Feasibility study of polymer flooding application in the heavy oil reservoir. Proceedings of the International Scientific Conference "Satbayev Readings – 2021" (in Russian)

7. **Sagyndikov**, M., Ogay, E., Kudaibergenov, S. 2020. Evaluation of Polymer Flooding Efficiency at Brownfield Development Stage of Giant Kalamkas Oilfield, Western Kazakhstan. Proceedings of the International Scientific Conference "Satbayev Readings – 2020"

Dissertation Organization. The dissertation is composed of six chapters. The introduction presents the general overview, relevance, objectives, hypotheses, and dissertation organization. Chapter I provides the Kalamkas oilfield geological properties and reservoir dynamics features. Chapters II, III, IV, and V are based on published papers, of which I am the first author, about topics of the Kalamkas polymer flood key aspects and EOR technology optimization. Chapter VI is conclusions. A summary of each chapter is shown as follows:

Chapter II is a comprehensive literature review of recent worldwide polymer EOR projects. Chapter III examines polymer in-situ mechanical stability and describes the development of a novel method for the field assessment of polymer degradation during a polymer flood of an oil reservoir. Chapter IV assesses polymer chemical stability and recommends mitigating viscosity loss and optimizing OPEX. Chapter V describes an unconventional approach to model a polymer flood at the Kalamkas oilfield.

The total volume is 116 pages, including 55 figures, 27 tables, references of 168 titles, and 6 appendices.

Next, I would like to thank Ilshat Salimgarayev, Nauryzbek Tuyakov, Ruslan Kushekov, Sattibek Baipakov, and other colleagues who have participated in the research works.

Finally, and most importantly, I would like to thank my father - Serik Sagyndykov, mother - Akzhunis Imanbayeva, and wife – Zarina Tlenova, for their continuous support and love.

1. THE KALAMKAS OILFIELD OVERVIEW

1.1 The Kalamkas oilfield geology and reservoir development features

This dissertation research object is related to the Kalamkas oil and gas field. The Kalamkas field, situated in the western part of Kazakhstan, was discovered in 1976 and brought on stream in 1979 according to the Field Development Project – FDP [18]. Oil and gas reservoirs were established in the Jurassic deposits, and Cretaceous deposits have massive gas and water reservoirs (Figure 1.1). Reservoirs mainly consist of sandstones deposited in deltaic, fluvial, and shallow marine environments.
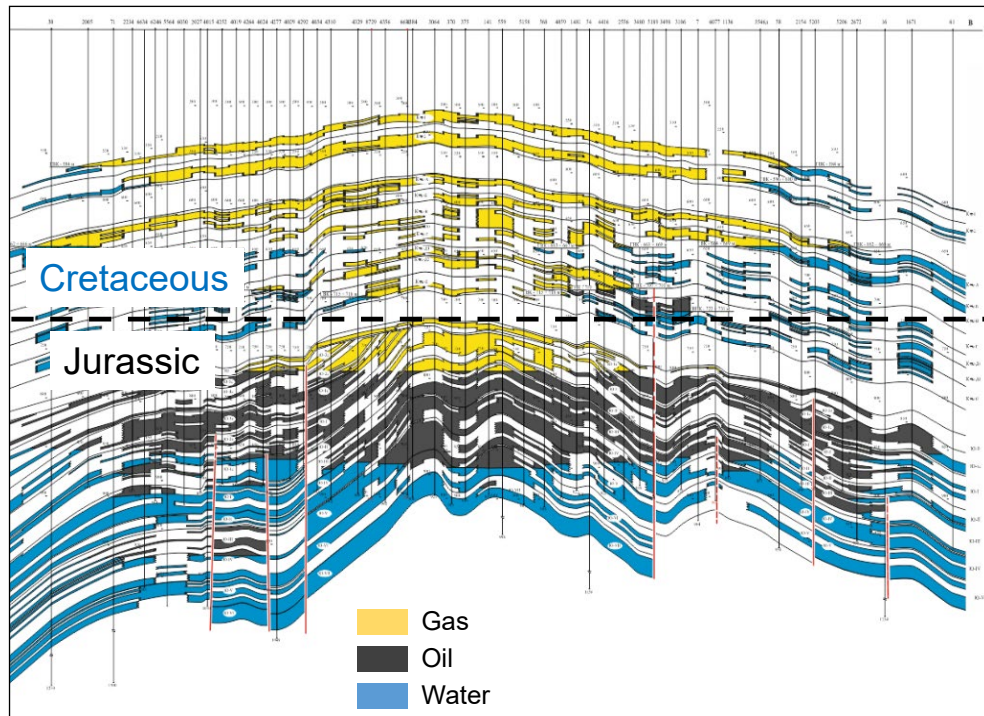
Figure 1.1 — Geological profile of the Kalamkas field

Taking into account the difference between reservoir pressures and bubble point pressures (2-3 MPa), predicted liquid production under the natural depletion, and other geological features, an FDP was designed with the following scenario:

- A uniform 9-spot pattern with 400-m well spacing.
- Well orientation – vertical.
- Pressure maintenance (or injection) started from the beginning of the development.
- The voidage replacement ratio was typically 100-120%.
- The injected water was either produced Jurassic brine and Cretaceous water reservoir brine.
- The injection bottom hole pressure (BHP) was below the initially measured formation parting pressure (12-14 MPa).
- Production BHP was not allowed to drop below the bubble point pressure (5-7 MPa).

Oil reservoirs have a high layered permeability contrast (>4) and unfavorable water-oil mobility ratio (M>7), which jeopardizes uniform depletion and oil recovery. To date, the water cut is significantly higher than expected considering the depletion of recoverable reserves (Figure 1.2). (In this case, the depletion of recoverable reserves is defined as a percentage ratio of cumulative oil production and recoverable oil reserves.)
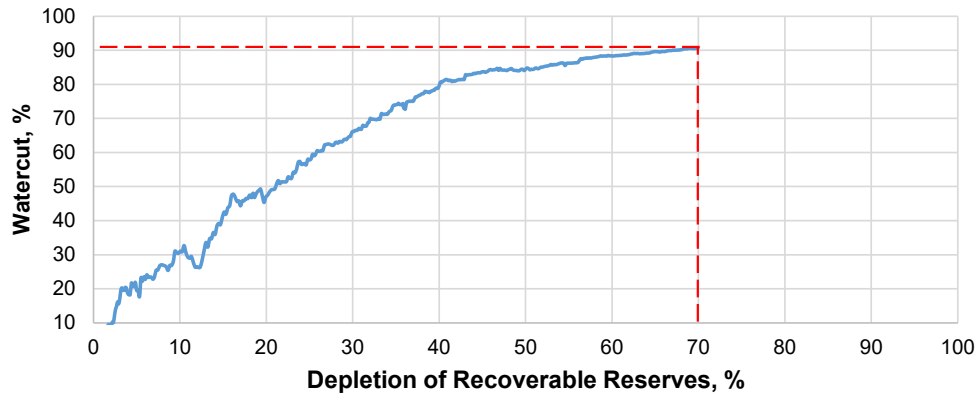

Figure 1.2 — History of the water cut versus recoverable reserves depletion for the Kalamkas field.

In contrast, high average formation permeability (>500 md) and relatively low reservoir temperature (40°C) attract the implementation of chemical enhanced oil recovery (EOR) methods, such as polymer flooding. In view of the low reservoir temperature, elevated mobility ratio, and high formation permeability, it was recognized that there is considerable potential for enhancing oil production by polymer flooding. For this reason, the Kalamkas polymer flood history started in 1981 [21]. Polymer flood was implemented as a secondary recovery method and utilized in 46 injection wells [22]. During 1981-1989 injected ~10 000 tons of dry HPAM or 8 million m^3 of polymer solution, incremental oil production by polymer flood was 1,16 million tons, with an average polymer utilization factor of 118 t/t (i.e., 118 tons of incremental oil is produced per 1 ton of polymer injected.) Kalamkas polymer flood project by scale and innovation was a pioneer in the Soviet Union. However, this effective EOR technology expansion was stopped due to the economic crisis.

After 25 years of intensive waterflooding, tertiary polymer flood was considered to enhance oil recovery at the brownfield development stage. Although polymer flood is not novel technology for the Kalamkas field, implementation at the late stage of development first needs a pilot to prove its feasibility [23; 24].

1.2 The Kalamkas Oilfield Polymer Flood Present State

Recent tertiary pilot tests was initiated September 2014 in two injectors in the West part of the field and the second in four injectors in the East part of the field, beginning March 2015 [25; 30]. The West pilot includes 2 injectors with a 9-spot pattern (red rectangle in Figure 1.3) as projected in the FDP, and the East pilot includes 4 injectors (red square in Figure 1.3) with an infilled 5-spot pattern. Based

on the pilots' results, the East polymer project was extended to the existing 9-spot well patterns using 11 injectors (blue polygon in Figure 1.3). The earliest 4 polymer injectors of the East pilot were returned to waterflooding.
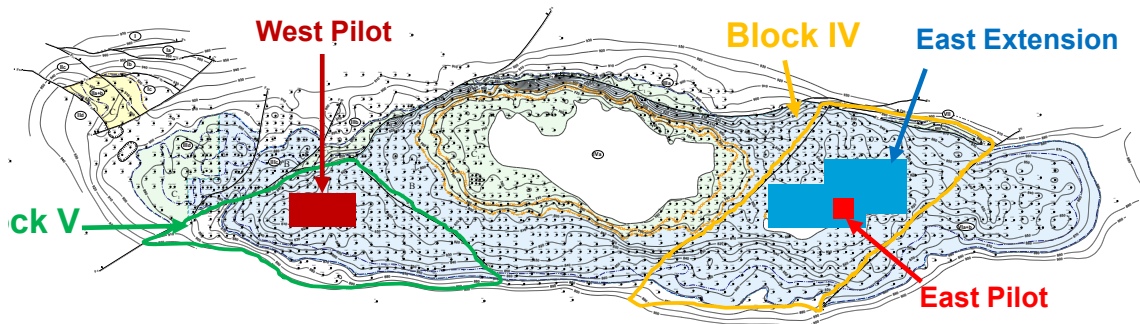

Figure 1.3 — Polymer flood project locations in the Kalamkas structural field map

West pilot was chosen with criteria to represent field-wide reservoir characteristics throughout Kalamkas oilfield. Accordingly, the reservoir at the pilot area has similar characteristics as whole Kalamkas oilfield with high layered heterogeneity (variation 1.6) and unfavorable oil-water viscosity ratio in reservoir conditions (>28). The permeability range is very wide with highest permeability of more than 2 000 md where average is 946 md (see Table 1.1).

Table 1.1 — Reservoir characteristics of the Kalamkas field and polymer flooding pilot area

#	Parameters	West PF pilot	Kalamkas field
1	Reservoir average TVD, m	746	725-879
2	Average permeability, md	946	55 – 1 273
3	Permeability variation degree, dim.	1,6	0,28-2,6
4	Vertical heterogeneity, dim.	3,3	1,15-3,41
5	Porosity, %	28	21-29
6	Initial oil saturation, %	70	50-71
7	Reservoir temperature, ºC	39	38-43
8	Initial reservoir pressure, MPa	9,3	9,18-9,53
9	Bubble-point pressure, MPa	7	5,1-7,2
10	Gas solubility, m^3/t	30,8	21-32,9
11	Reservoir oil density, g/cc	0,874	0,833-0,893
12	Pour point, ºC	-18	-15 - -20
13	Paraffin content, %	2,8	2,6-3,8
14	Sulphur content, %	1,09	1,21-1,45
15	Formation water salinity, g/l	118	101-121
16	Reservoir oil viscosity, cp	23,3	15,6-31
17	Reservoir water viscosity, cp	0,8	0,8

Table 1.2 provides a detailed chemical composition of the Cretaceous formation brine used in the polymer-solution injection process. This process includes preparing the mother solution and diluting it to the target concentration. The special production wells from a Cretaceous water reservoir supply the brine for West and East polymer flooding projects. We recognize that the formation salinities are quite high and that HPAM provides much more cost-effective viscosity in low-salinity brine than in high-salinity brine. Nevertheless, polymer flooding with HPAM under the conditions at Kalamkas still provides a substantial economic benefit. Further, given

the price and (lack of) availability of biopolymer (i.e., xanthan, scleroglucan, schizophyllan), the use of HPAM is still more cost-effective than alternatives.

Table 1.2 — The Kalamkas field formation brine physical and chemical properties

Parameter	Jurassic formation brine (from the production well)		Cretaceous formation brine (used for polymer dilution)	
	West Producer XX94	East Producer XX29	West PF	East PF
pH	6.1	6.3	5.8	6.1
Density, g/cm^3	1.089	1.081	1.072	1.080
Ca^{2+} content, ppm	4 500	4 400	4 609	5 410.8
Mg^{2+} content, ppm	2 640	2 400	2 189	2 432.0
Total salinity (TDS), ppm	136 211	123 445	98 722	108 913.7
Water type by Sulin	Cl-Ca	Cl-Ca	Cl-Ca	Cl-Ca
Water hardness, mg-eq/l	445	420	410	470
Fe^{2+} content, ppm	14	7.6	39.2	22.4
Fe^{3+} content, ppm	32	37	1.4	2.8
Total suspended solids (TSS) content, ppm	not measured	not measured	14.0	12.0
Dissolved oxygen content, ppm	not measured	not measured	0[1]	0[1]

[1] dissolved oxygen content measuring with CHEMets® express tests shows the undetectable value (less than 0.025ppm or 25 ppb)

The dissolved oxygen level has been measured at the wellhead of the water production well and the storage water tank of the polymer injection unit using CHEMets® colorimetric tests. Tests results reveal that the formation brine dissolved oxygen level is undetectable (less than 0.025 ppm or 25 ppb). This finding is consistent with the fact that Kalamkas oil reservoirs have a reducing environment due to iron-containing minerals up to 2-4% [31]. As can be seen from the brine chemical analysis, the brine has high salinity and high content of divalent cations (Ca^{2+}, Mg^{2+}, Fe^{2+}). The field brine iron content varies between 20-40 ppm. Consistent with Seright and Skjevrak (2015) experimental work [32], polymer solution viscosity losses at Kalamkas field conditions should be insignificant if the initial dissolved-oxygen concentration is 200 ppb or less.

At the Kalamkas field West pilot and East Extension polymer flood projects are using Polymer Slicing Unit (PSU) for the solution preparation and injection (Figure 1.4). For the East Pilot is using eductor-type unit, which will be shown in details in Chapter 4.

The PSU reduces the polymer particle size to a uniform and allows for significantly higher polymer concentrations [33] up to 1.5% or 15 000 ppm. In this unit, a polyacrylamide powder inlet is located at the upper part to supply polymer by gravity force (positive pressure) to the screw pump and PSU. The unit is completely isolated from air by a nitrogen blanketing system An individual low-shear pump was used for each injection well. The PSU at the Kalamkas field conditions shows high unit uptime [21]. Two powder-form partially hydrolyzed polyacrylamides (HPAM) (SNF products) were used: Superpusher K-129 (West Pilot) and Polyacrylamide R-1 (East Extension) They had a molecular weight of 14 million Daltons and a hydrolysis degree of 16%.These polymers are commercially available products. The chemical stability and good dissolving quality of the polymer were demonstrated

during the experimental work of Seright and Skjevrak (2015) [32] with polymers and conditions similar to those in our application.
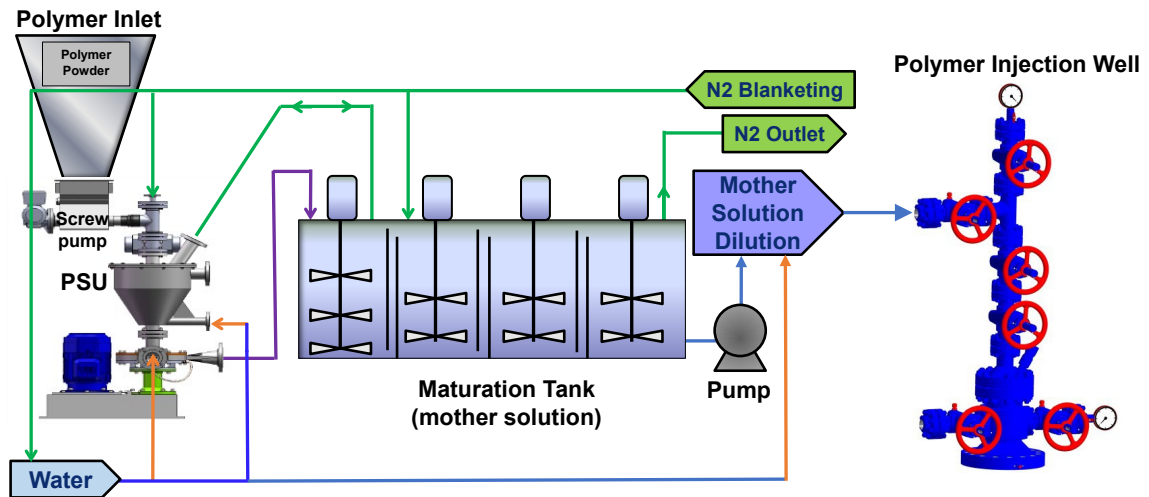
Figure 1.4 — Main components of the polymer solution injection unit.

Polymer Flood Performance. As mentioned earlier, West pilot was the first polymer flood project implemented at the Kalamkas field. The West pilot consists of 23 vertical producers and 2 vertical injectors (Figure 1.5). Production from the pattern began in June 1985 via the first drilled producer, and water injection began in July 1986 via the first vertical injector. According to the FDP pattern, initial drilling was completed in September 1990 with 400 m well spacing (17 producers and 2 injectors). Later, in 2011-2014 pattern was infilled with 6 producers with a spacing 200 m.

Before polymer flood for ~30 years of reservoir development cumulative oil production was 1 660 726 ton, cumulative liquid production – 6 831 612 ton, cumulative water injection – 3 604 614 m^3, and average water cut reached 90 %.

Figure 1.5 — West Pilot polymer flood pattern (red rectangle area) on the current oil production bubble map as of September 2014 (before polymer flood)

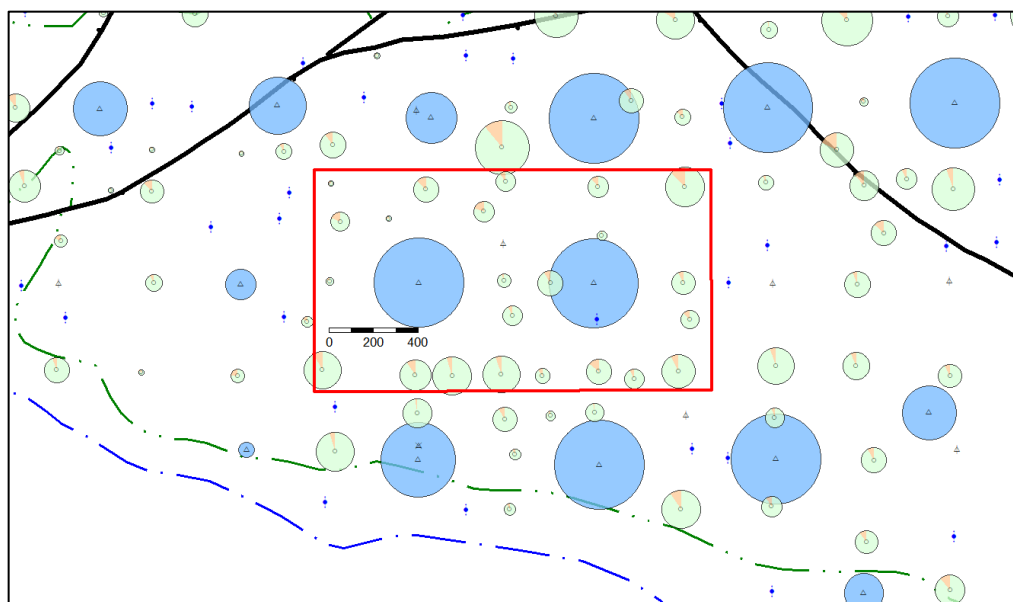Polymer flood began in September 2014 with the same injection rate as a water flood. Injecting polymer concentration was 1 800 – 1 900 mg/L with average viscosity of 20-22 cp (shear rate 7.34 1/s and T=25ºC). The watercut responded shortly after polymer solution injection and decreased 10% relative to the baseline. Polymer injected 20% of pattern pore volume, and no polymer production was observed. The incremental oil production was evaluated based on Buckley-Leverett fractional flow calculations [35], called "Displacement Characteristics." The West pilot pattern oil production and watercut response are shown in Figure 1.6.

The total incremental oil production by polymer flood was 303 214 tons, with an average polymer utilization factor of 97 t/t (i.e., 97 tons of incremental oil is produced per 1 ton of polymer injected.) Recovery factor enhanced by polymer flood for 5.2% and estimated 9% at the end of the project. Feasibility studies show an internal rate of return (IRR) – 131.5%, profitability index (PI) – 2.6, and payback period – 2.9 years.
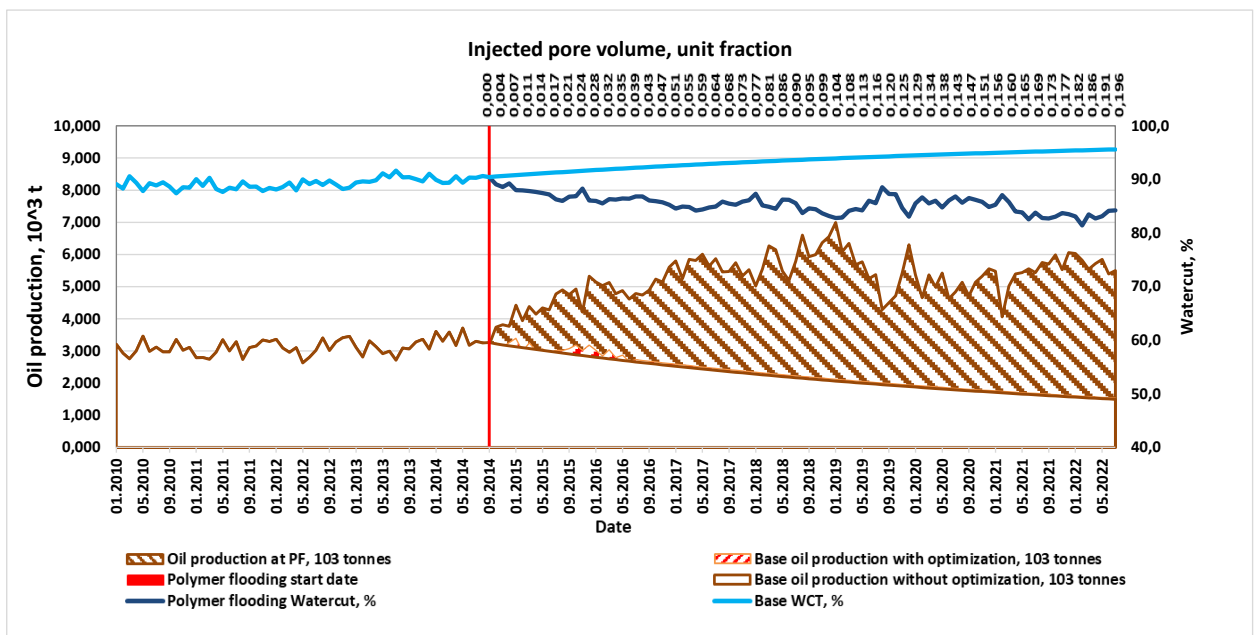
Figure 1.6 — Incremental oil production dynamics of West polymer flooding pilot

Additionally, for polymer flood efficiency assessment, we have analyzed the following oilfield data: cumulative and monthly production-injection data, oil reserves depletion, production logging test (PLT), injection logging test (ILT) interpretations before and after polymer flooding.

Figure 1.7 shows oil cut dynamics versus recoverable reserves depletion for the West polymer flood pilot pattern. Theoretical oil cuts at different mobility ratios are calculated based on Lysenko and Graifer's (2005) work [35; 36]. As shown in the Figure below, the mobility ratio before polymer flood was around 7, then decreased to 2 and further decline is expected.
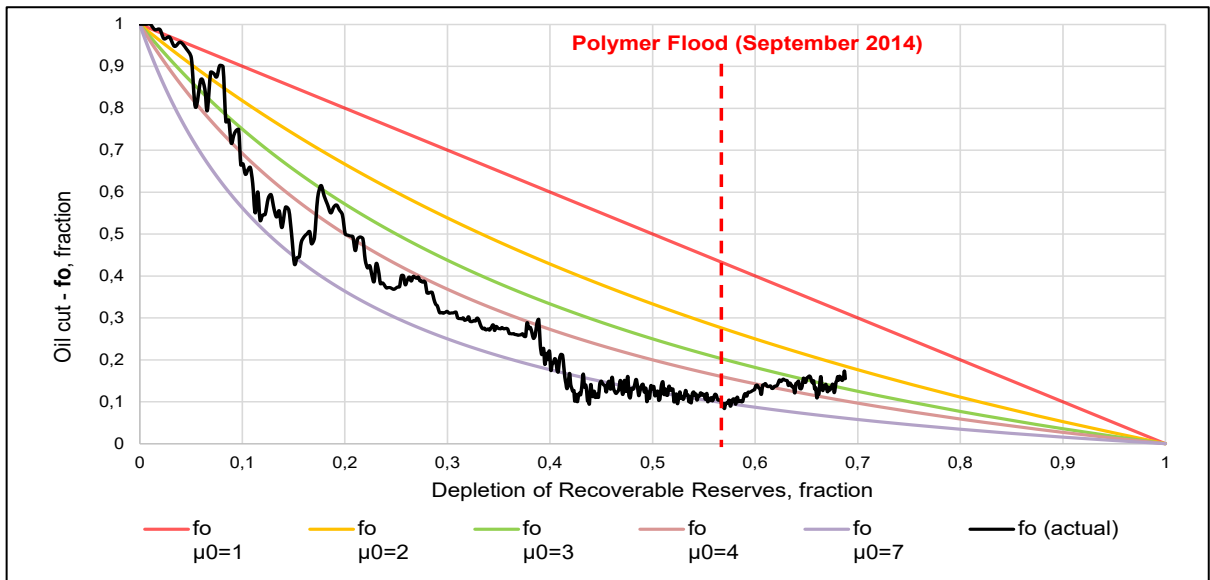
Figure 1.7 — Oil cuts actual and at different mobility ratios for the West polymer flood pilot

Figure 1.8 plots recovery factor vs. main reservoir dynamic indicators, i.e. watercut, oil/liquid production and injection rates. This figure respresents reservoir dynamics where development phases defined based on work [37]. The buildup phase (I) and plateau phase (II) are commingled, and it is a common image for the viscous and heterogeneous oil reservoirs. At those phases (I and II) recovery factor (RF) reaches 3% and watercut varied between 10-20%. Next, the drawdown phase (III) is characterized by an intensive water cut increase caused by water breakthrough shortly after water injection starts. At phase III watercut increased from 10% to 90% and RF reaches 21.3%. End of phase III indicated by significant watercut slope decrease and starting of brownfield phase (IV). Watercut at phase IV steadly and slowly increased. When recovery factor reaches 28.2% and watercut 90% polymer flood started. Polymer flood phase (V) characterized by noticeable watercut reduction and doubled oil rate. This phase can be called the new development stage, which extending the oilfield's' economic lifetime.

Figure 1.8 — Impact of conducting the polymer flooding pilot to the reservoir development

To obtain valuable well logs data, we proposed and ran ILT in injection wells and PLT in production wells. Figure 1.9 shows ILT results from XX41, XX49 injector wells before and after polymer flooding. Ther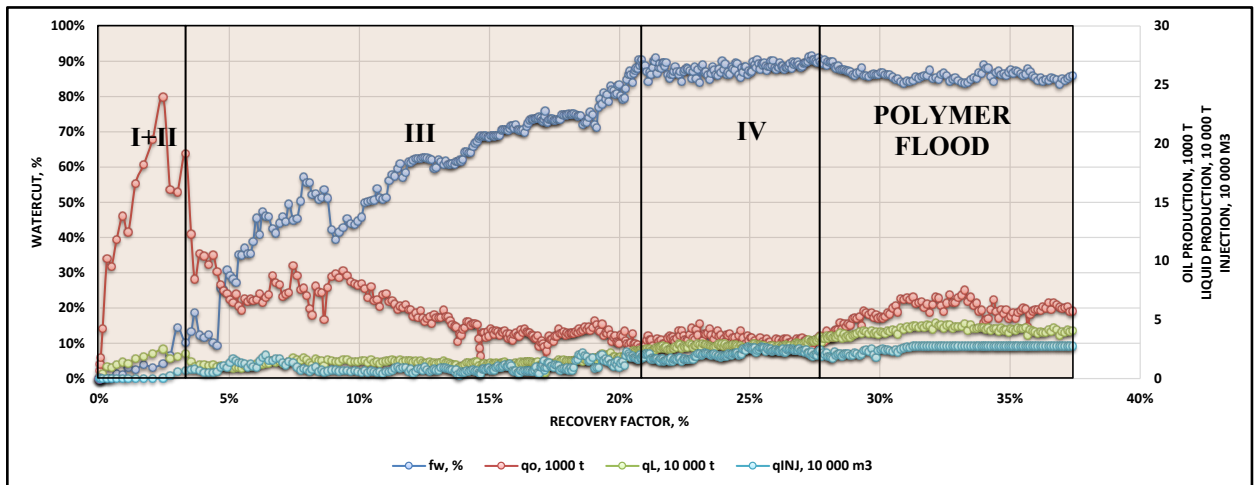e is an increase of vertical sweep efficiency approximately from 26% to 50% and 28% to 77% for XX41 and XX49 injector wells respectively. As observed, the polymer flooding process was able to redistribute the injected agent to maintain reservoir pressure in previously unaffected zones of the reservoir. It should be noted that the sweep efficiency of other injector wells drilled to reservoir J-C1 is much lower than polymer flooding pilot injector wells (Table 1.3).

The PLT interpretations from production wells are described in work [38]. According to the PLT interpretations, based on the flow contribution characteristics and amount to perforated intervals, production wells can be divided into the following categories:

- wells, where sweep efficiency is decreasing by blocking of washed water zones and increasing of the amount of oil;

- wells, where there is a redistribution of production profile and increasing of sweep efficiency;

- wells, were no dynamic change (constant flow profile and characteristics).

Our results show that there is an improvement of vertical sweep efficiency in injector wells and the blocking of washed water zones in production wells. The polymer flooding process was able to equally redistribute the injected agent to maintain reservoir pressure in previously unaffected zones of the reservoir.
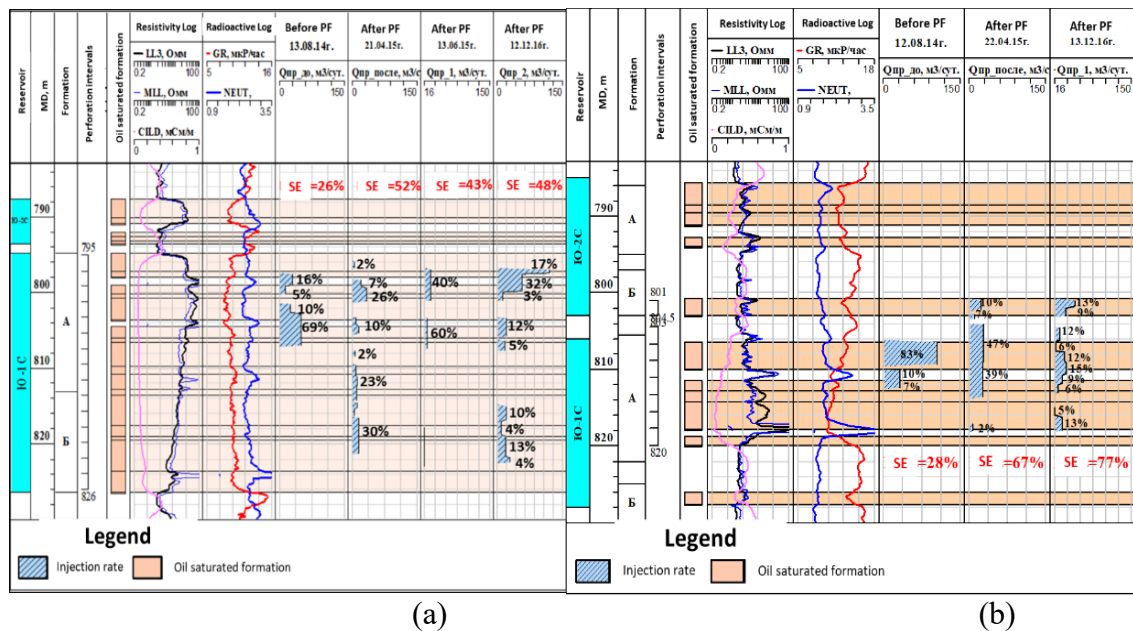

(a)   (b)

Figure 1.9 — Comparison of ILT acquired before and after the polymer flooding from wells XX41 (a) and XX49 (b)

Table 1.3 — ILT results of reservoir J-C1 injectors and wells XX41 и XX49

Parameters	Reservoir J-C1	Well XX41	Well XX49
Sweep efficiency			
Number of ILT	30	3	2
Arithmetical mean	42%	48%	72%
Variation	0,51	0,1	0,1
Max	90%	52%	77%
Min	14%	43%	67%
Average by thickness	39%	48%	72%

1.3 Chapter Conclusions

The Kalamkas oil reservoirs have a high layered permeability contrast (>4) and unfavorable water-oil mobility ratio (M>7), which jeopardizes uniform depletion and oil recovery. In view of the low reservoir temperature, elevated mobility ratio, and high formation permeability, it was recognized that the Kalamkas field has considerable potential for enhancing oil production by polymer flooding.

The Kalamkas polymer flood pilot conducting since 2014 and shows high technical and economic success. The following major performances were noted:
- HPAM polymer shows good dissolving quality and high uptime in injection units (PSU).
- The watercut responded shortly after polymer solution injection and decreased 10% relative to the baseline.
- PLT/ILT studies show an increase in sweep efficiency.
- A comparison of theoretical and actual oil cuts shows a decrease in mobility ratio.
- Polymer injected 20% of pattern pore volume, and no polymer production was observed.
- The total incremental oil production by polymer flood was 303 214 tons, with an average polymer utilization factor of 97 t/t.
- Recovery factor enhanced by polymer flood for 5.2% and estimated 9% at the end of the project.
- Feasibility studies show an internal rate of return (IRR) – 131.5%, profitability index (PI) – 2.6, and payback period – 2.9 years.

Taking into account above mentioned polymer flooding is a perspective EOR technique for the Kalamkas field that requires further development. The development requires (1) a comprehensive literature review of recent worldwide polymer EOR projects focusing on the Kalamkas field polymer flood aspects, (2) assess polyacrylamide solution chemical and mechanical stability, (3) experimental and numerical studies of the Kalamkas polymer flood technology for examining the oil recovery at various simulation scenarios, (4) feasibility studies for choosing the most rational concept for full field deployment.

2. REVIEW OF IMPORTANT ASPECTS AND PERFORMANCES OF POLYMER FLOODING VERSUS ASP FLOODING

2.1 Introduction

The principle of polymer flooding is to increase the viscosity of injected water and thereby develop a more favorable mobility ratio between displacing water and oil in place [16]. This approach reduces or avoids water fingering caused by geologic heterogeneities [17]. The favorable conditions for effective implementation of polymer flooding have been changed and improved by the augmented understanding of its mechanism over the last 60 years. The aim of this chapter is to understand how the range of these conditions has changed and the current stage of development. The chapter reviews some parameters such as oil viscosity, reservoir temperature, permeability, water ion composition, salinity, polymer concentrations, and injected volumes. Observations on required injection volumes have been described based on the Kalamkas oilfield experience. Water source selection has an essential role during pilot/field project design and is one of the most responsible technical and economic success decisions. Polymer slug design has been extensively analyzed, and it has been shown that achieving a unit oil-polymer viscosity ratio is not required, especially for high viscosity oil fields. Nevertheless, achieving a unit mobility ratio is desirable (to minimize viscous fingering), although it is not always practical because of injectivity constraints. Therefore, we placed significant emphasis on clarifying observed high polymer injectivities. Also, we performed a total acid number (TAN) analysis of three Kazakhstan oil fields for screening for ASP flood.

2.1 Polymer Flood Implemented Reservoir Conditions

Reservoir Depth, Temperature, and Salinity. Table 2.1 summarizes the main reservoir characteristics of many recent field projects. As the table shows, the majority of polymer flood projects are conducted in relatively shallow reservoirs with a depth of 1 600 m (except the Abu Dhabi case of 2 650 m). The reason is that shallow reservoirs have lower temperatures, which promotes polymer stability and favors economics as cheaper chemistry can be used. However, polymer degradation can be substantial at high temperatures (over 70 °C according to [30]). Thermal degradation of partially hydrolyzed polyacrylamides usually involves increased hydrolysis of amide groups, leading to precipitation with divalent cations (Ca^{2+}, Mg^{2+}). Incidentally, salinity and hardness often exhibit a linear relationship, which was obtained by analysis of several projects shown in Figure 2.1. Data were taken from fields such as West Koyot, Pelican Lake, Buracica, Bohai bay, Kalamkas, and others. Moreover, the interactions of hydrolyzed polymers with divalent cations lead to the reduction of polymer hydrodynamic volume. As a result, a decrease in solution viscosity or even polymer precipitation occurs [40; 41]. However, the inclusion of copolymers/monomers such as ATBS (Acrylamide-Tertiary-Butyl Sulfonate) and/or NVP (N-Vinyl-Pyrrolidone) enhances the thermal stability substantially [42; 43; 44]

and allow polymers to be tolerant up to 120 °C. According to the table, many polymer flooding projects, especially in Kazakhstan, are conducted using monomer-modified polymers and show promising results even at high salinities [21; 45; 30; 46; 47].
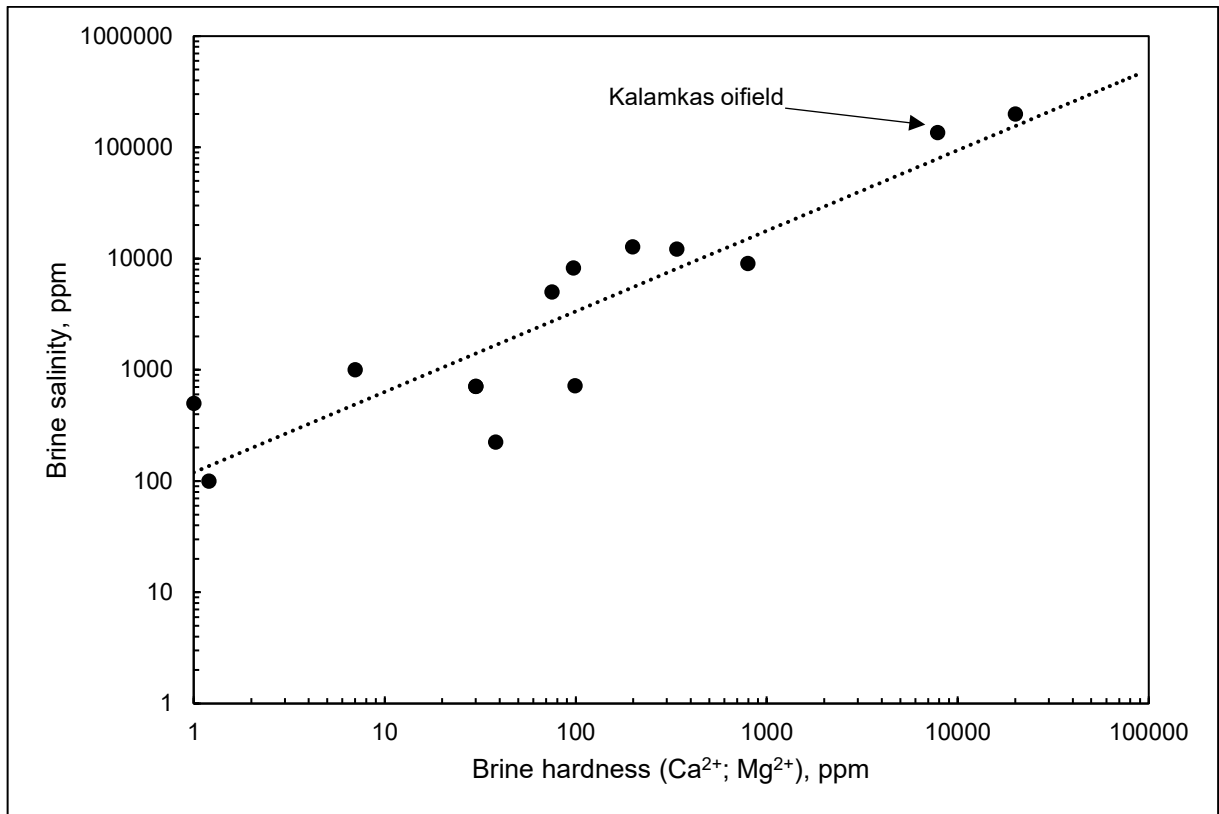
Figure 2.1 — Relationship of water hardness to water salinity from different polymer flood projects

Formation Permeability. The permeability of reservoirs affects the molecular weight (MW) of polymers used. The weight and size of polymer molecules are critical since larger polymer molecules tend to plug in relatively small pore throats, reducing the permeability and solution concentration. This process is called mechanical entrapment, which negatively affects the propagation of polymer in the reservoir [2; 17; 48]. Theoretically, less retention is expected as permeability increases. Therefore, experience-supported recommendations for polymer selection depending on polymer weight have been made by Wang et al. [49]. The minimum permeability required for successful polymer flooding is in the range of 100-300 md, and MW should generally be not greater than 17-25 million Daltons. This statement is supported by Table 2.1 based on actual field applications, where the permeability is mostly greater than 100 md, while the average permeability is around 2 000 md. However, Song et al. (2022) [50] showed promising laboratory results, where HPAM can effectively propagate through the tight low permeable (<50 md) carbonate rocks. The novel polymers can extend the minimum applicability range of permeability, and it has high relevance for future research & development.

Oil viscosity. Recent years in the history of polymer flooding (especially in Canada) have made it clear that achieving a favorable mobility ratio close to 1 or

less is not always the primary goal, but to reduce it as much as possible. As many field experiences show, injecting the same or close viscosity to live oil may be unnecessary. The fact that end-point relative permeability to water is usually much less than that to oil is often used to justify why the injected polymer viscosity can be less than oil viscosity. This approach has been applied to Canadian fields, where oil viscosity reaches 15 000 cP, and a "favorable" mobility ratio cannot even be achieved. Nevertheless, the experience of oilfields such as Pelican Lake, Seal, Mooney, East Bodo, etc. shows that polymer flooding can effectively produce more oil even if the oil is heavy. Many of these fields experienced an unsuccessful thermal injection, which becomes non-profitable in deep and/or thin reservoirs and requires a lot of energy [51]. Besides that, the design of the injected polymer viscosity is commonly based on the optimum economic output (i.e., net present value) according to reservoir modeling and feasibility studies. Some of these concepts are presented in literature sources [20; 47; 52].

Table 2.1 — Polymer flooding conditions in world projects

#	Field	Status	Depth, m	Formation thickness, m	Temperature, °C	Porosity, %	Permeability, md	Brine salinity, ppm	Live oil viscosity, cp
1	Marmul, Oman [53; 54; 55]	Field scale (Al Khalata)	550-675	-	46	25-30	100-2 000	4 600	90
2	Milne Point, Alaska, USA [56; 57; 58]	Pilot (J-Pad)	1 082	3-5.5	21.7	32	500-5 000	27 500	300
3	Captain (offshore), UK [59; 60; 61]	Pilot (SUCS)	914	<36.6	30.5	31	5 000	N/A	80
4	Dalia/Camelia (offshore), Angola [62; 63]	Pilot (DAL-710, 713, 729)	800-1 000	6-10	45-56	-	>1 000	117 700	1-11
5	Daqing, China [20; 64]	Field scale	1 000	6.1	45	25	1 100	3 000-7 000	9
6	Shengli, China [65]	Field scale	1 230	7.9-30.5	71	33.5	1 800	3 900	50-150
7	Shuanghe, China [66]	Pilot (Dong-Gudao)	1 460	25.2	72	20	422	4 356	7.8
8	Bohai bay, China [67]	Pilot (Layer II)	1 300-1 600	15-25	65	31	2 000	9 374	24-452
9	Tambaredjo, Suriname [68]	Pilot (Block-X)	375-425	13.7	36	33	3 000-10 000	10 000	300-1 100
10	East-Messoyakhskoe, Russia [69]	Pilot (T1-sand)	800	15-50	16	28-30	50-5 000	N/A	111
11	Matzen, Austria [70; 71; 72]	Pilot (PK1-3)	1150	20	50	20-30	500	25 000	19
12	Carmopolis, Brazil [73; 74]	Pilot (8 TH)	700	50	50	12-22	100	20 000	70-120
13	Canto do Amaro, Brazil [73; 74]	Pilot	500	8	55	22	204	500	7
14	Buracica, Brazil [73; 74]	Pilot (Pilot-1)	305	20-40	60	20	150-400	33 000	11
15	Diadema, Argentina [75; 76]	Pilot (Pilot-1)	900	4-12	50	30	500	16 000	100
16	El Corcobo, Argentina [77; 78]	Pilot	650	0.5-18	38	27-33	500-4 000	46 000	160-300
17	Bockstedt, Germany [79]	Pilot	1 200	15	54	24-30	2 000	186 000	11-29
18	East Bodo, Canada [9]	Pilot	794	3.2	27	30	1 000	25 000-29 000	600-2 000

#	Field	Status	Depth, m	Formation thickness, m	Temperature, °C	Porosity, %	Permeability, md	Brine salinity, ppm	Live oil viscosity, cp
19	Mooney, Canada [80; 81]	Pilot (11-14 pattern)	875-925	3-5	29	26	1 500	N/A	300-600
20	Seal, Canada [10; 81]	Pilot	600-650	8.5	20	27-33	3 000-5 800	N/A	3 000-7 000
21	Caen, Canada [10; 82]	Pilot	930	2.9	21	26.5	500-2 000	13 509	69.5-99
22	Wainwright, Canada [83]	Pilot (Suffield area)	650	-	-	30	300	72 000	100-200
23	Pelican Lake, Canada [11;84]	Pilot (B pool)	300-450	1-9	12-17	28-32	300-5 000	N/A	1 650-15 000
24	Mangala, India [85; 86; 87]	Pilot (NE-5)	600	24-40	<62	21-28	5 000	7 140	9-22
25	Abu Dhabi [88]	Single well injection test	2 650	20	>93	20-30	10-1 000	>200 000	1
26	Nuraly	Pilot	1 550	10	81	19	368	57 000	0,91
27	East-Moldabek, Kazakhstan [45]	Pilot scale	250	10	25	35	1 500	140 000	400
28	Zaburunje, Kazakhstan [45]	Pilot (FM1)	875	10	38	30	230-1 000	145 000	20
29	Kalamkas, Kazakhstan [21; 46; 47]	Industrial pilot scale	746	10-20	39	28	946	136 211	16

Note: all 29 fields are sandstone reservoirs except the Abu Dhabi (carbonate-limestone) oil field

Figure 2.2 shows a radar diagram of the major screening parameters for polymer flooding, showing the polymer flooding applicablity range. Wide ranges are associated with most parameters, and the ranges have been expanded due to the growth in the understanding of the technology and its refinement during the past 60 years. However, temperature and depth of formation remain the weakest side of polymer flooding. Even if new monomer-modified co- and terpolymers are showing promising laboratory results [42; 43; 89; 90; 91], there are no real field implementations where the formation temperature is greater than 109 °C [92]. Nevertheless, the radar chart provides an excellent visual representation of observations made previously in this work.
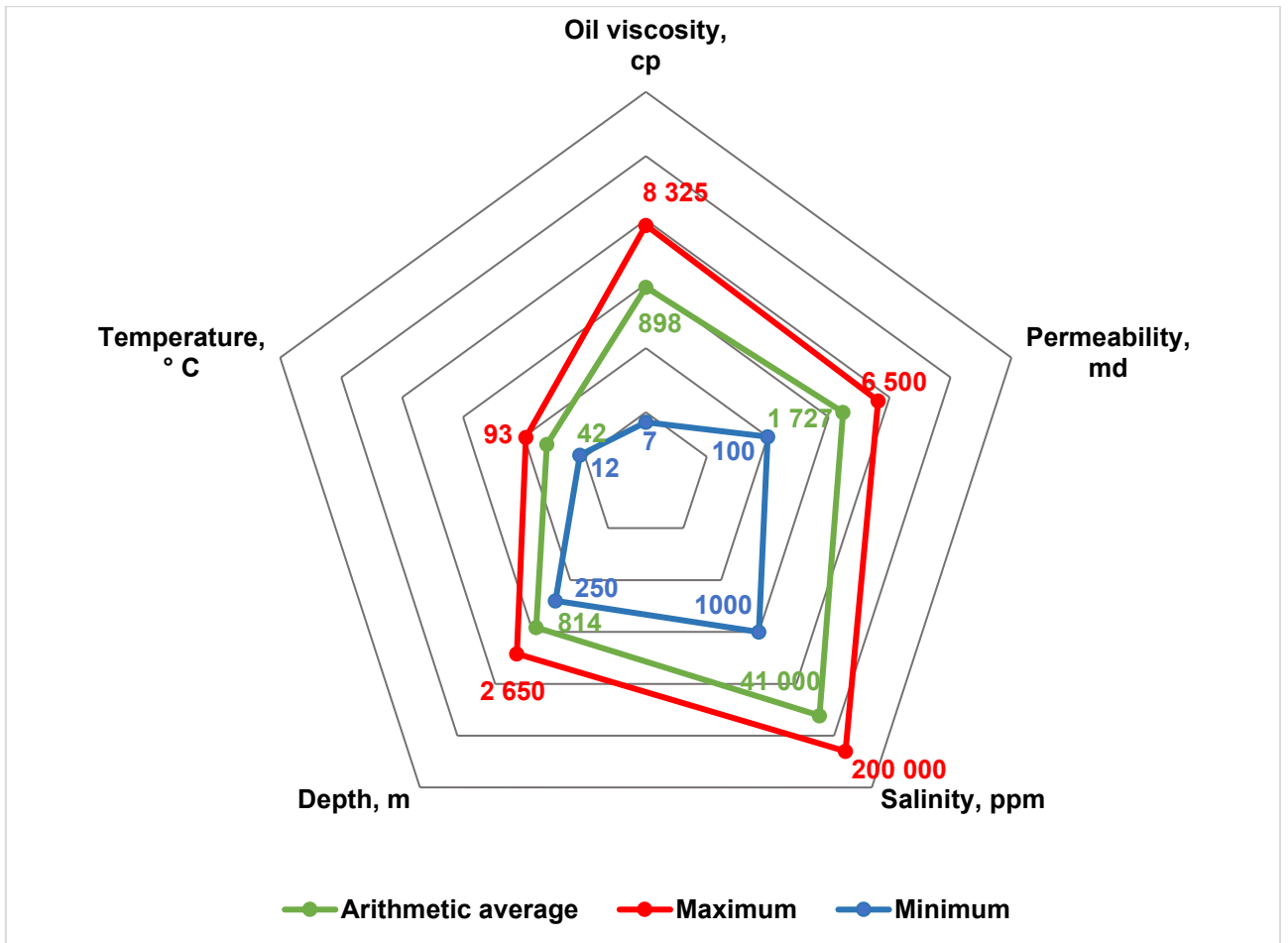
Figure 2.2 — Main screening parameters for polymer flood according Table 2.1

2.2 Polymers and Injection Parameters

Polymers used in EOR. Table 2.2 summarizes the main injection parameters during the polymer flooding. According to many authors [2; 16; 17; 28; 93], there are two main types of polymers in terms of their origin: synthetic polymers or polyacrylamides (PAM) used in paper production, and biopolymers used in the food industry as a thickener. In early polymer flood applications, polyacrylamides were used much more frequently than biopolymers due to their efficient manufacturing environment and commercial availability. This tendency continues these days because over 95% of polymer floods are based on polyacrylamides. Also, it is essential to highlight that polyacrylamide is mainly used in its partially hydrolyzed or anionic form (HPAM). Since anionic PAM (or HPAM) provide high viscosifying power and less retention on anionicly charged clays. In contrast, cationic PAM is too shear sensitive and has lower Mw. Non-ionic PAM is adsorbing on the rock surface too much [94].

The main representative of biopolymers is xanthan gum (derivation of micro-organism *Xanthomonas campestris*) [95; 96], which is characterized by semi-rigid molecules, whereas the structure of polyacrylamide molecules is flexible long chains [97]. Understanding the structure of molecules and microscale studies reveals each

polymer type's key features. Thus, the primary polymer parameters such as stability to temperature, high water salinity, mechanical degradation, biodegradation, dissolvability, viscosifying characteristics, adsorption to the rock surface, etc. are noted.

There are many laboratory and simulation studies [98; 99; 100; 101] that confirm HPAM benefits in viscosifying characteristics, absence of biodegradation, and injectivity over biopolymers. Alagic et al. [100] state that biopolymers are often sensitive to biodegradation, and it is important to protect them against potential microbial degradation. On the other hand, Al-Murayri et al. [102] indicated that biopolymers are more stable in the presence of oxygen and H_2S in any concentration, while high concentrations limit stability for HPAM. Seright and Skjevrak [32] suggest that HPAM degradation can be mitigated by keeping dissolved oxygen at an undetectable or acceptable level (as close to zero as practical). For this reason, modern polymer injection units provide nitrogen blanketing in the polymer preparation system to prevent air contact with the solution [30]. Specialized equipment for HPAM solutions was also mentioned in many works [56; 63; 103]. For example, Abbas et al. [103] argue that specialized equipment is essential in the field conditions to overcome problems with dissolving HPAMs (e.g. fish-eyes and gels). In contrast, such dissolution problems are not observed for hydroxyethylcellulose (HEC) biopolymers. Seright et al. [104] confirmed that xanthan solution is more resistant to mechanical degradation showing pseudoplastic behaviour during coreflooding experiments. In addition, synthetic HPAMs lack thermal and brine hardness stability, as will be discussed below. But, the main conclusion for the polymer's limitations is made by Ryles [30], who observed that the main challenge lies with high temperature rather than high salinity. Despite these disadvantages, HPAM is still the most widely used polymer in the world. An internet search suggests that ~1.2x10^6 tones of HPAM/PAM are produced each year, whereas only ~1.2x10^4 tons of xanthan are produced. Thus, HPAM production (and availability) is roughly 100 times greater than xanthan (the most extensively produced biopolymer). The price of xanthan (per weight) is 3-6 times greater than that of HPAM. This information is from a combination of internet and confidential sources. Also, biopolymers oil field application is associated with the problems of high purity, active content, and neediness of using biocides [94].

A major factor that aids the application of polymer flooding is the the current price for large HPAM purchases (~\$2-2.5/kg) is actually less than that in 1980 (~\$4-5/kg). This fact is remarkable because the Consumer Price Index in the USA (the average cost of goods and services) has more than tripled since 1980. Much of the credit for keeping HPAM prices must go to the HPAM manufacturers. However, some credit must also be given to several large-scale polymer floods (Daqing, Mangala, Pelican Lake) that played a significant role in providing the market and promoting low-cost polymers. Interestingly, the primary justification (used by big oil companies) for eliminating EOR in 1986 was that the "cost of chemicals would always rise in direct proportion to the price of oil." The reality of HPAM price history emphasizes that

technical and economic advances can upend conventional wisdom at a particular time.

Polymer Injection Design. A literature review reveals that polymer concentrations were in a wide range of $300 - 2\,750$ ppm and, on average, was $1\,570$ ppm, as shown in Figure 2.3. Furthermore, the viscosity range was 3-300 cp and in average was 41 cp. Only a minority of field projects used polymer viscosity higher than 40 cp. On the other hand, some projects used relatively low polymer concentrations and achieved considerable viscosity–because low-salinity (or fresh) water was used [105; 106; 107] (#26 line in Table 2.2). The selection of the process water source has crucial importance and should satisfy the following concepts: 1) compatibility with reservoir rock & fluids (no clay swelling/migration should occur; 2) low cost and existing infrastructure; 3) high potential production capacity; 4) salinity (especially divalent cations) as lower as practical; 5) chemical stability; 6) dissolved iron, oxygen, TDS, oil contents as low as possible (absence is an ideal case); 7) if dissolved iron exists in the process water dissolved oxygen level should be controlled as low as possible (at a maximum <200 ppb based on [32] and <46 ppb based [108]).

Polymer Injectivity. Injectivity issues are important and of high current interest in polymer flooding technology. Besides creating a high-pressure displacement front in-situ, providing a sufficient injection rate is also essential. Moreover, in unfractured vertical injection wells, simple Darcy-law calculations reveal that polymer injectivity relative to water should be reduced by at least 80% [85]. In contrast, most field projects summarized in Table 2.2 reported relatively high polymer injectivity. Furthermore, the Kalamkas field case [30] demonstrated that polymer injectivity was roughly 4 times greater than water injectivity. Previous work has shown that the viscoelastic (or shear-thickening) behavior of HPAM polymers occurs at high fluxes, and as a consequence induces a fracture to form and extend in the well [109]. The presence of fractures during the polymer flood is consistent with the fact that most of the worldwide polymer flood projects inject into vertical wells above the formation parting pressure [52; 104; 106; 110; 111; 112]. In contrast, if fractures or fracture-like features are not present during polymer injection, achieving a favorable economical injection rate and acceptable voidage replacement ratio (e.g., the same as during a waterflood) are not practical. Also, Sagyndikov et al. [46] demonstrated that these induced fractures reduce polymer mechanical degradation to a level that mitigates this degradation concern in a field setting.

Thomas et al. [113] have investigated injectivity prediction difficulties by reviewing some polymer field projects. The authors conclude that improving injectivity prediction is needed as pessimistic predictions are often obtained and can lead to the evaluation of polymer volumes that can be injected. The paper suggests further investigations using simulation processes, especially in reconsidering reservoir properties such as near-wellbore fractures and modeling polymer rheology and its features. Table 2.2 represents a modified summary of the polymer projects injectivity data presented by Thomas et al. [113].

Table 2.2 — Polymer formulation and injectivity of PF projects

#	Field	Polymer type	Mw, million Da	Polymer concentration, ppm	Polymer viscosity, cP	Porcess water salinity, ppm	Injection rate, m³/d	Injectivity issues
1	Marmul, Oman	HPAM	18-20	-	15	4 500	250-750*	No (fractures)
2	Milne Point, Alaska, USA	HPAM	N/A	1 600-1 800	45	2 500	350 and 95*	Initially no (decreased after 7 months)
3	Captain (offshore), UK	HPAM	18	~2 000	20	-	4 710 then 2 041*	No
4	Dalia/Camelia (offshore), Angola	HPAM	12-16	900	2.9	25 000-52 000	2 385*	No
5	Daqing, China	HPAM	N/A	2 000-2 500	40-300	700	0.14-0.2 PV/yr**	Mostly no (hydraulic fracturing applied if needed)
6	Shengli, China	HPAM	17	2 000	25-35	3 900	-	-
7	Shuanghe, China	HPAM (S625+S525)	N/A	1 090	93 at 3 rpm	fresh water	-	-
8	Bohai bay, China	Associative polymer	20	1 750	77.6-131	-	-	-
9	Tambaredjo, Suriname	HPAM Flopaam 3630S	N/A	<2 500	45 then 125	500	150-450*	No (fractures)
10	East-Messoyakhskoe, Russia	HPAM	20	1 830	30 at 7.34 s-1 60 at res. cond.	-	150-300*	No
11	Matzen, Austria	HPAM Flopaam 3630S	5-10	800	1.6-4.6 at res. cond.	23 000	400*	No (fractures)
12	Carmopolis, Brazil	HPAM	5-10	1 000	30	500	165*	No
13	Canto do Amaro, Brazil	HPAM	5-10	750	10	-	200-300**	No
14	Buracica, Brazil	HPAM	20	500	40	100	60-120**	No
15	Diadema, Argentina	HPAM Flopaam 3630S	N/A	1 500-3 000	70	16 000	1 000**	No
16	El Corcobo, Argentina	HPAM	N/A	500	20-25	1 044	1 000**	No
17	Bockstedt, Germany	Biopolymer Schizophyllan	18-20	300	25	-	135**	No (after reperforation and acidizing)
18	East Bodo, Canada	HPAM	20-25	1 500	50-60	-	200*	No (horizontal wells)
19	Mooney, Canada	HPAM	20	1 500	20-30	-	-	No (horizontal wells)
20	Seal, Canada	HPAM Flopaam 3630S	20	1 000-1 500	25-45	2 500-11 000	-	No (horizontal wells)
21	Caen, Canada	HPAM Flopaam 3630S	N/A	1 300	32	15 287	800*	No
22	Wainwright, Canada	HPAM	20	2 100-3 000	25	72 000	-	No (after installing booster pumps)

#	Field	Polymer type	Mw, million Da	Polymer concentration, ppm	Polymer viscosity, cP	Porcess water salinity, ppm	Injection rate, m³/d	Injectivity issues
23	Pelican Lake, Canada (2006-...)	HPAM Flopaam 3630S	20	600-3 000	13-25	-	-	No
24	Mangala, India (2014-…)	HPAM Flopaam 3630S	18-20	2 500-3 000	15-20	5 400	~740*	No
25	Abu Dhabi	HPAM (ATBS)	N/A	500-2 400	1.2-5.5	>200 000	144*	No
26	Nuraly (2014-2019)	HPAM Flopaam 5115 VHM AL-777	14	500	6	1 300	80-220*	No
27	East-Moldabek, Kazakhstan (2019-…)	HPAM Flopaam 1630S	N/A	2 400	23	140 000	50*	No
28	Zaburunje, Kazakhstan (2014-…)	HPAM	N/A	1 950	15	135 000	740**	No
29	Kalamkas, Kazakhstan (2014-…)	HPAM R-1 and Superpusher K129	14	2 000	24	98 722-108 914	300*	No (fractures)
30	West Salym [114]	HPAM FLOPAAM 3230	8	2 500	14	soft water (Ca^{2+}, Mg^{2+} <1.6 ppm)	150*	No (fractures)

* - injection rate for 1 well; ** - full field injection rate

Volokitin et al. (2018) [114] during West Salym ASP project concluded that injection below fracture pressure could not be achieved a reasonable rates. Thus, decided to inject under fracturing conditions. Fracture initiated by the temperature reduction and ramping up the injection rate (thermo-elastic stress reduction). The fracture length (determined by well tests analysis) have remained small compared to the well spacing and therefore not expected to harm sweep efficiency. Also, this work showed practical approach to monitor fracture propagation by combination of temperature logs and presurre fall-off tests, which can be utilized at the Kalamkas PF project.
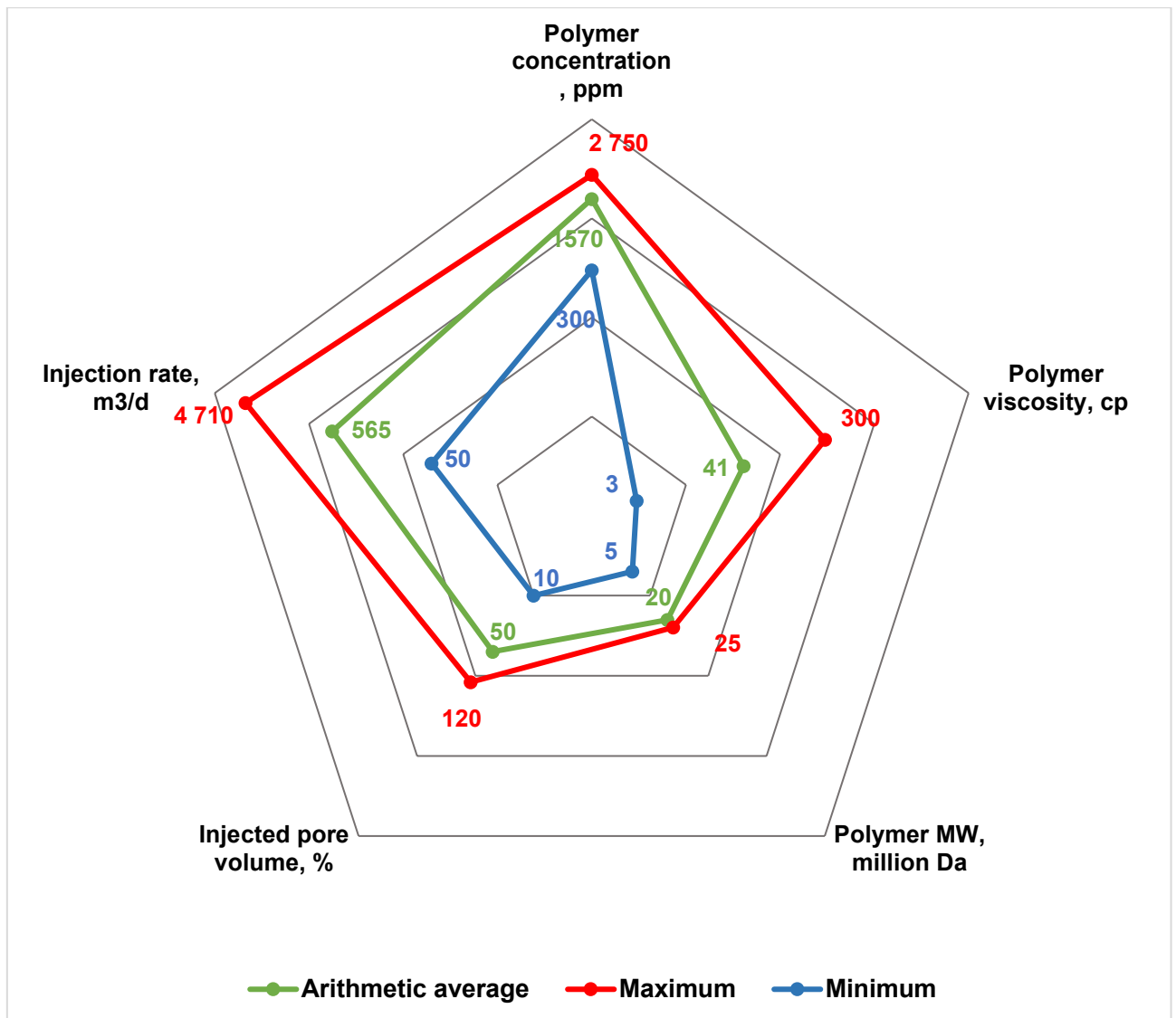
Figure 2.3 — Polymer injection parameters for polymer flood according Table 2.2

Polymer viscosity and slug design. Determining the desired viscosity of the polymer solution is a key objective of designing the polymer flooding project since it strictly affects project feasibility. A simple method to estimate desired viscosity has been developed by Sorbie and Seright [115]. As the authors say, the base-case method helps determine the target polymer viscosity by simply multiplying waterflood end-point mobility ratio times the permeability contrast (highest permeability divided by the lowest permeability. Thus, the measurement of water and oil relative permeabilities is key for the polymer flood design.

Table 2.3 summarizes the main reservoir development parameters (mobility ratio & permeability contrast) in the comparison of PF design (viscosity, slug size), implemented conditions (number of injectors & producer, watercut) and an achieved result (incremental recovery factor - RF).

As the polymer solution is a shear-thinning (non-Newtonian) agent, it is strongly recommended to consider its apparent viscosity (dependent on the shear rate). Typically, polymer viscosities are evaluated at a shear rate of 7,34 s^{-1}, which has been accepted as the industry standard (corresponds to 6 rpm of UL adapter on

Brookfield viscosimeter). In fact, typical shear rates in reservoir conditions (deep from well perforations) can be lower (depending on permeability, well spacing, and injection rate, so the apparent viscosity could be higher. In addition, reservoir temperature should be considered while measuring the polymer solution viscosity since the higher the temperature, the lower the viscosity is expected.

Sheng [116] and Seright [52] show that over the 60-year history of polymer flooding (PF), the concentration and volume of polymer injection have increased over time. Whereas the slug volume in the 1960-1980 period was around 5-17% of the pore volume, in the last 20 years the volume has reached 120% (Daqing field, PRC). The increase in volume is due to the absence of a residual resistance factor effect, i.e., the absence of a post-effect when polymer wells are converted to water injection. Testing on physical reservoir models has shown that the viscous fingering of the polymer bank has occurred in the high permeable zone, thereby not involving the low-permeable zone. This phenomenon has been clearly demonstrated by a field example from the Kalamkas field [47].

Horizontal wells for polymer flooding. Up to the mid 1990s, before the widespread use of horizontal wells, accepted screening criteria [117] advocated that 150 cp was the upper limit of oil viscosity for polymer flooding applicability. The introduction of horizontal wells has allowed polymer flood applications with much higher oil viscosities [11; 52; 106; 31]. In particular, horizontal wells considerably increase injectivity, reservoir acess, and sweep efficiency, relative to vertical wells.

Table 2.3 — Reservoir development parameters accepted for polymer flooding projects

#	Field	End Mobility Ratio	Perm. Contrast	Polymer viscosity, cP	Injected Volume, PV	I/P*	Water Cut before PF, %	Incremental RF, %
1	Marmul, Oman (2010-…)	~40	10:1	15	-	27/-	~90	~10 expected
2	Milne Point, Alaska, USA (2018-…)	>20	10:1	45	-	2/2 (horizontal)	~65	~10 expected
3	Captain (offshore), UK (2011-2013)	31	-	20	-	1/1 (horizontal)	85	~16
4	Dalia/Camelia (offshore), Angola (2010-…)	-	10:1	2.9	0.5 expected	3/- (deviated)	>40	3-7 expected
5	Daqing, China (2008-…)	9,4	4:1	40-300	0.4-1.2	-	95	15-18
6	Shengli, China (2008-2013)	-	-	25-35	>0.4	55/84	95	3.7
7	Shuanghe, China (1994-1999)	-	4:1	93 at 3 rpm	0.4	-	91	10.4
8	Bohai bay, China (2005-…)	-	4:1	77.6-131	0.31	10/35	>80	7.1
9	Tambaredjo, Suriname (2008-2015)	-	12:1	45 then 125	0.65	3/9	80	11
10	East-Messoyakhskoe, Russia (2017-2019)	30	-	30 at 7.34 s-1 80 at res. cond.	0.1	2/4 (horizontal)	>90	-
11	Matzen, Austria (2011-...)	-	-	1.6-4.6 at res. cond.	-	2/6	~90	~10 expected
12	Carmopolis, Brazil (1997-2003)	12	-	30	0.1	4/21	10	-

#	Field	End Mobility Ratio	Perm. Contrast	Polymer viscosity, cP	Injected Volume, PV	I/P*	Water Cut before PF, %	Incremental RF, %
13	Canto do Amaro, Brazil (2001-2008)	2-5	-	10	0.16	2/6	6	-
14	Buracica, Brazil (1999-2003)	3	-	40	0.73	2/7	8	-
15	Diadema, Argentina (2007-...)	80	9:1	70	0.8	5/19	96	6-8 expected
16	El Corcobo, Argentina (2012-…)	-	-	20-25	-	6/22	~85	6-10 expected
17	Bockstedt, Germany (2013-…)	-	3:1	25	-	-/4	>90	-
18	East Bodo, Canada (2006-…)	42	-	50-60	-	1/12	95	20 expected
19	Mooney, Canada (2008-2010)	-	-	20-30	-	2/3 (horizontal)	90	18
20	Seal, Canada (2010-…)	-	-	25-45	-	3/4 (horizontal)	~18	8.8
21	Caen, Canada (2010-…)	44-64	4:1	32	0.6	2/10 (horizontal)	96	7-12 expected
22	Wainwright, Canada (2009-…)	-	-	25	0.5	13/24	-	-
23	Pelican Lake, Canada (2006-...)	165	4:1	13-25	-	-	90	25 expected
24	Mangala, India (2014-…)	28	10:1	15-20	~0.7	86/-	77	23
25	Abu Dhabi (2021-2022)	1.8	10:1	5.5	N/A	1/-	N/A	N/A
26	Nuraly (2014-2019)	0.7	30	6	0,153	4/22	81	
27	East-Moldabek, Kazakhstan (2019-…)	-	-	30	0.035	2/17	~85	5.7-7.7
28	Zaburunje, Kazakhstan (2014-…)	-	-	19	0.17	4/63	~90	2.3
29	Kalamkas, Kazakhstan (2014-…)	7	4:1	24	0.075	2/23	~90	9 (expected)

2.3 Chemical (ASP) flood risks and feasibility assessment

The alkali/surfactant/polymer injection was first invented in 1983 by Krumrin and Falcone in the laboratory to achieve the synergetic effect of the chemicals. After 10 years, in 1993, the first field-scale implementation was conducted in the West Kiehl Field, Wyoming, USA, reported by Clark et al. [118]. The pilot test was successful, leading to the production of 26% of original oil in place (OOIP) in 2.5 years. Later, other countries such as Canada, India, and Russia implemented field pilot tests. Finally, the largest field-scale implementations were started in China in 2014. According to Wang et al. [119], the widespread use of polymers in Chinese fields provided solid foundations for ASP flooding. This point of view was also supported by laboratory experiments conducted by Aitkulov et al. [120], which indicated more enhanced oil recovery of ASP after polymer flooding rather than after waterflooding.

The synergetic effect of ASP flooding is based on mechanisms induced by each of three chemicals: polymers, which create a stable piston-like displacement front; surfactants, which decrease interfacial tension (IFT) between oil and water; and alkalis, which mitigate surfactant adsorption and create in-situ soaps to decrease IFT.

These three mechanisms improve the ability of the oil to flow in porous media involving untouched zones of reservoir.

To better understand the effect of ASP on oil production growth, especially the mechanism underlying the surfactant-oil interaction, it is necessary to examine the main studies on microemulsion types [121; 122]. There are three types of microemulsions formed when oil and surfactant come into contact in the reservoir, based on Windor's [104] terminology. Thus, Type II (-), Type III, and Type II (+) have been detected depending on brine salinity level. These Windsor types can be well described by ternary diagrams. Type II (-) means a two-phase environment at low salinities where only water and oil are presented. Then, it moves to the Type III microemulsion at medium salinity where three phases exist in equilibrium: water, oil, and microemulsion (middle phase). Type III is the transitional stage from Type II (-) to Type II (+) or vice versa, where Type II (+) also has two phases, but at high salinity: water and microemulsion. Type II (-) and Type II (+) can coexist in the Type III environment since Nelson and Pope [122] did not observe type-to-type behaviour in EOR processes. In general, Type III is the most favorable condition for effective oil displacement in porous media since the pure oil phase and lowest IFT are achieved. Based on this theory and these processes, the evaluation of ASP formulation (phase behaviour tests) is conducted to reach successful ASP flooding projects. If the formulation fits reservoir conditions, over 20% of incremental oil recovery can be accomplished, which is almost two times greater than polymer flooding.

Although ASP flooding seems promising in the laboratory as a tertiary recovery method, field experience has revealed several complicating features of the technology. One of the main problems is a chemical cost, i.e., the surfactant is roughly 2 times more expensive than polymer (Table 2.4), and the consumption is 5 times more, resulting in a factor of 10 for cost. Another ASP flooding major problem is related to operational arrays [12; 13; 14; 15]. The scaling problem is the most common among ASP flood projects, and it creates the need to redesign surface facilities from ASP solution preparation units to production and processing units. Experience in China has shown that frequent pump failures have greatly shortened pump-checking time to tens of days [124]. Figure 2.4 represents some pictures of scaling accumulated on stators of progressing-cavity pumps (PCP) in the Daqing oilfield. ASP flooding in the Mangala field led to the impairment of the artificial lifting system. As a result, jet pumps were accepted as suitable instead electrical submersible pumps (ESP) [125]. The simple explanation for scale formation in the tubes is the significantly high pH level of the injected water, caused by the large amounts of alkali added [126]. Apart from reconsidering the artificial lift systems, it is also required to implement chemical techniques such as scale inhibitors and chemical-feeding systems [15], which certainly increases project operational costs.

Figure 2.4 — Scaling PCP rotors in Daqing ASP flooding area [105]

Another complicating feature during production can be viscous hard-to-break emulsions, as was observed in several pilots in China. Guo et al. [15] reported that the maximum emulsion viscosity of the produced fluid reached 487 cp during strong alkali injection (NaOH). Some cases show great emulsion viscosities which are 10 times greater than injected ASP solution. The authors acknowledge that the phenomenon is not well understood, but the presence of emulsions and their problems remain a fact. The main associated problem is the loss of production. Therefore, potential emulsification issues should be envisaged preliminary as it was done in the Bhagyam field having additional demulsifier injection wells near producers [12]. Also, Finol et al. [13] have reported preliminary laboratory experiments on identifying cost-effective demulsifiers in the designing stage of the Al Khalata pilot test.

Feasibility study on ASP flooding projects. According to Dean et al. [127], the development of ASP formulations and their implementation in the field/pilot units has two main objectives: 1) academic applications aiming at a better understanding of the mechanism, and 2) practical applications pursuing economic benefits through the production of incremental oil. Based on a number of publications that are describing any ASP technology implementation at a pilot scale, it is observed that the authors refrain from providing the economic performance of any given project. This is the main reason for the difficulty in determining the real purpose of ASP projects. Moreover, some projects were evaluated without considering capital and/or operating expenditures, i.e. only the benefit from incremental oil was estimated, and the proj'ct's profitability was not adequately assessed. Such cases can misrepresent the understanding of the economic feasibility of ASP flooding, which is critical due to its complexity and use of expensive chemicals.

This section focuses on the economic evaluation of ASP flooding projects conducted on Daqing (China) and Mangala (India) oilfields. It is worth noting that the economics of the projects have been evaluated based only on the data presented in the scientific articles of Gao et al. [128] and Pandey et al. [125]. Both projects were successful, providing additive oil recovery. Nevertheless, the economics behind them were not properly assessed. Therefore, the main question to answer is: does the extra oil produced by ASP flooding pay for itself?

Gao et al. [128] presented an ASP flooding project, which involved 16 injection and 25 production wells. Injection of the main ASP slug started in 2014 and by 2019 the accumulated oil increment was 0.647 million barrels which refers to 7.89% of

the incremental recovery. Considering the size of the pilot area and the number of wells involved, the complications of water treatment and production that are common in ASP projects, it can be assumed that the project does not achieve economic benefit. In evidence, the simplified feasibility study considering only the costs of chemicals as the main part of operational expenditures is presented in this section. The consumption of chemicals has been pre-compiled based on the given injected pore volumes and the slug formulations, and chemical prices have been taken as industry average prices. Thus, the following assumptions over prices were accepted (Table 2.4):

Table 2.4 — Chemical prices according to industry averages

Chemicals	USD/kg
Alkaline	0.65
Surfactant	7
Polymer	3.5

ASP project was held on the N3D block with an area of 0.49 km^2 and a pore volume of 1 798 200 m^3, which is located on the East side of the Daqing oilfield. According to Guo et al. [15], the chemical formulations of ASP floods in China were analyzed. The authors presented data on 27 ASP flooding projects with slug concentrations. From the data, the average concentrations of each slug were identified and fitted to the injection volumes of the N3D block (Table 2.5). Combining all this available information and correct calculations makes it easy for us to imagine the costs of this project. It is estimated that around $41 million was spent on chemicals only to provide such slug volumes (Table 2.6). The author states that the economic benefit of performed ASP project is $32.35 million (calculated at $50/bbl), which is about $10 million more than the chemical cost. It is important to note that apart from the cost of chemicals, nothing else has been taken into account, i.e. the actual cost of the project could be times higher with capital and other operating costs caused by different challenges.

Table 2.5 — Assumed design of Daqing ASP flooding [15; 128]

1st year		2nd -4th years		5th year		6th year		
Pre-Slug (polymer)		ASP Main Slug		ASP Vice Slug		Post-Slug (polymer)		Total injected
PV	Concentration, %	PV	Concentration, %	PV	Concentration, %	PV	Concentration, %	PV
0,2	0.14	0.505	0.3%S+1%A+0.18%P	0.21	0.1%S+1.2%A+0.16%P	0.18	0.12	1.0924

Table 2.6 — Cost of chemicals used in Daqing ASP pilot

Slug consequence	Chemicals	Injected weight, tonnes	Cost for chemicals, USD	Cost for chemicals over the pilot period, USD
Pre-Slug (polymer)	A	0	0	1 762 236
	S	0	0	
	P	503.50	1 762 236	
ASP Main Slug	A	9 080.91	5 902 592	30 693 476
	S	2 724.27	19 069 911	
	P	1 634.56	5 720 973	
ASP Vice Slug	A	4 479.68	2 911 789	7 615 449
	S	373.31	2 613 144	
	P	597.29	2 090 515	
Post-Slug (polymer)	A	0	0	1 357 929
	S	0	0	
	P	387.98	1 357 929	
Total				41 429 089

A similar approach was applied to evaluate an Indian ASP experience performed in the Mangala oilfield in 2014 [125]. The critical reason for evaluating its economic efficiency is the involved well locations. According to the authors, the ASP pilot project was carried out on a 5-spot pattern block with 4 injection wells and 1 production well, and an area of 10 000 m². The main reason to investigate this case is the well locations that lead to injected volume loss 3/4. It suggests that the crucial part of injected volume abandons outside of the well grid. Therefore, the economic effect is questionable, as the cost of chemicals for effective sweeping increases by a factor of 4.

As reported by Pandey et al. [129] at the design stage of the ASP pilot, the thickness of the pilot formation is 70 m with a net-to-gross of 40%. Considering the area of 10 000 m² and average porosity, the volume of pores is 70 000 m³. Later, after a technically successful pilot, the slug formulations were presented in 2016 (Table 2.7). Table 2.8 presents chemical cost estimation for each stage of ASP flooding at Mangala. Since the incremental oil reached 23 000 bbl, which the authors describe, the project will not be appropriate for returning investments spent even if the oil cost is 90 $/bbl. It should be noted that there was polymer flooding at the same pilot area for 3 years before the ASP flooding. The polymer slugs were graded, and the pilot performed well generating incremental oil, referring to 10-15% of STOIIP compared to waterflood [85]. Despite this fact, ASP flooding was technically justified, giving extra-incremental oil from the pilot area, but proved to be uneconomical.

Table 2.7 — Chemical slug compositions prepared in Mangala ASP pilot [125]

ASP Main Slug		Polymer Drive-1		Polymer Drive-2		Chase Water Drive	
PV	Concentration, %	PV	Concentration, %	PV	Concentration, %	PV	Concentration, %
0.5	0.3%S+3%A+0.25%P	0.3	1.5%A+0.23%P	0.2	1%A+0.2%P	0.1	1%A

Table 2.8 — Cost of chemicals used in Mangala ASP pilot

Slug consequence	Chemicals	Injected weight, tons	Cost for chemicals, USD	Cost for chemicals over the pilot period, USD
ASP Main Slug	A	1 050	682 500	1 638 000
	S	105	735 000	
	P	63	220 500	
Polymer Drive-1	A	315	204 750	373 800
	S	0	0	
	P	48.3	169 050	
Polymer Drive-2	A	140	91 000	189 000
	S	0	0	
	P	28	98 000	
Chase Water Drive	A	70	45 500	45 500
	S	0	0	
	P	0	0	
Total				2 246 300

ASP applicability studies on Kazakhstani fields. The previous section described the economic issues attributed to ASP flooding. Apart from this, the other critical property oil total acid number (TAN) for ASP applicability was studied. The high acidic constituents react with alkaline solutions to create in-situ surfactants [17]. Surfactants, for their part, obtain ultralow interfacial tension (IFT) between displacing agent and crude oil. Thus, several mechanisms are in place to enhance oil recovery. In the case of low TAN, alkalines may mitigate surfactant retention, which improves chemical consumption volumes.

In this regard, the TAN analysis of several Kazakhstan oilfields was carried out. The TAN analysis of the Mangistau (West Kazakhstan) oilfields, combined with actual ASP feasibility studies from other companies, argues that ASP is not a promising cEOR method for extending the life of brownfields (Table 2.9). According to Guo et al. [15], in 1987 the threshold value of the acid number for the effective reaction was considered 0.20 mg KOH/g, but then this number was reduced by several times, which can be noted in Table 2.9. Nevertheless, underestimating the importance of oil TAN, using highly reactive surfactants, is too risky because of production issues, such as scaling and hard-to-break emulsions. These problems, coupled with the expensive surfactant cost, only complicate and worsen the economics of projects.

Table 2.9 — TAN analysis of Mangistau oilfields in comparison with worldwide ASP projects

Oilfields	Oil TAN, mg KOH/g	ASP flood conducted	Incremental RF, %	Complications
Bhagyam, India [12]	2,00	Yes	20	Emulsion, scaling, corrosion
Al Khalata, Oman [13]	0,78	Yes	-	Emulsion, scaling
Karazhanbas, Kazakhstan	0,251	No	-	-
Kalamkas, Kazakhstan	0,132	No	-	-
Uzen, Kazakhstan	0,048	No	-	-
West Salym, Russia [14]	0,040	Yes	16	Scaling
Daqing, China [15]	0,020	Yes	>20	Emulsion, scaling, repairment of surface equipment

2.4 Chapter Conclusions

The goal of this chapter was to review important aspects and performances during polymer flooding. These aspects include reservoir conditions for effective implementation, polymer injection, and reservoir development parameters. The growing large-scale application polymer flooding demonstrates that it is the most feasible chemical EOR technology. In contrast, ASP/SP flood is not profitable and causes severe on-site problems. The primary novel finding from this review and analysis of field projects is to cast doubt on the economic feasibility of ASP flooding—especially in Kazakhstan. This work also provides a perspective on the TAN (total acid number) for Kazakhstan oilfields, especially for applicability to ASP flooding. Many insights into applicability of polymer flooding were also noted. In particular, the fact that HPAM prices are actually lower now than they were 40 years ago has greatly aided the ability for polymer flooding to be applied on a large scale today. The development of horizontal wells has greatly enhanced polymer injectivity and allowed the upper limit of oil viscosity for polymer flooding to be increased from ~150 cp to over 3000 cp. Controlled injection above the formation parting pressure has also played a major role in this regard. Until recently, commercially available EOR polymers were not sufficiently stable in reservoirs with temperatures exceeding ~70°C. However, the recent availabity of an ATBS polymer has the potential to allow feasible polymer flooding in reservoirs at temperatures up to 120°C. A major difference from waterflooding is that the dissolved oxygen level as close to zero as practical—certainly less than 200 parts per billion. Above 60°C, dissolved oxygen levels must be much closer to zero. In theory, polymer flooding can be applied in formations with any water salinity. However, practical considerations favor using the least saline water that is available. Field experience, as well as laboratory and theory, consistently reveal that the polymer bank size should be as large as practical (typically ~1 pore volume). Once injection is switched from polymer back to water injection, water cuts will quickly rise to high values. The vast majority of polymer floods have been applied in moderate-to-high permeabilty reservoirs (>100 md). This fact is due first to the need for high polymer injectivity and second because high-Mw polymers exhibit difficult in penetrating into less-permeability rock. However, Song et al. (2022) [50] showed promising laboratory results, where HPAM can effectively propagate through the tight low permeable (<50 md) carbonate rocks. The novel polymers can extend the minimum applicability range of permeability, and it has high relevance for future research & development.

3. FIELD DEMONSTRATION OF THE IMPACT OF FRACTURES ON HYDROLYZED POLYACRYLAMIDE INJECTIVITY, PROPAGATION AND DEGRADATION

3.1 Introduction

The investment in chemicals during a polymer flood can amount to tens of millions to hundreds of millions of dollars. Thus, any polymer degradation (and consequently reduced polymer solution viscosity) can incur a substantial cost. Mechanical and oxidative degradation are two major concerns during a polymer flood [31; 32; 104; 106; 108; 130; 131]. Straightforward calculations, coupled with laboratory results, reveals that mechanical degradation of HPAM (hydrolyzed polyacrylamide) polymers will be quite high during injection into unfractured vertical wells [104]. In contrast, if a fracture is open at the injection well, calculations suggest that the increased rock-face area associated with the fracture reduces fluid velocities to the point that mechanical degradation of HPAM is no longer a concern [104; 106]. (The fracture could be newly created, a previously induced hydraulic fracture, or an existing natural fracture.) A significant part of this chapter is dedicated to testing/confirming this prediction in a field application. This confirmation required developing a method to back-produce polymer solutions without inducing further mechanical or oxidative degradation. As will be revealed in our literature review, most previous attempts to collect polymer from a reservoir have induced substantial degradation during the sampling/measurement process. In contrast, our method is quick, simple, cheap, and reliable.

Previous calculations [52; 104; 109; 111] suggested that polymer injectivity into vertical wells would be unfeasible without open fractures. In contrast, others [26; 27; 28; 29] attempted to justify observed field polymer injectivities using controversial assumptions about HPAM rheology during radial flow (i.e., in unfractured vertical wells). This raises the question: "How do we know that we actually have a fracture intersecting our injection well?" In this chapter, this question will be answered using a combination of calculations, laboratory tests of polymer rheology in porous media, and field tests using pressure transient analysis and step-rate tests.

An additional benefit from this study was confirmation that contact of HPAM solutions with the reservoir rock promoted polymer stability by removing dissolved oxygen. As will be shown, solutions that were back-produced from the injection well and those that propagated from an injector to a producer (Chapter 4) contained dissolved oxygen levels that were substantially lower than those of injected fluids. This finding is consistent with known geochemistry and results from other field tests [31; 106].

3.2 Literature Review

Viscosity/molecular weight of produced polymer solutions. If polymer solutions are produced from reservoir production wells with no loss of viscosity or molecular weight, that knowledge could comfort the operator that the polymer did not deteriorate by any degradation mechanism. Several field applications attempted to quantify polymer degradation of produced fluids and suggested severe loss of polymer molecular weight. A sampling of production wells at Daqing revealed ~80% viscosity loss for HPAM after traveling ~800 ft through the Daqing sand at 45°C [19; 20; 106; 133]. After 2-3 years of residence time in the Daqing reservoir, You et al. (2007) [134] reported that polymer molecular weight decreased by 92% (from 19.8 million daltons to 0.89 million daltons), and the degree of hydrolysis increased from 28% to 36.2%. You et al. (2007) [134] also reported that HPAM molecular weight decreased by 77.2% (from 17.3 million daltons to 3.94 million daltons), and the degree of hydrolysis increased from 22.3% to 38.2% upon flowing through the Shengli reservoir (70°C, 2-3 years residence time). After transiting the Shuanghe (Henan) reservoir (70°C, 2-4 years residence time), You et al. (2007) [134] reported HPAM molecular weight decreased by 84.6% (from 15.2 million daltons to 2.35 million daltons), and the degree of hydrolysis increased from 23.7% to 59.5%. For HPAM produced from the Courtenay polymer flood (30°C), Putz et al. (1994) [135] noted that the HPAM lost about half of its viscosifying ability. Manichand et al. (2013) [106] reported that early efforts at characterization suggested an 83% decrease in polymer molecular weight after flow through the Tambaredjo field (Suriname, 38°C). These losses seemed excessive, considering the temperatures of the fields. Previous laboratory work indicated that HPAM solutions should be quite stable, considering the conditions present in most low-temperature reservoirs [31; 40; 136; 137]. So, the field observations are troubling since they raise questions about when and how polymer degradation occurred. If the polymer degraded during or shortly after injection, the polymer flood may not be viable. On the other hand, if degradation occurs at or near the production wells, the degradation has little or no negative impact. For the cases mentioned above where pessimistic assessments of polymer degradation were made, it is prudent to ask whether an improved sampling method might result in less observed degradation (i.e., more in line with the predictions made from laboratory results).

Fortunately, Manichand et al. (2013) [106] demonstrated that at least for the Suriname case, the observed degradation was an artifact of the method used to sample and measure the viscosities of the produced polymer solutions. This method used the traditional method of first flushing the sample cylinder from the bottom to the top and producing several cylinder volumes of fluid before closing the cylinder valves. However, in addition, after the cylinder arrived at the lab, a plastic attachment was placed at the bottom of the cup of the UL (ultra-low) adapter of the Brookfield viscometer. Tubing was connected from the bottom of the sample cylinder to this plastic attachment on the viscometer. Then nitrogen was introduced into the top of the sample cylinder to force the fluid sample into the viscometer cup.

The flow was allowed to overflow from the top of the viscometer cup to flush out all oxygen. After this fluid overflow showed undetectable dissolved oxygen, the viscometer was turned on to measure the viscosity of the anaerobic sample. Using this improved sample collection and analysis method, they proved that the HPAM solutions propagated through 330 ft of the Tamboredjo reservoir with no significant degradation. Their work confirmed that although polymer solutions may have high dissolved oxygen levels upon injection, iron minerals in the formation quickly removed that oxygen. Oxygen-free polymer solutions can then readily dissolve iron during propagation through the reservoir. This dissolved iron (Fe^{2+}) is not detrimental to the polymer so long as oxygen is not redissolved in the solution [32]. Thus, an effective sampling method must keep the sample anaerobic; otherwise, oxidation may mislead the operator that severe polymer degradation occurs. This is an important lesson that we incorporated in our methodology.

Laboratory assessment of mechanical degradation. Many laboratory methods were developed to predict mechanical degradation in tubing, the near-wellbore zone, and under reservoir conditions [28; 104; 106; 108; 130; 131; 138; 139; 140; 141; 142; 143]. A common feature of these methods is the determination of the viscosity of polymer solutions before and after the test. Tests were performed using field cores, sand-packs, outcrop cores, and blenders. These laboratory tests injected polymer solutions at different flow rates (flux or Darcy velocity) to model fluid velocities through perforations, the near wellbore, and within the reservoir. Assumptions made for different flow regimes (velocities) were often based on the Darcy radial-flow equation. In contrast, most of the worldwide polymer flood projects injection in vertical wells occurs above the formation parting pressure [52; 104; 112], where the linear flow was expected. (Here, in our terminology, "parting pressure" is simply the pressure at which a fracture or fracture-like feature opens. It may be the first time the fracture was created or alternatively that a fracture that was created previously but subsequently closed when the pressure was reduced.) To test and complement these ideas, there is considerable value in reviewing field experiments where polymer degradation was assessed directly using downhole sampling from a polymer injector [142; 144], samples collected from an observation well near the injector [145], or from a polymer production well [106].

Field assessment of mechanical degradation. Field operators in Austria [142], Angola [145], China [144], and Suriname [106] conducted field tests to assess polymer degradation near wellbore and deep in the formation by direct methods. These field cases used partially-hydrolyzed polyacrylamide, which is the same type of polymer used in the Kalamkas field.

In the Austrian field test, the injected polymer solution was back-produced using a swabbing unit. In addition, swabbing was performed after injection. The test results showed that molecular weight decreased from 20 MDalton to 8 MDalton (60% degradation).

The Dalia (offshore Angola) field test collected bottom-hole samples from a special observation well, which was drilled 80 m from a polymer injector. This observation well was located upstream of the polymer front (which was located

using 4D seismic monitoring). A Modular Dynamic Tester was tested onshore to confirm that the polymer solution did not suffer severe degradation during sampling. Based on onshore test results, the operator added precautions, such as using new valves, coated pipes (i.e., with Sulfinert™), flushing dead volumes with ultrapure nitrogen to remove oxygen, and careful flow rate control. The analyses of samples showed that the average degradation was 75% and polymer concentration was in the same range as the injected solution.

During a field test in China [144], downhole polymer solutions were recovered using coiled tubing and a nitrogen-assisted flow-back technique. Direct measurements of the concentration and viscosity revealed that the polymer solution was degraded, with the viscosity of the polymer reduced to one-third of injected value. Initial viscosity was 21.5 cp and, after flow-back from 0.24-m into the reservoir formation, was degraded to 7.7 cp.

The above field tests might be viewed as disheartening because so much polymer degradation was noted. However, one must ask whether the sampling method is the source of the apparent degradation. A field test in Suriname collected anaerobic polymer solution samples from production wells. Manichand et al. (2013) [106] using a simple sampling procedure that allows collection of polymer samples from a well, introduction into a Brookfield viscometer, and viscosity measurement – all under anaerobic conditions. Viscosity measurements of samples revealed that the polymer solution effectively propagated from an injector to a producer (~330 ft) with no significant degradation. In their case, based on analytical calculations, polymer solution injectivity was 61 times greater than expected for injection into an open-hole completion, and the fracture area was roughly 61 times greater than that associated with an open hole. This area equated to a fracture that extended radially 20 ft from the well. By increasing the sand-face area by a factor 61, the velocity when the polymer enters the formation is reduced in proportion, and as a consequence, the possibility of HPAM mechanical degradation is reduced.

Importance of fractures. Because of a fear that fractures might cause severe channeling, one might desire to inject polymer solutions under conditions where fractures are not open near an injection well. However, in vertical injection wells, simple Darcy-law calculations reveal that without open fractures, polymer injection below the formation parting pressure will reduce injectivity (relative to water injection) by at least 80% [104]. One can easily test this idea in any existing polymer flood field injector to prove its validity [19; 106; 52]. Consequently, it is commonly argued that all vertical polymer injection wells, and even most water injection wells have open fractures [104; 109; 111]. For horizontal wells, the necessity to inject polymer above the formation parting pressure is significantly less [104]. Nevertheless, horizontal wells may still intersect fractures or fracture-like features [104; 147]. For those cases, fluid flow profiles should be used to identify the location of the fracture-like feature—and consideration can be given to the value of plugging this feature (e.g., using a gel treatment [148]).

Alternative views of polymer injectivity and mechanical degradation. Much of the literature mentioned above argues that fractures or fracture-like features must

be open during most/all previous field polymer floods where polymer solutions were injected into vertical wells. At the heart of this argument is the observation in most/all previous field polymer floods that the injectivity during polymer injection was not substantially different than that during previous water injection [19; 20; 52; 104; 106; 111]. For example, suppose a 10-cp Newtonian polymer solution is injected into a vertical well with no fractures. In that case, the Darcy equation predicts substantially lower injectivity (e.g., perhaps, roughly 10 times lower) than 1-cp water—especially because viscous behavior near the wellbore dominates flow resistance during radial flow. However, contrasting viewpoints have been argued in the literature.

Delamaide (2019) [29] advocated an analytical method to estimate injectivity of HPAM solutions in vertical wells with no fractures. His model assumed shear-thinning rheology for HPAM solutions at near-wellbore velocities, which contradicts all experimental studies [104; 108; 130; 131; 141; 149; 150; 151]. Thus, this model appears to use two opposing incorrect assumptions (i.e., no fractures and no shear-thickening behavior at high velocities) in an attempt to match observed field injectivities. Even with these assumptions, the author had difficulty matching observed field injectivities.

Skauge et al. (2016) [27] performed radial and linear core floods with HPAM solutions. They advocated that transient phenomena during radial flow caused substantial differences in polymer rheology in porous media that were not consistent with observations during linear flow. They suggested that these differences might explain why injectivities during polymer injection during field applications were not much lower than those during water injection. However, no calculations or analyses were performed to examine whether this suggestion was possible. In their work, throughout the full range of examined fluid velocities (0.01 to 40 ft/d), the apparent viscosity never fell below 80 cp. Thus, the injectivity loss could not be less than that of a 80-cp Newtonian fluid [104]. Consequently, Skauge et al. (2016) [27] arguments can not quantitatively rationalize observed field injectivities as similar to water.

Asen et al. (2019) [28] argued that mechanical degradation of HPAM solutions in linear flow was significantly overestimated compared to that in radial flow. They predicted this result because during many cycles of injection of a single HPAM solution and re-injection into a linear core at a fixed velocity, they observed additional degradation during each cycle. They advocated that HPAM mechanical degradation would continue through up to 20 meters during linear flow in porous media. In contrast, all other previous researchers [108; 130; 131] consistently reported that HPAM mechanical degradation in linear flow was stabilized within 1-cm after entering the porous media. Close examination of the work of Asen et al. suggests that their extended degradation results were due to oxidative degradation that occurred between each cycle of HPAM re-injection. Whether or not the results of Asen et al. are accepted, all authors agree that HPAM that passed the sandface in radial flow would retain a significant resistance factor (e.g., 10 or greater for most practical HPAM solutions). Straightforward Darcy flow calculations consistently

reveal that such polymer solutions would cause injectivity reductions (relative to water) of at least 80% in radial flow [104; 131].

Lottollahi et al. (2016) [152] performed a "mechanistic simulation" of polymer injectivity associated with selected field tests. Their model purported to include shear-thickening/viscoelastic behavior of HPAM solutions, shear-thinning at low rates, presence of "junk" (undissolved particulates) in the polymer, polymer retention, and permeability reduction effects, but did not include the presence of fractures or fracture-like features (i.e., the radial flow was assumed around vertical polymer injection wells). The absence of fractures was assumed in the simulation, despite literature stating fractures were present in the modeled field (Matzen, Austria) and also despite a substantial initial water saturation (50%) and water breakthrough noted in the field. The work of Lottollahi et al. predicted very modest injectivity declines (no more than 50%) even for cases where the injected polymer viscosity was 10-100 cp and the polymer penetrated substantial fractions of the distance between injectors and producers. These predictions appear to be a strong violation of the Darcy equation, and the apparent contradictions were not addressed in the paper. One would have expected "mechanistic simulations" to explain such surprising results. "Black-box" predictions from a simulator are difficult to understand without first benchmarking against basic physics and common sense.

Tai et al. (2021) [153] provided an improved method for calculating pressures in vertical polymer injection wells during simulations. They acknowledged that fractures might cause enhanced polymer injectivity. However, they pointed out that the concept of "pressure-equivalent radius" was commonly used to characterize bottom-hole pressures and injectivities during simulations. In effect, the gridblock that contains the vertical injection well is assumed to contain a much larger effective wellbore radius than actually exists in any unfractured open-hole completion. This procedure substantially increases the sandface area available to polymer entry into the porous medium—just as a fracture would. We respect this approach for accommodating observed injectivities during simulations. However, since the procedure assumes a circular "wellbore", it does not account for the directional nature of fractures and fracture growth.

Perhaps the great lengths that some have taken to deny the presence of fractures during polymer injection into vertical wells stem from government regulatory policies to "stay below the fracture or parting pressure during injection." These policies were understandably implemented to prevent fractures from developing that caused either severe channeling between injectors and producers or flow "out of zone" (i.e., breaking through flow barriers above or below the target formation). In the present paper and work, rather than to deny the presence of fractures, our approach is to accept and take advantage of the fact that fractures can have a very beneficial effect on injectivity, sweep improvement, and reduction of mechanical degradation during HPAM injection into vertical wells [52]—if the fractures do not extend too far to cause channeling problems.

One could argue that the most definitive way to establish that open fractures were responsible for mitigating HPAM mechanical degradation during a field project is

to compare viscosities of back-produced solutions while injecting polymer below the formation parting pressure versus above the parting pressure. Unfortunately, this suggestion is not practical in a real field setting, because the rates and injectivities are prohibitively low when the fractures (or fracture-like features) are not open during polymer injection into vertical wells. We have consciously looked for such a case throughout the literature and in discussions with field operators over the past 43 years—and have found none.

3.3 Methods, procedures, equipment

Injector back-produced sampling. At the Kalamkas field, a special scheme (Figure 3.2) and procedure were developed to gather back-produced samples at the wellhead of polymer Injectors 20XX, XX24 and XX41, and assess in-situ polymer mechanical degradation. The polymer injectors geological and technical information are shown in Table 3.1. A dedicated process pipe was installed for connection to a mobile pump unit. The sampling procedure operated as follows. First, after stopping the polymer injection unit, close all valves at the wellhead. Subsequently, open the sampler to decrease pressure between the check and wing valve. Then connect the mobile pump unit and the pressurized cylinder to the sampler. At this stage, the well is ready for back-flow sampling. Further, open required valves and allow polymer back-flow through the measuring tank of the mobile pump unit. Then, collect samples and change cylinders when certain volumes of polymer solution are reached. Sampling should be carried out with sufficient flushing of the cylinders (3-5 volumes of the cylinder) with the polymer solution to prevent air from entering the sample.

After collecting samples, immediately transport the pressurized cylinders to the field lab to measure viscosity, using a high-precision rheometer (Anton Paar MCR 502) and aerobic conditions. Because the field laboratory does not have a glove box that provides oxygen-free conditions, polymer solutions must be tested immediately (i.e., within 10-15 minutes after collection in the pressurized cylinder).

Measurement of viscosity of each sample should be repeated twice and averaged under conditions of minimal divergence. If the values are not similar, the measurement should be repeated. Test conditions: shear rate 7.34 s^{-1} at room temperature (~25°C). The use of a shear rate 7.34 s^{-1} is commonly used as a standard single-point for comparison of viscosities for non-Newtonian enhanced oil recovery fluids (2; 52; 106; 141). The test temperature of ~25°C is convenient and reasonably close to the reservoir temperature (40°C). The viscosity ratio at ~25°C (room condition) to that at 40°C (reservoir condition) is roughly equal to 0.85, i.e., if the test temperature increases from room to reservoir temperature, polymer solution viscosity simply decreases 15%. Because most liquids (including polymer solution) are incompressible at low or medium pressures, a considerable change in pressure from 14.5 to 4350 psi causes no significant change in viscosity [154]. Therefore, the reservoir pressure condition for polymer solution viscosity measurement is not essential.

This test procedure was carried out during planned repair work of the polymer injection unit. Consequently, the test did not affect the injection unit uptime. Also, the test has a low cost and can be done in a short time (< 6 hours).

The new method to evaluate polymer mechanical degradation was tested in Injection Well 20XX of the West Pilot area and Injection Wells XX24, XX41, XX37 of the East Extension area (Figure 3.1).
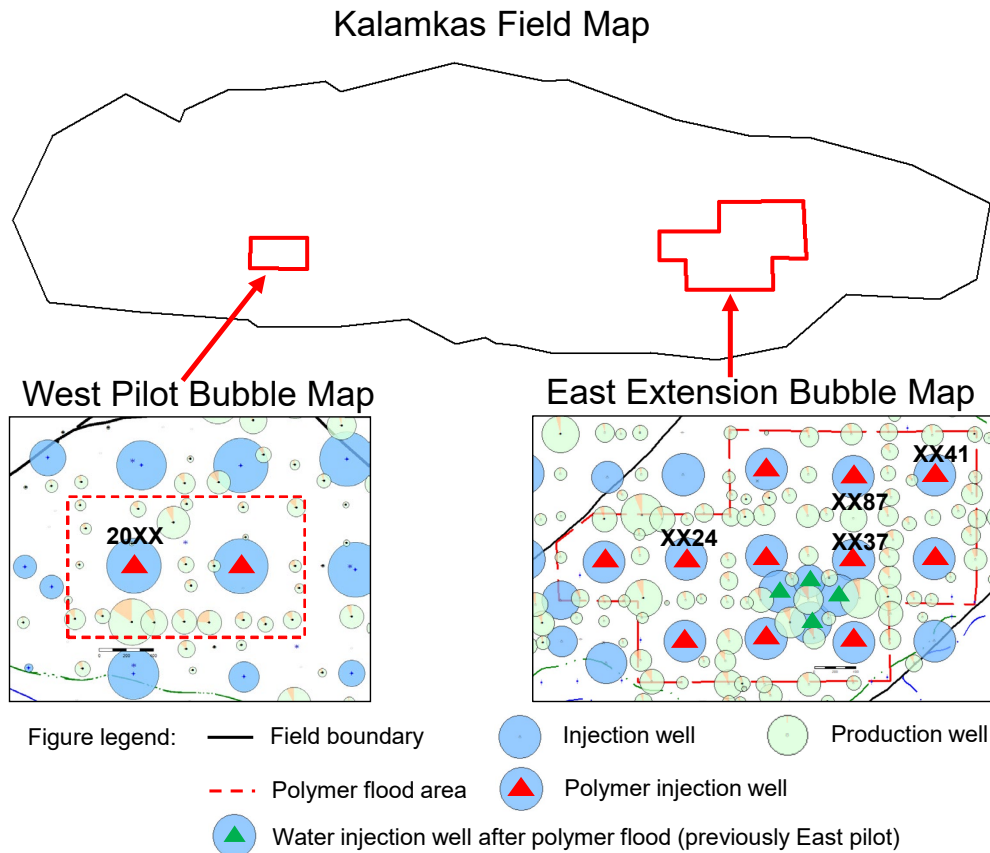
Figure 3.1 — Polymer flood project locations in the Kalamkas field.

Estimated depths (Dsample) away from the wellbore of the collected samples were calculated based on three equations with different assumptions: Eq. 3.1 is based on the radial flow geometrical calculation; Eq. 3.2 is based on Eq. 3.1 and additionally considering connate water (S_{wc}) and residual oil saturation (S_{or}); Eq. 3.3 is based on fracture flow geometrical calculations:

$$Dsample = 100 \text{x} \sqrt{\left(\frac{Vp - Vtubing - Vcasing}{\pi \cdot h \cdot \emptyset}\right)} \dots\dots\dots\dots\dots\dots\dots\dots\dots\dots\dots\dots(3.1)$$

$$Dsample = 100 \text{x} \sqrt{\left(\frac{Vp - Vtubing - Vcasing}{(1 - Swc - Sor) \cdot \pi \cdot h \cdot \emptyset}\right)} \dots\dots\dots\dots\dots\dots\dots\dots\dots\dots(3.2)$$

$$Dsample = 100 \text{x} \left(\frac{Vp - Vtubing - Vcasing}{2 \cdot w \cdot h}\right) \dots\dots\dots\dots\dots\dots\dots\dots\dots\dots\dots(3.3)$$

Estimated depths for different assumptions (equations) and detailed injection wells information are shown in Table 3.1. Note that no matter which equation is

applied, the calculations reveal that the back-produced volume from the injection wells was large enough to gather samples that were previously within the formation.

Table 3.1 — Wells' detailed information and the sample depth estimation for different assumptions (equations)

| Parameters	Well XX24	Well XX41	Well 20XX
Tubing length (MD), m	775	780.05	735.06
Formation top (MD), m	780	804	795
Inner Diameter of Tubing, m	0.062	0.0503	0.062
Inner Diameter of Casing, m	0.14	0.0995	0.14
Perforated reservoir thickness (h), m	10	8.5	10
Porosity (ø), unit fraction	0.29	0.29	0.31
Swc, unit fraction	0.2	0.2	0.2
Sor, unit fraction	0.3	0.3	0.3
w, m	0.00381	0.00381	0.00381
Vtubing	2.340	1.550	2.228
Vcasing	0.077	0.186	0.877
Vp	4	7.2	12
Vf	1.583	5.464	8.895
Deepest Dsample (1), cm	42	84	146
Deepest Dsample (2), cm	59	119	207
Deepest Dsample (3), cm	2078	8436	27422
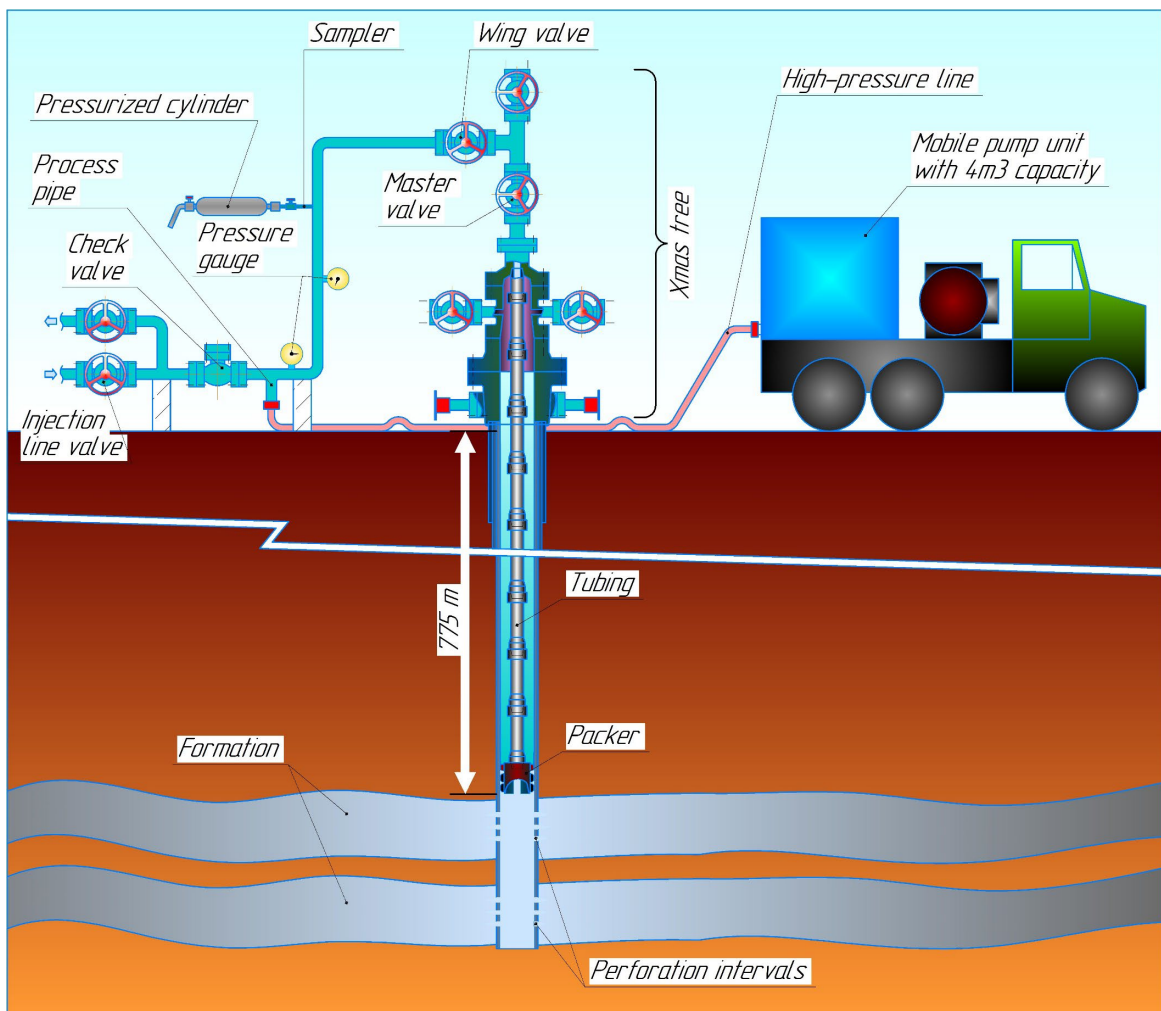
Figure 3.2 — Scheme to collect back-produced polymer solutions from Injector XX24.

Polymer-solution sampling used a pressurized cylinder. The pressurized cylinders and collection procedure were specially designed for the polymer flood project to protect the solution from oxidative degradation [106; 139]. These cylinders are made of stainless steel and coated with an inert material to prevent corrosion and any iron contamination. Oxygen can be effectively excluded by carefully flushing air from the cylinder with polymer solution while collecting the sample.

Overall, the above methods, processes, and special surface equipment schemes to assess polymer solution mechanical degradation are quick, simple, cheap, and (most importantly) reliable. They were considerably easier and perhaps more reliable than those described in some other field tests [142; 144; 145]. Based on these other field tests where substantial degradation was observed, one could argue that our methods are more reliable since they revealed only minor mechanical and/or oxidative degradation of HPAM samples and since laboratory and theoretical findings suggested that degradation should not have occurred under the conditions of the other field tests.
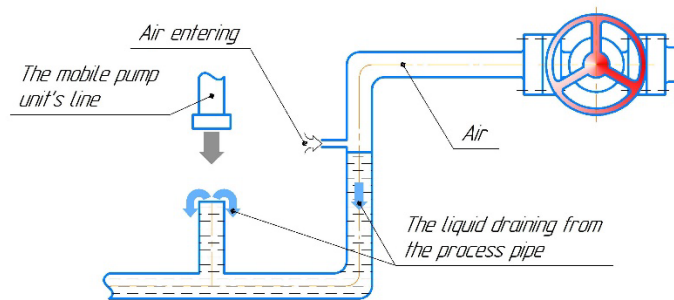
3.4 Field test results and discussion

Injector back-produced sampling. Our method for collecting back-produced HPAM solution samples was applied in three polymer injection wells: XX24, XX41, and 20XX. The first two applications allowed us to perfect the technique, while the third (in Well 20XX) was most successful and definitive. In each case, 6-7 samples were collected as the injection well was depressurized and flowed-back. The starting and ending wellhead pressures were 696 and 145 psi for Well XX24, 465 and 392 psi for Well XX41, and 640 and 162 psi for Well 20XX, respectively. The total volumes of back-produced fluid were 4 m^3 for Well XX24, 7.2 m^3 for Well XX41, and 24 m^3 for Well 20XX. The maximum distance of sample penetration of fluid radially into the formation (as estimated using the radial flow equation, Eq. 1) was 42 cm for Well XX24, 83.5 cm for Well XX41, and 146 cm for Well 20XX. Table 3.2 lists results for the third and most successful test (in Well 20XX).

For our first attempt using the procedure (in Well XX24), most of the back-flowed samples contained suspended solids—apparently, because depressurization dislodged some loose sand from the formation. Viscosities on these samples were measured both before and after filtration to remove the suspended solids. Filtration caused a very little reduction in viscosity, indicating that the suspended solids did not strongly affect the viscosity measurements. After filtration, the last six of the seven samples collected (representing fluid origins from 10 to 42-cm into the formation sand) experienced viscosities no lower than the injected polymer solution. The exception was that the first sample was collected after 1.2 m^3 of back-flow. This sample originated from 390 m along the tubing (about the middle of the total tubing length) and exhibited 32% lower viscosity than the originally injected fluid. We suspect that this viscosity loss was due to oxidative degradation because some air leaked into the piping during the process of setting up our collection system.

In the second test (in Well XX41), the first five (of six total) back-produced polymer samples exhibited viscosity losses ranging from 50-75% of original viscosity. This case particularly introduced a significant amount of air while preparing for the test. Specifically, the air was introduced when the sample cylinder was (see Figure 3.3) added/connected between the check valve and the wing valve (which required depressurization of the system). The air subsequently contributed to oxidative degradation, as seen in the first five back-produced samples. In contrast, the sixth and final sample collected (after 7.2 m^3 of flow-back and originating from an estimated 83.5 cm into the formation) exhibited no viscosity loss relative to the injected polymer solution.
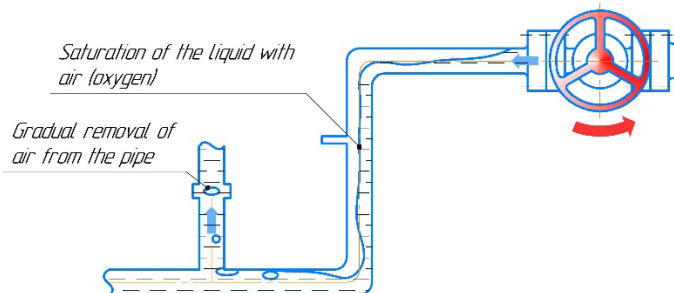

Figure 3.3 — Illustration of air (oxygen) entering the pipe and its influence during the test

The test results from Wells XX24 and XX41 revealed that samples recovered relatively early in the sample-recovery process experienced some level of oxidative degradation. Therefore, we prepared a special adapter and improved our sampling method. In this improvement, this adapter was connected to the top valve (Figure 3.4), thereby preventing oxygen from entering the pipe and wellbore space. To confirm this improvement, we measured dissolved oxygen levels throughout the testing procedure.

For Well 20XX, the planned back-produced volume was increased to 24 m^3 (3 times more than previous tests). The beginning wellhead pressure was 640 psi and the test-ending pressure was 162 psi.
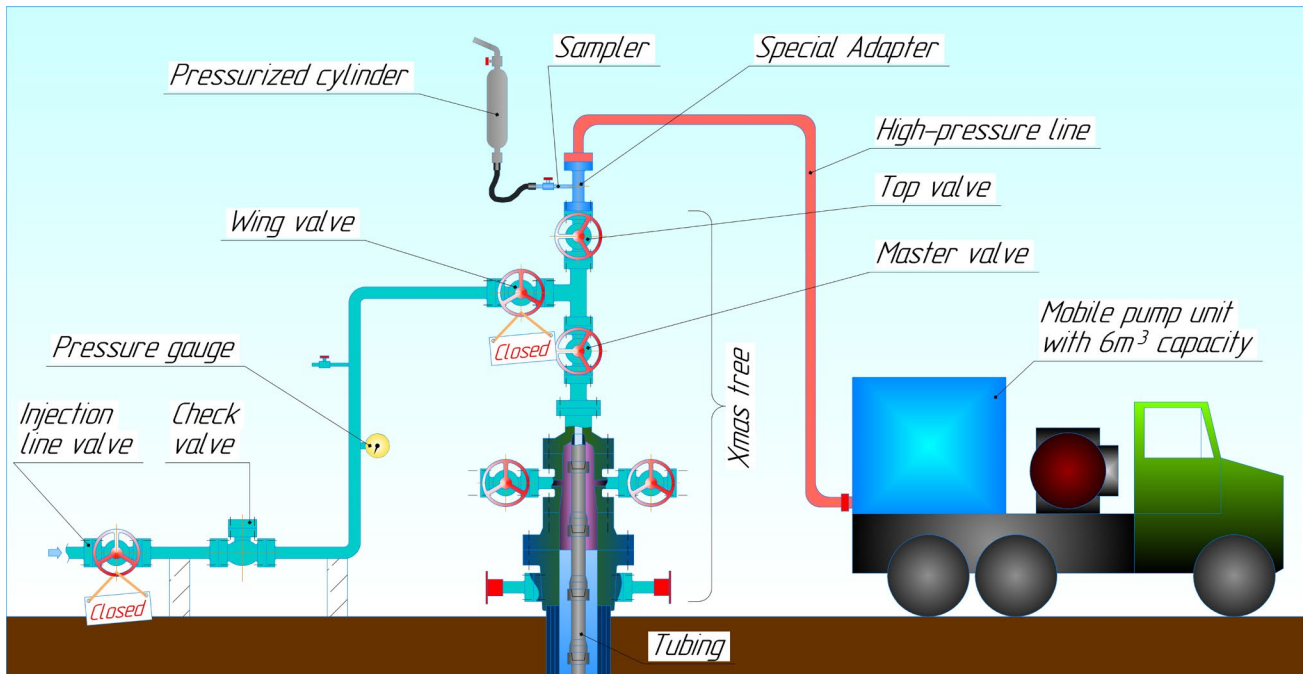
Figure 3.4 — The improved scheme to collect back-produced polymer solutions from Injector 20XX.

Back-produced sampling for Well 20XX occurred on 24th August of 2021. During the test, six samples were collected, including the first sample at the wellhead as a base sample. The typical surface temperature was 33ºC during the collection.

Table 3.2 — Rheology measurements of the back-produced polymer solution from Injector 20XX

No. cylinder	Back-produced volume at the measuring tank, m³	The estimated location of the collected sample	Loss of viscosity	Dissolved O₂ concentration, ppm
1	0	wellhead (initial viscosity)	0%	0.2-0.3
2	8	71 cm away from the wellbore	8%	0
3	12	96 cm away from the wellbore	0%	0
4	16	115 cm away from the wellbore	0%	0
5	20	132 cm away from the wellbore	0%	0
6	24	146 cm away from the wellbore	0%	0
[1](API RP 63 1990)				
The distance away from the wellbore calculated based on Eq. (1)				

Well 20XX wellhead injected initial viscosity was 15.7 cp. The samples of the back-produced polymer solution (Table 3.2) did not suffer oxidative degradation, except a minor viscosity loss of 8% for Sample No. 2. This small viscosity loss may have been associated with a small amount of oxidation because of the 0.2-0.3 ppm oxygen that was injected. The first sample from the wellhead showed 0.2-0.3 ppm dissolved oxygen, and other samples from the formation contained no detectable dissolved oxygen—thus, demonstrating the effectiveness of our improved sample-collection method. Polymer solution Samples No. 2 to 6 that temporarily penetrated a few meters into the formation were depleted of dissolved oxygen, even though injected solutions contained 0.2-0.3 ppm oxygen. Presumably, the 2-4%-iron mineral content of the reservoir rock caused this oxygen depletion. Even though this process added dissolved iron to the solutions, the HPAM did not degrade so long as

the dissolved oxygen level remained low. To our knowledge, this is the first time that back-produced HPAM samples from an injection well have been demonstrated to contain no dissolved oxygen.

Overall, rheology measurements demonstrated the absence of polymer solution mechanical degradation during polymer injection in Wells 20XX, XX24 and XX41.

Figure 3.5 plots flux versus distance from the wellbore dependence for Injectors 20XX, XX24 and XX41. This calculation was based on Eq. 3.4 and specific conditions of the injection wells (Table 3.3). (In this case, the flux is defined as a ratio of injection rate to radial flow filtration area.)

$$\text{Flux} = 3.28084 \text{x} \left(\frac{\text{Injection rate}}{2 \cdot \pi \cdot R \cdot h} \right) \dots\dots\dots\dots\dots\dots\dots\dots\dots\dots\dots(3.4)$$

where, Flux = ft/d;

3.28084 = multiplier to convert meters to feet;

Injection rate = m^3/d;

$2 \cdot \pi \cdot R \cdot h$ = the filtration area based on a radial flow, m^2;

R = distance from the wellbore, m;

h = perforation thickness, m.

Table 3.3 — Injection conditions for Wells 20XX, XX24 and XX41

Parameters	Well XX24	Well XX41	Well 20XX
Injection rate, m^3/d	400	295	326
Perforation thickness, m	10	8,5	10
Distance from the wellbore, m	0.10 – 0.42	0.086 – 0.835	0.71-1.46
Calculation assumptions	Open hole with no fracture present		

Calculations using Eq. 3.4 assume an open hole completion (i.e., assuming no fracture was present), so a certain distance (radius) from the wellbore corresponded to the estimated depth of collected samples (based on Eq. 1). In Figure 3.5, Sample No. 3 for Well XX24 and No. 4 for Well XX41 exhibited the highest flux (>200 ft/d). Of course, flux decreased with increased distance (radius) from the wellbore. Sample No. 6 for Well 20XX exhibited the lowest flux (~12 ft/d). Based on our laboratory experiments in a 769 md Kalamkas reservoir core for 1800 ppm R-1 HPAM polymer in Cretaceous formation brine (10.9% TDS), and consistent with other analog works [104; 130], mechanical degradation occurs at a flux higher than 5 ft/d. Those results suggest that for polymer injection wells, such as 20XX, XX24 and XX41, if injection occurs without open fractures, polymer solutions should exhibit substantial mechanical degradation. In contrast, our rheology study of formation samples revealed that the polymer solution did not exhibit mechanical degradation. This confirms that those injectors have open fractures with a high injection area which allows flux to be lower than 5 ft/d.
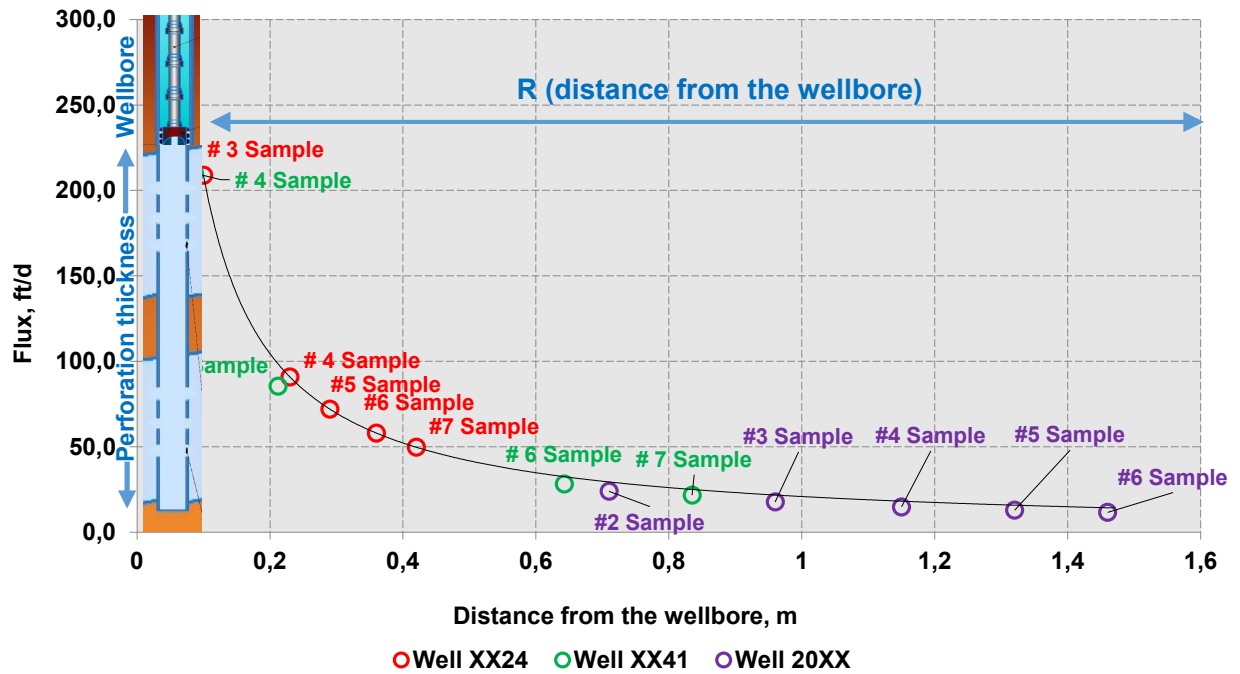
Figure 3.5 — Flux versus distance from the wellbore, Well XX24 and XX41.

Pressure fall-off tests. To obtain valuable well test data, we ran pressure fall-off tests in injection wells. These tests were perfomed during polymer injection for Wells XX24, XX41, 20XX and XX37 in 2020 and during the water flood in 2019, except Wells 20XX and XX37 (well tests not conducted). For Wells XX24 and XX41, two combined pressure transient analyses are presented in Figure 3.6 and Figure 3.7, and their interpretations are in Table 3.4 and Table 3.5. For Well XX37, pressure fall-off test analysis during polymer injection is presented in Figure 3.8 and Table 3.6. For Well 20XX, pressure fall-off test analysis during polymer injection is presented in Figure 3.9 and Table 3.7. The pressure transient analysis includes plotting pressure versus time and the Bourdet derivative on a log-log scale (based on [156]). Comparison and analysis of two pressure curves (original and derivative) for each flood can reveal signatures of numerous well, reservoir, and boundary behaviors. In our case, the analyses of pressure fall-off tests indicated the absence of fractures during water flood (green curves), but during the polymer flood (red curves), injection occurred above the formation parting pressure. The fracture half-lengths for Wells 20XX, XX24 and XX41 were about 100 m. For Well XX37, where severe channeling and polymer breakthrough was observed, fracture half-length was close to the well spacing. We can see that polymer injection leads to natural well stimulation and as a consequence, the polymer solution flows through the perforations and near wellbore zone with an area high enough to ensure mechanical stability of the solution. If Wells 20XX, XX24, XX41 and XX37 were not fractured, injection of viscous polymer solution would necessarily decrease injectivity, roughly in proportion to the polymer solution viscosity [104; 106]. In our case, the expected injectivity without open fractures would be 16 times lower than that for water. But in fact, our injectivity was enhanced by a factor from 1.3-2.1.
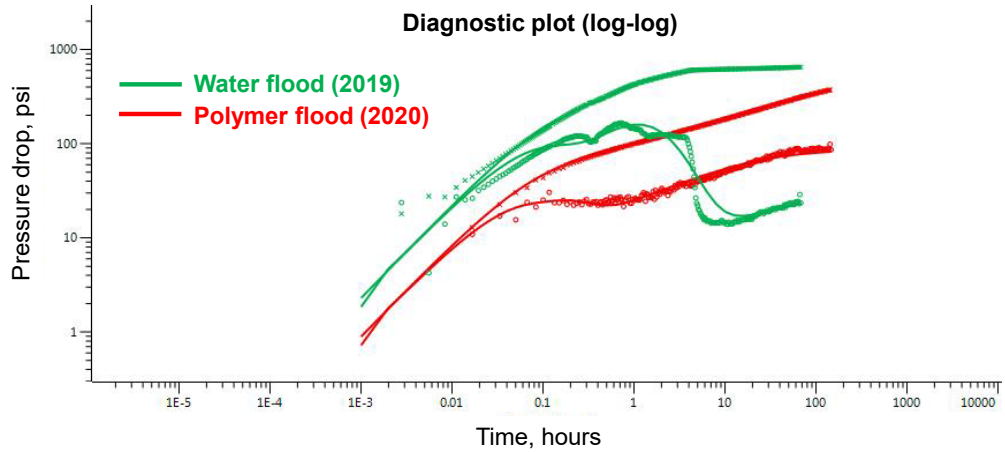
Figure 3.6 — Analysis of pressure fall-off tests during water and polymer injection into Well XX24.

Table 3.4 — Analysis of pressure fall-off tests during water and polymer injection into Well XX24

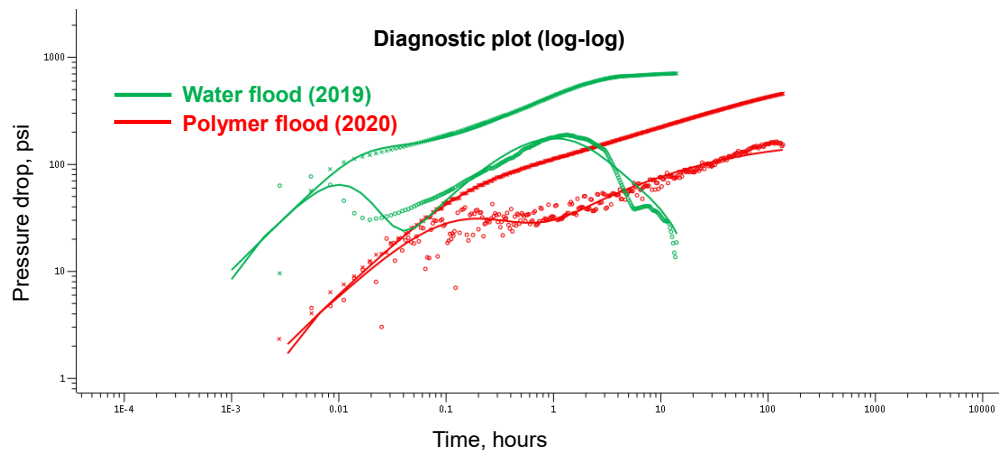| No.	Parameter	Value	
		During water flood (2019)	During polymer flood (2020)
1	Perforation interval, Top-Bottom	780-805 m	780-805 m
2	Test duration, hours	69.2	146
3	Wellbore storage (WBS) model	Changing WBS	Changing WBS
4	Well model	Vertical	Vertical fractured finite conductivity
5	Reservoir model	Homogenous	Homogenous
6	Boundary model	One fault	Infinite
7	Reservoir pressure, psi	1075	1270
8	Conductivity, mD·m	3 764	8 596
9	Average permeability, mD	362	860
10	Total skin	13.4	-5.8
11	Geometrical skin	-	-6.1
12	Fracture half length, m	-	101.0
13	Fracture conductivity, mD·m	-	7.93E+6
14	Fracture permeability, mD	-	39 292
15	Injectivity index, bbl/(d·psi)	3.17	6.62

Figure 3.7 — Analysis of pressure fall-off tests during water and polymer injection into Well XX41.

Table 3.5 — Analysis of pressure fall-off tests during water and polymer injection into Well XX41

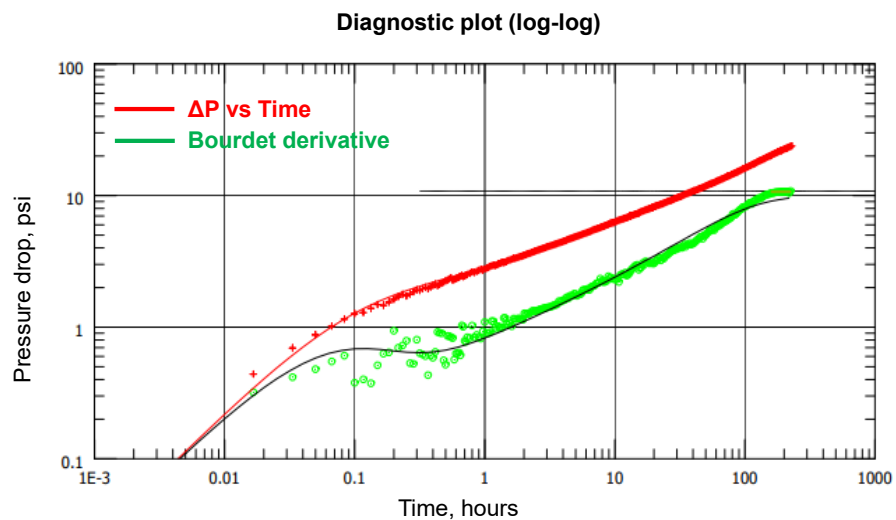| No.	Parameter	Value	
		During water flood (2019)	During polymer flood (2020)
1	Perforation interval, Top-Bottom	804-807, 810-812, 813.5-817 m	804-807, 810-812, 813.5-817 m
2	Test duration, hours	71.8	140.9
3	Wellbore storage (WBS) model	Changing WBS	Changing WBS
4	Well model	Vertical	Vertical fractured finite conductivity
5	Reservoir model	Homogenous	Homogenous
6	Boundary model	Circle (Re-P-const)	Infinite
7	Bottomhole pressure, psi	1822	1874
8	Conductivity, mD·m	972	3 604
9	Average permeability, mD	135	424
10	Total skin	1.46	-5.9
11	Geometrical skin	-	-6.0
12	Fracture half length, m	-	102.3
13	Fracture conductivity, mD·m	-	4.45E+6
14	Fracture permeability, mD	-	2 174
15	Injectivity index, bbl/(d·psi)	2.08	3.77

Figure 3.8 — Analysis of pressure fall-off test during polymer injection into Well XX37.

Table 3.6 — Analysis of pressure fall-off test during polymer injection into Well XX37

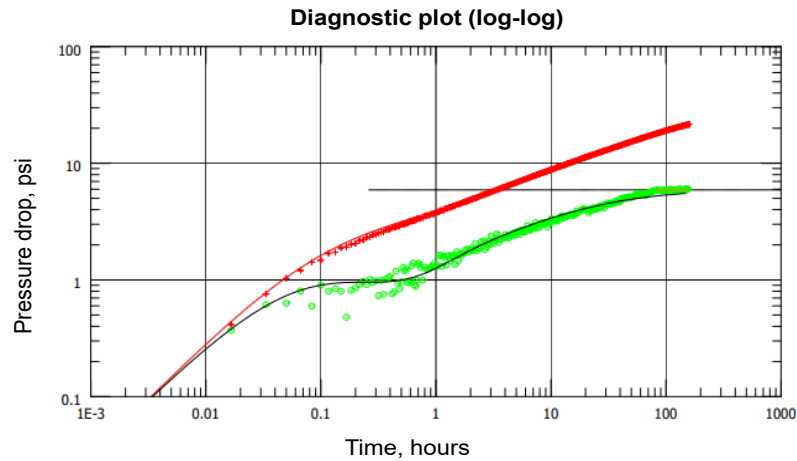| No.	Parameter	Value	
		During polymer flood (2020)	During water flood (2018)
1	Perforation interval, Top-Bottom	806-810, 812.5-820.5 m	806-810, 812.5-820.5 m
2	Test duration, hours	233.6	
3	Wellbore storage (WBS) model	Changing WBS	
4	Well model	Vertical fractured finite conductivity	
5	Reservoir model	Homogenous	
6	Boundary model	Infinite	
7	Reservoir pressure, psi	1252	N/A
8	Conductivity, mD·m	5 630	
9	Average permeability, mD	503.1	
10	Total skin	-7.13	
11	Geometrical skin	0.1	
12	Fracture half length, m	308	
13	Fracture conductivity, mD·m	0.384E+6	
14	Fracture permeability, mD	623	
15	Injectivity index, bbl/(d·psi)	2.47	1.86

Figure 3.9 — Analysis of pressure fall-off test during polymer injection into Well 20XX.

Table 3.7 — Analysis of pressure fall-off test during polymer injection into Well 20XX

No.	Parameter	Value	
		During polymer flood (2020)	During water flood (2014)
1	Perforation interval, Top-Bottom	795-826 m	795-826 m
2	Test duration, hours	163.5	
3	Well model	Vertical fractured finite conductivity	
4	Reservoir model	Homogenous	
5	Boundary model	Infinite	
6	Reservoir pressure, psi	1099	
7	BHP, psi	1794	N/A
8	Conductivity, mD·m	1 260	
9	Average permeability, mD	440.5	
10	Total skin	-6.16	
11	Geometrical skin	0.12	
12	Fracture half length, m	116	
13	Fracture conductivity, mD·m	0.1E+6	
14	Injectivity index, bbl/(d·psi)	3.86	2.21

Step-rate tests. To evaluate and confirm obtained results from pressure fall-off tests, we ran step-rate tests in water and polymer injection wells. These tests were performed at Polymer Injectors XX24 and XX41, and at Water Injector XX47, which is an offset well for polymer injectors, so it has the same reservoir characteristics (formation height, layering, permeability) and technical conditions (perforation intervals, injection rate, number of surrounded production wells, voidage replacement ratio, well spacing). Figure 3.10 plots injection rate vs. pressure drop for Wells XX24, XX41, and XX47. Step rate tests results and analysis are in Table 3.8.

The step rate test was performed as follows. First, the injector current operating flow rate and wellhead pressure were measured. Next, we decreased the injection rate to the next step and allowed pressures to stabilize, and wellhead pressure was determined again. This process was repeated in stages to determine the wellhead pressures at lower flow rates. Then we converted wellhead pressures to the well flowing bottom hole pressures (BHP) and the reservoir pressure was determined by extrapolating the inflow performance relationship (IPR) curve to zero flow rate. Finally, we plotted flow rate and pressure drop associated with solid circles for Water Injector XX47, solid triangles for Polymer Injector XX41, and solid squares for Polymer Injector XX24. The resulting dashed lines are IPRs, and their slopes (a multiplier of "x" variable in the linear equation) are injectivity indexes. For the water injector, the flow rate was controlled by the choke. In contrast, for the polymer injector flow rate control was achieved by reducing the engine speed of individual plunger pumps. A flow rate of 144 m^3/d was the lowest operating rate and 400 m^3/d was the highest technical flow rate for an individual plunger pump within the polymer injection system.

Comparison and analysis of IPRs during water and polymer injection confirms pressure fall-off test analysis that the injectivity index during polymer injection was much higher than during waterflood. The step rate test showed enhanced injectivity during the polymer flood relative to waterflooding (i.e., roughly 4 times greater than expected). Previous work has shown that viscoelastic (or shear thickening) behavior of HPAM polymers occurs at high fluxes, and as a consequence induces a fracture to form and extend in the well [109].

The presence of fractures during the polymer flood is consistent with the fact that most of the worldwide polymer flood projects inject into vertical wells above the formation parting pressure [52; 104; 111; 112], where linear flow is expected. In contrast, if fractures or fracture-like features are not present during polymer injection, achieving a favorable economical injection rate and acceptable voidage replacement ratio (e.g., the same as during a waterflood) is not practical. Additionally, according to the analytical calculations of Seright (2017) [52] and the work of Dyes et al. (1958) [157], fractures may not seriously affect a sweep efficiency if the fracture half-length is less than 1/3 of the well spacing. These findings reveal that the advantages of fracture features during polymer flooding (i.e., little or no injectivity loss and mechanical stability of the polymer solution) outweigh its disadvantages (e.g., possible severe channeling, jeopardized sweep efficiency).

Table 3.8 — Analysis of pressure step rate tests during water and polymer injection into Wells XX47, XX24, and XX41

| # Step	Injection Rate (bbl/d)	Water Injector XX47			Polymer Injector XX24			Polymer Injector XX41		
		Pwellhead (psi)	BHP (psi)	dP (psi)	Pwellhead (psi)	BHP (psi)	dP (psi)	Pwellhead (psi)	BHP (psi)	dP (psi)
1	906	319	1625	182	653	1851	40	544	1773	56
2	1238	406	1709	266	682	1877	66	557	1783	66
3	1630	450	1749	306						
4	1751							595	1815	98
5	1887	537	1833	390	718	1907	95			
6	2521	638	1926	483	740	1933	122	638	1862	145
7	3140	812	2090	647						
Reservoir pressure (psi)		1443			1811			1717		
Injectivity bbl/(d·psi)		4,9			20,0			17,4		
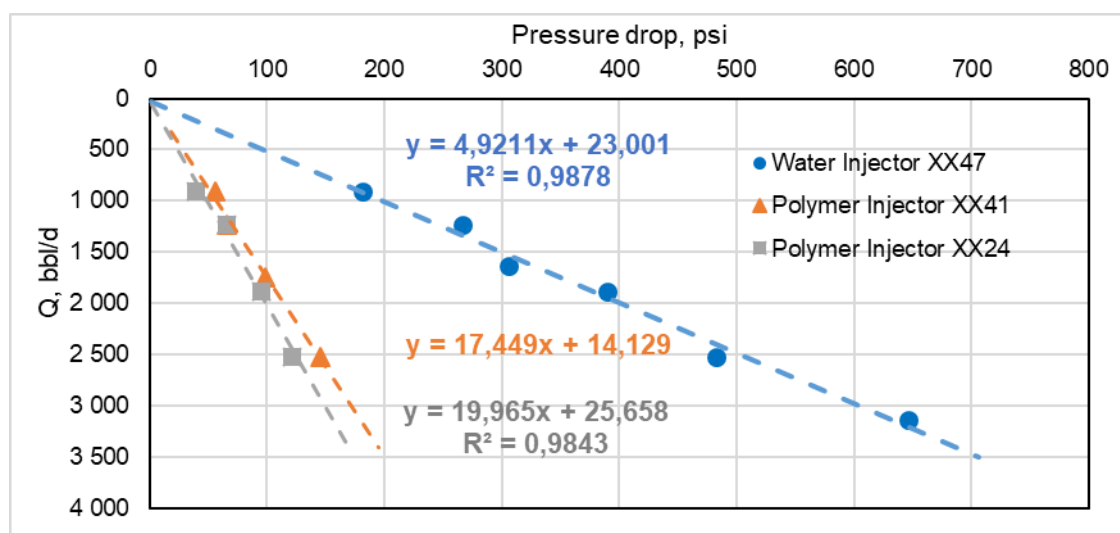
Figure 3.10 — Analysis of pressure step rate tests during water and polymer injection into Wells XX47, XX24, and XX41.

Rheology in porous media and mechanical degradation. The purpose of this section is to demonstrate (using laboratory measurements) that severe mechanical degradation would have been observed during HPAM injection of our wells if fractures or fracture-like features were not present. Rheology in porous media and mechanical degradation are directly related to the fluid velocity or flux in porous media [104; 130; 106; 141]. Consequently, using the methods described in Seright et al. (2011) [141], we determined rheology in a 769-md Kalamkas reservoir core for 1800-ppm R-1 HPAM polymer in Cretaceous formation brine (10.9% TDS). Figure 3.11 plots resistance factor vs. flux for this solution. (Resistance factor is the effective viscosity in porous media relative to water.) Figure 3.12 plots viscosity (measured at 7.34 s^{-1} and 25ºC, and expressed as a percentage of the injected polymer-solution viscosity) for the effluent vs. flux at which the polymer solution was forced through the core. Figure 3.13 plots fresh polymer solution viscosity vs. shear rate before injecting in the reservoir core.

Figure 3.11 was generated as follows. First, we performed standard core analysis to determine porosity and permeability. Next, the core was saturated with Kalamkas Cretaceous formation brine and permeability was determined. Subsequently, we injected freshly prepared 1800-ppm R-1 HPAM (in the Kalamkas Cretaceous formation brine) at moderate flux (50 ft/d) and measured the stabilized resistance factor. Then we decreased flux to 30 ft/d and allowed pressures to stabilize and resistance factor to be determined again. This process was repeated in stages to determine the resistance factors associated with the solid squares in Figure 3.11. The dashed curve in Figure 3.11 shows viscosity vs. flux which corresponds to the calculated shear rate using the model described in Hirasaki and Pope (1974) [150]. Between 50 and 11 ft/d, the resistance factor appeared to be constant with decreasing flux. As flux was lowered from 11 to 1 ft/d, the resistance factor decreased dramatically with decreasing flux. The literature has reported this behavior [130; 141] as a shear thickening or dilatant or viscoelastic effect. Shear thickening in porous media has been attributed to increased stresses and energy expenditure associated with disentanglement and elongation of coiled HPAM molecules as they flow through the sequentially contracting/dilating flow paths within porous media. For each flux between 50 and 5.2 ft/d, the polymer was mechanically degraded to a different extent, as demonstrated by the solid squares in Figure 3.12.

For flux values lower than 1 ft/d, a modest shear thinning was seen, as resistance factor increased with decreasing flux (Figure 3.11) and no mechanical degradation occurred. Furthermore, this resistance factor increase correlated reasonably well with the polymer viscosity increase as shear rate (or flux) decreased.
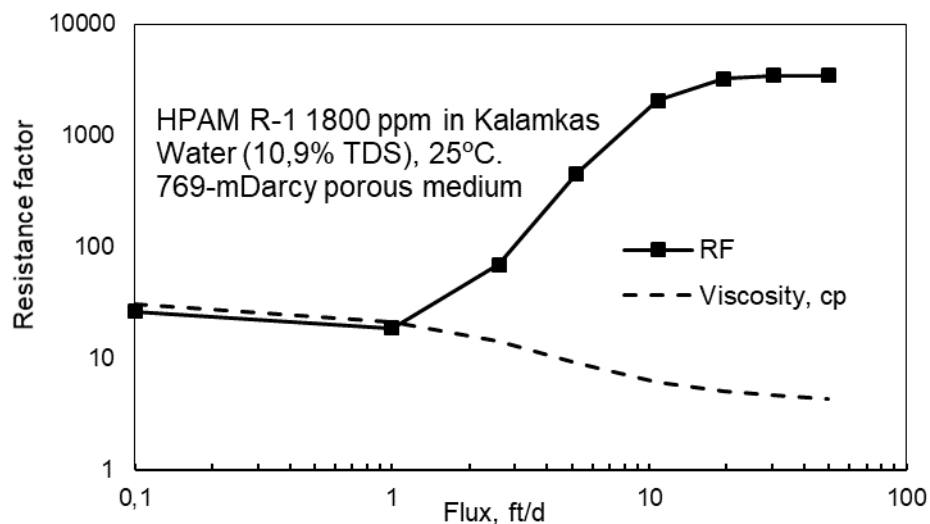

Figure 3.11 — Resistance factor vs. flux for R-1 HPAM in the Kalamkas water.
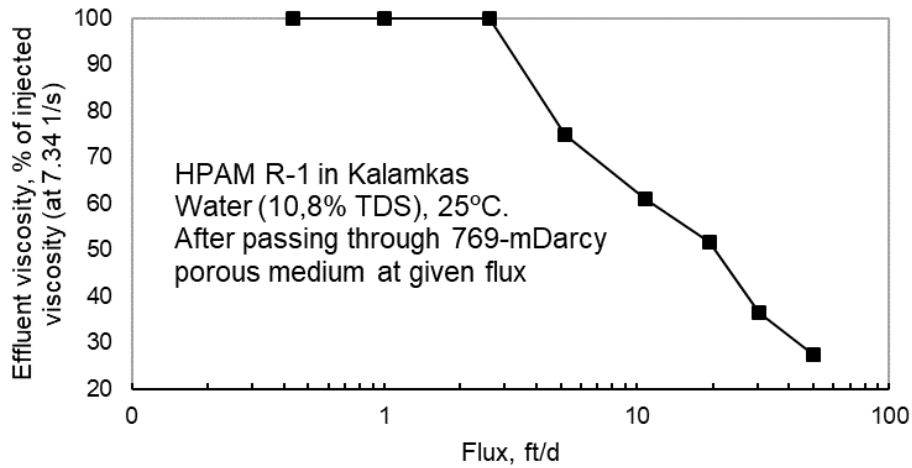
Figure 3.12 — Viscosities of solutions after being forced through the core at a given flux.
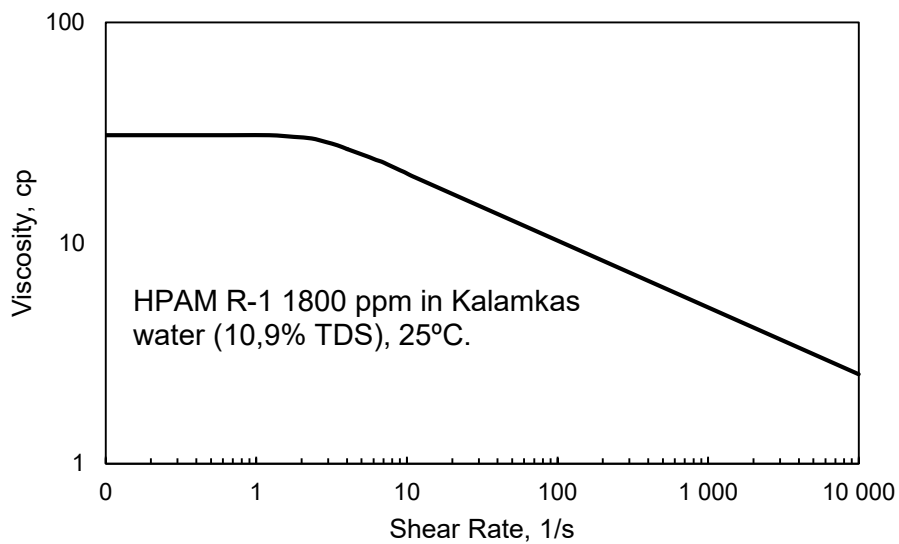
Figure 3.13 — Viscosity vs. shear rate for 1800 ppm R-1 HPAM in the Kalamkas water.

Recall from Figure 3.5 that the Darcy velocity (flux) at the injection sand face for an open hole completion would be over 200 ft/d. Thus, from Figure 3.11, the anticipated mechanical degradation would have been over 70% if the completion was the open hole with no fracture present. Therefore, the presence of the open fracture provides the logical explanation for both the observed lack of severe degradation and lack of severe injectivity loss for the HPAM injection well.

Significant of the results. As mentioned earlier, the very large investment associated with the polymer bank during a polymer flood necessitates a determination that the polymer is not substantially degraded during the process of injection. This paper provides a new methodology that is much more cost-effective for assessing near-wellbore polymer degradation than in previous methods, and the methodology is demonstrated for an important field application in Kazakhstan. In addition, this paper provides field-based support that vertical polymer injection wells have open fractures that enhance injectivity. We especially demonstrate that these

fractures reduce polymer mechanical degradation to a level that mitigates this degradation concern in a field setting.

3.5 Chapter Conclusions

The goal of this chapter was to demonstrate certain predictions about the existence and effects of fractures on injectivity during injection of HPAM solutions into vertical wells during a polymer flood in the Kalamkas field. This chapter provides field evidence to clarify the utility of near wellbore fractures to promote injectivity and mitigate mechanical degradation of HPAM solutions. It also provides a sampling methodology that demonstrated minimum mechanical and oxidative degradation under field circumstances, whereas previous sampling methods may have provided overly pessimistic indications of HPAM stability. The following findings were noted:

- Step rate tests indicated that fractures were not open during water injection before polymer injection. In contrast, during polymer injection, open fractures were confirmed using step rate tests, pressure transient analysis, and comparison of actual injectivities versus those calculated using the Darcy radial flow equation coupled with laboratory measurements of HPAM rheology in Kalamkas cores.
- We developed a novel method to assess in-situ polymer solution mechanical stability during a polymer flood. Under Kalamkas field conditions, we demonstrated the collection of formation samples using the natural energy of a reservoir at the wellhead. This process protected polymer solution samples from oxidative degradation. Compared to other lab and field methods, this novel method is quick, simple, and inexpensive. Compared with other field tests where substantial degradation was observed, one could argue that our methods are more reliable since they revealed only minor mechanical and/or oxidative degradation of HPAM samples and since laboratory and theoretical findings suggested that degradation should not have occurred under the conditions of the other field tests.
- Rheology measurements of back-produced polymer solutions showed the absence of the mechanical degradation. This finding provided further confirmation that polymer injection occurred above the formation parting pressure and that the injection area associated with the fracture was large enough to ensure the stability of the solution.
- These findings confirm that the advantages of fractures or fracture-like features during a polymer flood (i.e., little or no injectivity loss; mechanical stability of the polymer solution) can outweigh their disadvantages (e.g., possible severe channeling, jeopardized sweep efficiency).
- Polymer solutions that were back-produced from injection wells were depleted of dissolved oxygen, even though injected solutions contained 200-300 ppb of dissolved oxygen and the polymer solutions only penetrated

a few meters into the formation. Presumably, the 2-4%-iron mineral content of the reservoir rock caused this oxygen depletion. Even though this process added dissolved iron to the solutions, the HPAM did not degrade so long as the dissolved oxygen level remained low.

- As will be shown later in Chapter IV, Polymer solutions that propagated over 400 meters through a fracture from an injector to a producer were also depleted of dissolved oxygen, but suffered only minor viscosity loss (15%) after traveling all the way through the formation.

- The significance and novelty of the last four conclusions may be appreciated by realizing that virtually all previous field tests (where produced samples were analyzed from production wells or back-produced samples were analyzed from injection wells) indicated substantial HPAM degradation (as revealed in our literature review). If accepted at face value, those previous results would cast serious doubt on the viability of all HPAM floods. In contrast, our results alleviate those doubts by demonstrating that HPAM stability in a field application is consistent with present and previous laboratory and theoretical expectations. Our results suggest that the lack of stability observed in the previous tests may have been due to problems with the sampling procedures—rather than degradation that jeopardized the polymer in the reservoir.

4. ASSESSING POLYACRYLAMIDE SOLUTION CHEMICAL STABILITY

4.1 Introduction

Most Kazakhstan oil fields formation water (including the Kalamkas field) have high salinity and iron content. Commonly, those oil fields have no alternative fresh or low salinity (i.e., without iron content) water source similar to Daqing [105] or Milne Point [107]. It is well known that the HPAM solution at sealed and anaerobic conditions is very stable if iron ions exist in the process water [32]. That is why a sealing system for a polymer injection unit is crucial. But in a field application, controlling dissolved oxygen content at "zero" level is challenging. [32] suggested that 200 ppb oxygen is the highest value where viscosity losses will be insignificant. In contrast, [108] found that 46 ppb can lead to 10% viscosity loss. [31] based on the geochemical calculation and laboratory experiment, revealed that high dissolved oxygen content (which can be introduced during polymer solution preparation and injection) after entering the sandstone with 1% pyrite (FeS_2)—as in case of Kalamkas formation—can rapidly be depleted. Unquestionably, lower dissolved oxygen content leads to higher polymer chemical stability, and the "zero" (undetectable) level is an ideal case. So how much-dissolved oxygen will be feasibly acceptable in a real field setting? A significant part of this chapter is dedicated to testing and confirming those predictions in a field application at the Kalamkas polymer project.

As mentioned in Chapter 1, the PSU was used for the West pilot and for the seven injectors East extension. The other four wells of East Extension were supplied by the eductor-type polymer unit. This conventional eductor works on the Venturi principle, and polymer powder is supplied by air injection. There is no action to isolate air from the unit (Figure 4.1). The time to fully dissolve the polymer in water for the PSU is ~45 minutes and for the eductor-type is ~3 hours.

The water's dissolved oxygen level has been measured at the wellhead of production wells supplying West and East polymer projects. It was also measured in the water at storage tanks and in the mother solution from maturation tanks of the West PSU, the East PSU, and the East eductor-type polymer unit using CHEMets® express tests. The measurement results are shown in Table 4.1. Tests results reveal that at the formation, brine (from the wellhead) dissolved oxygen level is undetectable (less than 0.025 ppm or 25 ppb). This finding is consistent with the fact that Kalamkas oil reservoirs have a reducing environment due to iron-containing minerals up to 2-4% [31].

As shown in Table 4.1 at the West polymer project, oxygen was introduced during water transportation from the production well to the storage tank, and its level was at 0.3-0.4 ppm. In contrast, this problem did not occur at the East polymer project, where the oxygen level at the storage tanks was undetectable. But during the polymer dissolving process, the oxygen was introduced into the mother solution. The oxygen level was 0.3-0.4 ppm for the PSU type system, and for the eductor-type unit was 2-

3 ppm. For the PSU, the dissolved oxygen was close to the acceptable safe range, according to [32]. But for the eductor-type, this value is over 10 times higher than the acceptable level. As will be shown later, this unacceptable oxygen level resulted in 45% viscosity loss and the equivalent of 25% polymer concentration loss.

Table 4.1 — The dissolved oxygen measurement results during polymer injection in the Kalamkas field

Polymer injection unit	Dissolved oxygen content, ppm			
	Water producer	Water storage tank	Polymer mother solution	Polymer Injector
West PSU	0	0.2 - 0.3	0.3 - 0.4	0 – 0.3
East PSU	0	0	0.3 - 0.4	0.3
East eductor	0	0	2 - 3	1 - 2
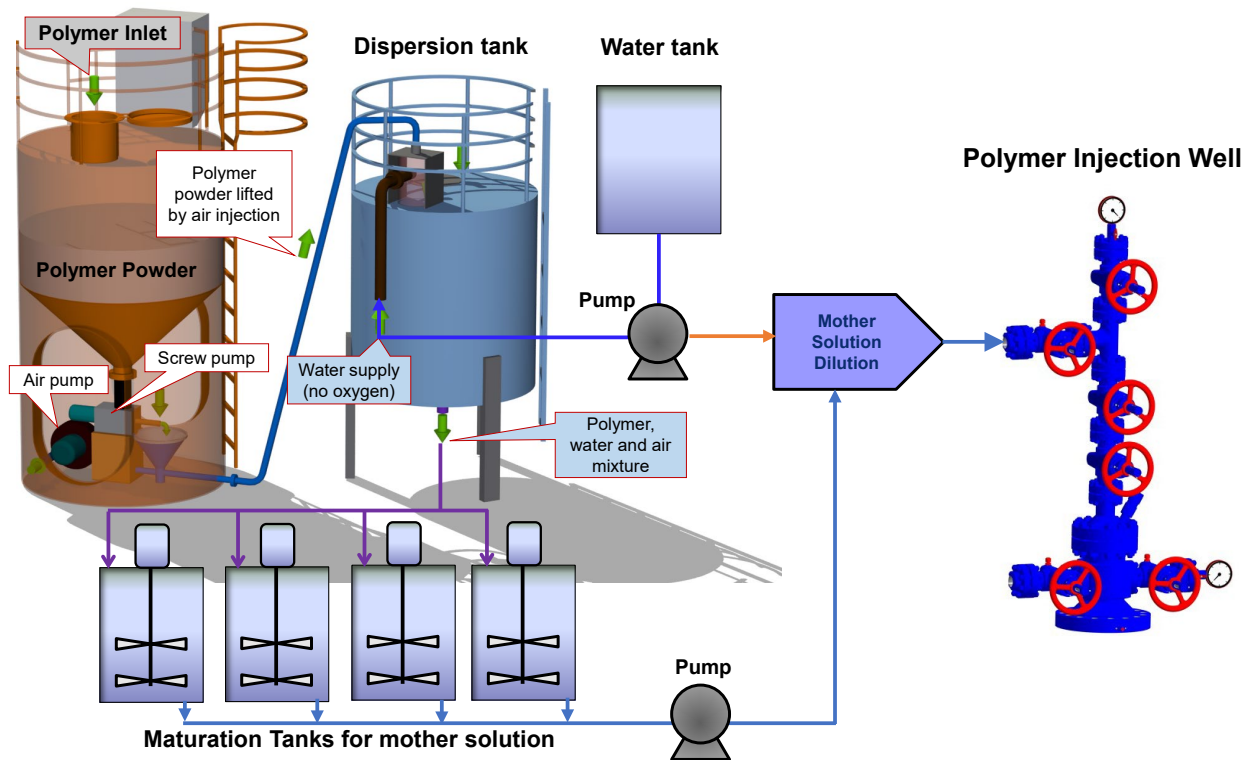
Figure 4.1 — Main components of the eductor-type polymer unit

4.2 Experimental

A field sampling of polymer solutions. To assess chemical stability, we compared laboratory prepared and sampled polymer solutions viscosities where polymer concentrations were the same as at the field. Mother solutions were sampled from polymer dissolving units (PSU and eductor type) and polymer solution from injectors wellhead. As a baseline for comparison, we used fresh polymer solution viscosities (the methodology will be shown later in this section). Viscosities were measured using a high-precision rheometer Anton Paar MCR 502 (Austria) at a shear rate of 7.34 s-1, at room temperature (25°C), and aerobic conditions. The use of a shear rate 7.34 s-1 is commonly used as a standard single-point for comparison of viscosities for non-Newtonian enhanced oil recovery fluids [2; 52; 106; 141].

Because most liquids (including polymer solution) are incompressible at low or medium pressures, a considerable change in pressure from 14.5 to 4350 psi causes no significant change in viscosity [154]. Therefore, the reservoir pressure condition for polymer solution viscosity measurement is not essential. The viscosity of each sample was usually measured twice and then averaged.

Polymer solution at the wellhead was collected in pressurized cylinders (Figure 4.2). Pressurized cylinders and collection procedures were specially designed for the polymer flood project to protect the solution from oxidative degradation [106; 139]. These cylinders are made of stainless steel and coated with an inert material to prevent corrosion and any iron contamination. Oxygen can be effectively excluded by carefully flushing air from the cylinder with polymer solution while collecting the sample.

Figure 4.2 — Pressurized cylinders for a polymer solution sampling at the wellhead

The Brine, Polymers and Concentrations. Formation brine in this work was collected from the dedicated production wells of the Cretaceous water reservoir (which is used for polymer dilution, as shown in Table 4.2). Brines (West and East Producers) have high iron content. Consequently, after exposure to the air, Fe^{2+} reacts with oxygen. Therefore, to eliminate the effect of oxidized products, both brines are pumped by air to oxidize all iron from the solution and then passed through paper filters before further use.

Table 4.2 — Cretaceous formation brine physical and chemical properties

Parameter	Cretaceous formation brine (used for polymer dilution)	
	West Producer	East Producer
pH	5.8	6.0
Density, g/cm^3	1.071	1.082
Ca^{2+} content, ppm	4 809.6	5 611.2
Mg^{2+} content, ppm	1 702.4	2 067.2
K$^+$ and Na$^+$ content, ppm	32 722.5	35 890.9
Cl$^-$ content, ppm	63 810	71 254.5
SO$_4^{2-}$ content, ppm	118.5	21.4
CO$_3^{2-}$ content, ppm	0	0
Total salinity, ppm	103 187.4	114 857.4
Water type by Sulin 1946[1]	Cl-Ca	Cl-Ca
Water hardness, mg-eq/l	410	470
Iron (Fe) content, ppm	40.6	18.2
Total suspended solids (TSS) content, ppm	14.0	12.0
Dissolved oxygen content, ppm	0[2]	0[2]

[1] [22]
[2] dissolved oxygen content measured with CHEMets® express tests shows the undetectable value (less than 0.025ppm or 25 ppb)

Two powder-form partially hydrolyzed polyacrylamides (HPAM) (SNF products) were used: Superpusher K-129 and Polyacrylamide R-1. They had a molecular weight of 14 million Daltons and a hydrolysis degree of 16%.

Polymer solutions were prepared by sprinkling the appropriate mass of polymer powder onto the brine vortex created by an overhead stirrer with a four-blade propeller. After mixing for several hours at a high rate, the stir rate was reduced for at least four hours and led to solution stand overnight. As in the field application, our target polymer concentrations for the three projects are in Table 4.3.

Table 4.3 — Polymer concentrations for the laboratory study

Polymer injection unit	Polymer type	Active polymer concentration, ppm	
		Mother solution	Injector wellhead
West PSU	Superpusher K-129	9 200	1 600
East PSU	Polyacrylamide R-1	15 000	1 700
East eductor	Polyacrylamide R-1	4 900	2 200

A sampling of producer fluid. Many polymer flood projects reported that production wells responded to polymer flooding by watercut decreases and increased produced polymer concentration [20; 106; 132; 134; 155; 161]. In some cases, the polymer channeled directly from an injector to a producer through a fracture, i.e., producing the same polymer concentration as injected. This circumstance occurred at Kalamkas field, where severe channeling and polymer breakthrough was observed from Injector XX37 to Producer XX87 in June 2019. Note that this polymer-channeling problem developed only once during over 7 years of polymer injection (i.e., since 2014). The distance between the producer and injector was 400 m. After the breakthrough, polymer concentration increased roughly from undetectable values (i.e., <1 ppm) to the injected values. Injector pressure fall-off tests after polymer injection revealed that injection occurred above the formation parting pressure and the fracture half-length was close to 400 m. This

value is very close to the well spacing (Figure 3.8 and Table 3.6). Thus, in this particular case, the fracture was detrimental to sweep efficiency because it extended all the way from the injector to the producer. After several unsuccessful attempts to plug the fracture (both from the production and injection sides), the production well was shut down.

Figure 4.3 shows Injector XX37 and Producer XX87 operation history before and after polymer breakthrough. This history indicates a powerful hydrodynamic connection expressed by a quick change of producer dynamic fluid level during an injector workover and after restoring injection. After the polymer breakthrough, the watercut increased from 87% to 100%. Tracer tests (Table 4.4 and Figure 4.4) during water and polymer injection confirmed that the source of polymer breakthrough was Injector XX37.

This unusual case provided the opportunity to assess polymer solution chemical and mechanical stability that traveled all the way from the injector to the producer through the reservoir.

Table 4.4 — The interwell tracer tests results on Polymer Injector XX37 and surrounding producers

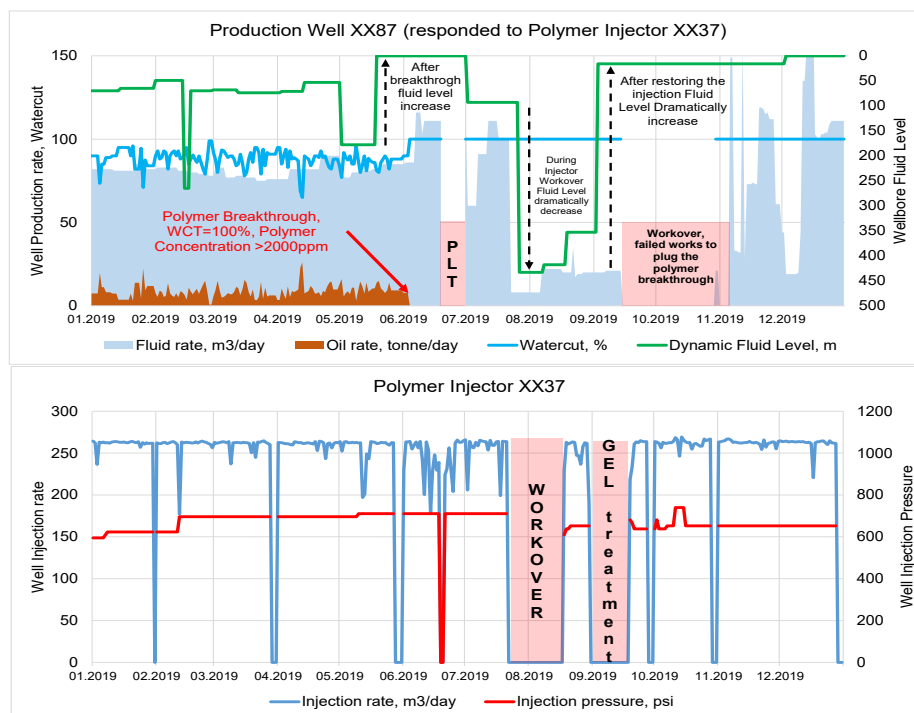| Date	Tracer type	Injected Mass, kg	Injected V, m3	Prod-ed M, kg	Prod/Inj M, %	A tracer reached well number	Tracer max velocity, m/d	Tracer min velocity, m/d	Tracer average velocity, m/d
Nov. 2017	Urea	5000	18	147,8	2,96	25	1808	188	638
Nov. 2019	Fluorescein (Uranin)	60	9	0,6172	1,03	1 (XX87)	2781	2781	2781
Nov. 2020	Rhodamine C	60	18	0,1	0,11	6	1162	62	210

Figure 4.3 — Well XX87 production and Well XX37 injection history, where polymer breakthrough was observed
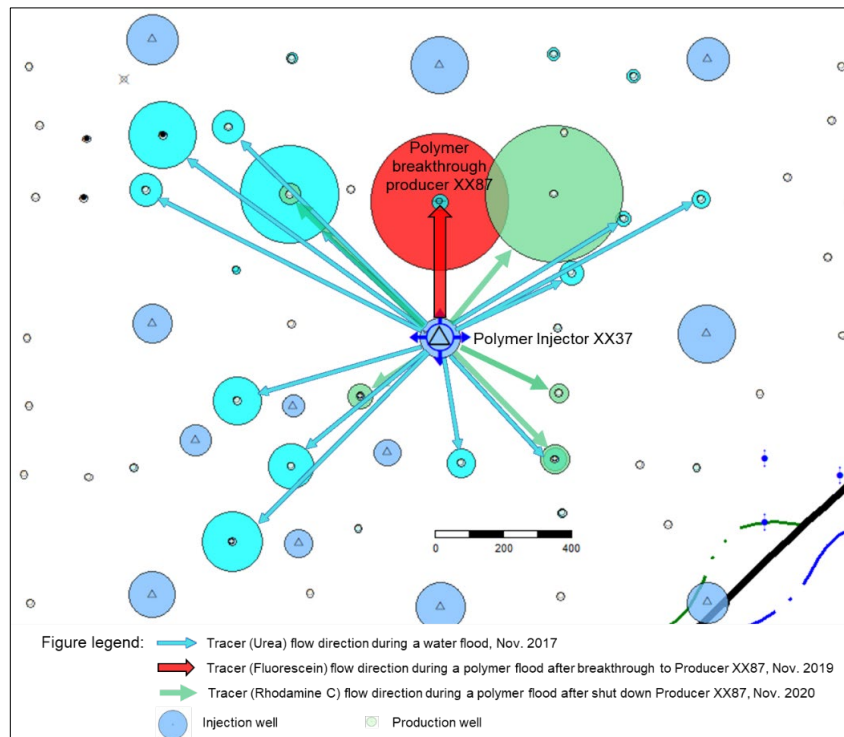
Figure 4.4 — The interwell tracer tests results on Injection well XX37 and surrounding producers

A special scheme (Figure 4.5) and procedure were developed to collect produced polymer solution samples from Producer XX87, and assess in-situ polymer stability. The production well was equipped with a production line valve, check valve, annulus valve, wing valve, pressure gauge, sampler, and X-mas tree. The well downhole was equipped with tubing and a rod pump. The top of the perforation interval was located at 806 m MD (measured depth), and the tubing end was at 590 m MD. A dedicated high-pressure hose was installed to connect the sampler to the pressurized cylinder to collect polymer solution samples at the wellhead. The special procedure was as follows as applied in Well XX87:

- Stop polymer solution injection unit (including Injector XX37) for planned repair work for >6 hours.
- Install pressure gauge, flow meter, and connect the pressurized cylinder to collect samples before putting on production well XX87.
- Open wing and production line valve to put the well on the production and start to collect samples.
- Open the sampler valve and flush several cylinder volumes with the produced polymer solution to prevent air from entering the sample.
- Collect six samples (total) at different cumulative production volumes with the same procedure as described above and measure dissolved oxygen level.
- Collect injecting polymer solution at Well XX37 (source of the polymer breakthrough) and measure dissolved oxygen level.
- After collecting all samples, immediately transport pressurized cylinders to the field lab to measure viscosity.

- Viscosity measurements proceed as described above in the subsection "*A field sampling of polymer solutions*" and additionally determine the rheological power law index [21].
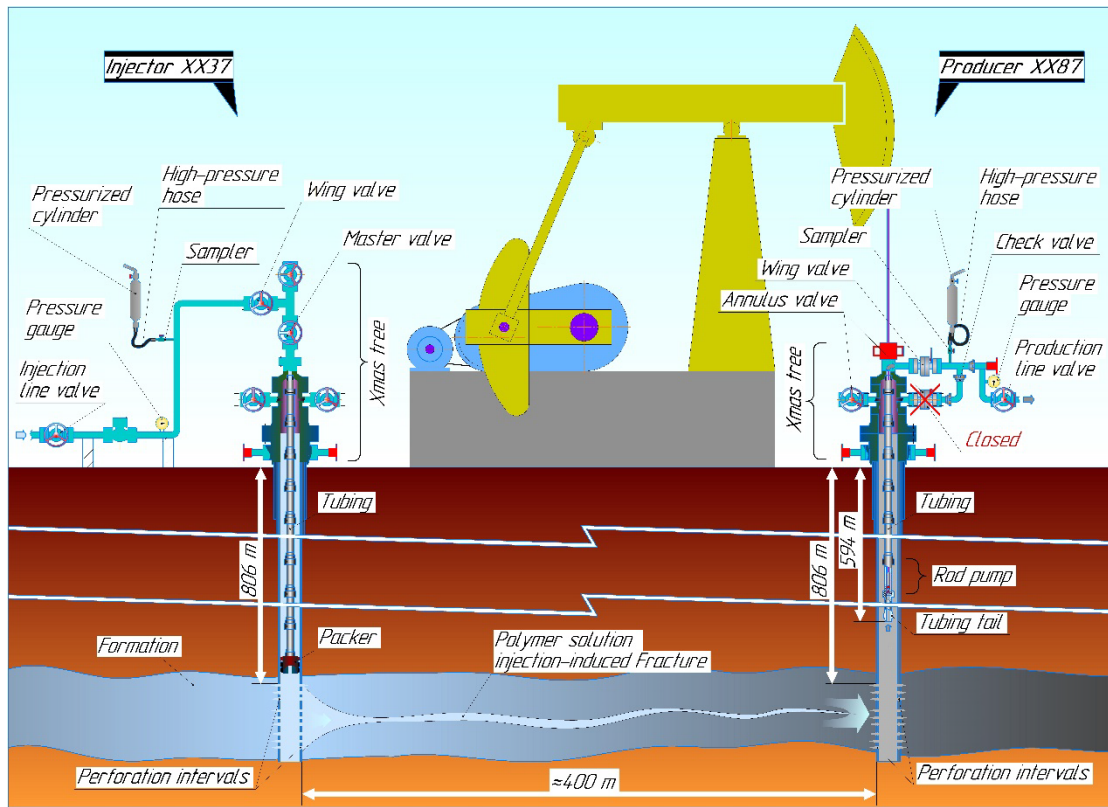

Figure 4.5 — Scheme to collect polymer solutions from Producer XX87

4.3 Results and Discussion

Effect of Dissolved Oxygen. As shown in Table 4.2, process water has a high content of dissolved iron. Therefore, if dissolved oxygen is introduced to the polymer injection system, it will cause chemical degradation. The PSU is designed to keep dissolved oxygen very low, and the Eductor type unit has no action to treat the oxygen or iron. Further, the effects of dissolved oxygen and Fe2+ on polymer viscosity for three polymer units are demonstrated in Table 4.5. Examination of this table first reveals that the PSU for both projects (West and East) has a good performance due to chemical stability. Chemical stability provided by nitrogen blanketing system and its efficiency is consistent with [32] work. The field viscosity of the PSU mother solution did not reach the lab viscosity. However, after subsequent dissolution processes, the solution reached the required polymer viscosity and dissolving quality at the wellhead. Finally, we can see that viscosity losses were zero at the injector wellhead for the West and East PSUs, demonstrating high technical efficiency.

For the East eductor, both mother and polymer solutions showed a very high level of viscosity losses. The viscosity loss for the mother solution and at the injector wellhead were 36 and 45%, respectively. These losses are unrelated to dissolving

quality, but instead is due to oxidative (chemical) degradation caused by dissolved oxygen and divalent iron reactions. As shown in Figure 4.1, the dissolved oxygen was introduced by air injection associated with the polymer powder supply. At the first mixing step, the mother solution had 2-3 ppm dissolved oxygen. Due to the absence of oxygen in the process water and the polymer dilution process, the oxygen level at the wellhead decreased to 1.5 ppm (Table 4.1). This oxygen content was higher than the acceptable range - by roughly 10 times. The final viscosity loss was about 45% or equivalent to 25% loss of polymer concentration. The primary oxidative degradation location in the system is the dispersion tank. Subsequently, during transit from the injection unit to the wellhead, it additionally loses about 10% more viscosity. We assume that this process continues in the tubing before entering the formation. As will be shown later, after the polymer solution enters the formation, all oxygen will be consumed by the surrounding rock very quickly and provide subsequent chemical stability. But still, severe degradation at the surface affects project economics and feasibility.

Table 4.5 — The viscosity measurement results at different injection units

Polymer injection unit	Lab viscosity, cp		Field viscosity, cp		Viscosity loss, %		Polymer concentration loss, %
	Mother solution	Injector wellhead	Mother solution	Injector wellhead	Mother solution	Injector wellhead	
West PSU	680	20	652	20	4	0	0
East PSU	1 980	23	1 850	23	14	0	0
East eductor	240	38	154	21	36	45	25%

The viscosity of the polymer solution measured at $7.34s^{-1}$ T=25°C

The polymer rheology and concentration loss. Figure 4.6 shows polymer concentration and viscosity relationship for two types of used polymers in the field. For our case, polymer viscosity roughly depended on the square of its concentration. This figure analysis reveals that 45% viscosity loss for the East eductor polymer injection unit corresponds to 25% equivalent polymer concentration loss.

Several views exist on how to solve this problem. They include: (1) chemical/mechanical treatment of the process water to remove all iron from the solution [162], (2) chemical additives such as free-radical scavengers or pH adjustment [89; 163], (3) keeping dissolved oxygen at an undetectable or acceptable level (as close to zero) [31], and (4) no action [20] as in our example of the East eductor unit.

The viscosity measurement results at different injection units (Table 4.5) reveal that removing all oxygen from the system is the feasible and effective way to provide the chemical stability of the solution. Thus, we suggest modifying the East eductor injection unit to ensure an undetectable or acceptable oxygen level that will save 25% cost of chemicals.
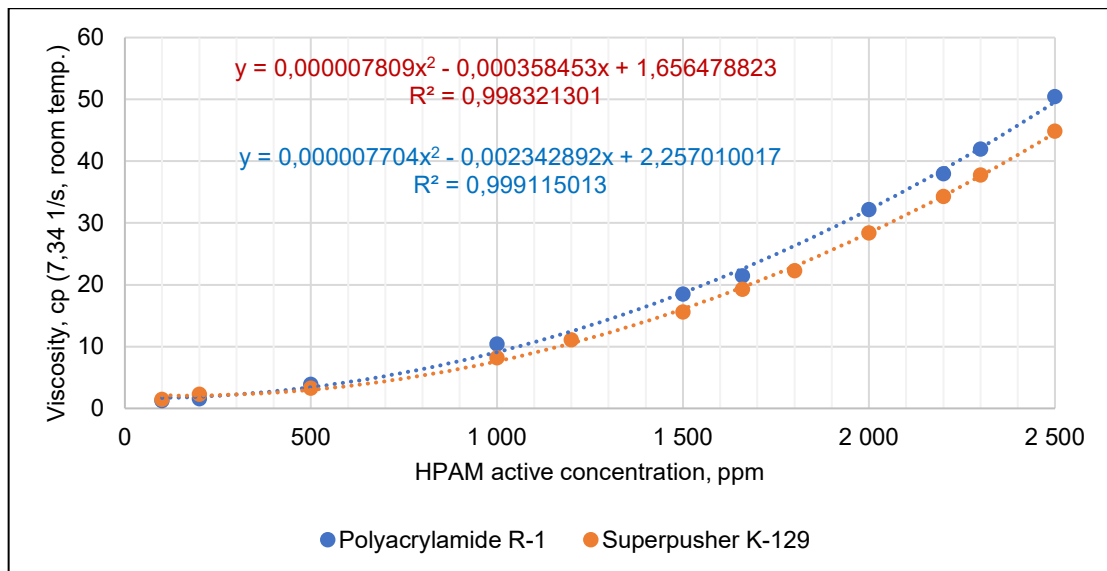
Figure 4.6 — Polymer solution viscosities at different concentrations

Effect of the formation on the polymer stability. Fluid sampling for Producer XX87 and injection of polymer solution at the wellhead of Well XX37 occurred on 30th April 2021, as described above in the section "*A sampling of producer fluid*". The typical surface temperature was +20ºC during the test. As shown in Figure 4.5, samples from Producer XX87 were collected after polymer breakthrough and that polymer solution propagated over 400 m through the reservoir from Injector XX37. Additionally, the dissolved oxygen level was measured at the wellhead of Polymer Injection Well XX37 and the last four produced samples (# 3, 4, 5, 6) using CHEMets® colorimetric tests. The viscosity and oxygen measurement results are shown in Figure 4.7 and Table 4.6. Note in Table 4.6 that after the first listing (the original sample that was injected), the samples are listed in reverse chronological order of collection—i.e., Sample 6 was collected last from the formation, and Sample 1 was collected first in the tubing). Test results show that injected solution from Well XX37 had roughly 1.5 ppm (i.e., between 1 and 2 ppm) dissolved oxygen content and viscosity of 25.1 cp with power law index of 0.763. The first three produced samples (originating closest to the surface) contained 0.2 ppm dissolved oxygen and different degrees of viscosity loss relative to the injected (25-50%). The last three samples show undetectable dissolved oxygen levels (less than 0.025 ppm or 25 ppb) and only modest viscosity loss (15%), with a power law index close to that of the injected solution.. We presume that significant degradation was seen for the first collected samples because oxygen (air) was introduced into the production well during the well repair work. The gradual decrease in the level of degradation (i.e., increase in viscosity) with time reflected flushing this oxygen out of the system. These findings indicate that injected oxygen in the polymer solution (that transported 400 m through the Kalamkas reservoir) was consumed by the surrounding reservoir rock provided chemical (oxidative) stability of the solution (due to iron-containing minerals up to 2-4% [31]). The small viscosity loss (from 25 to 21 cp) was probably associated with oxidative viscosity decrease in the wellbore of the Injection Well XX37. (Viscosity was measured at the wellhead, then solution passed through the

tubing about 30 min before entering the formation. This time was sufficient to degrade the solution viscosity by 15%.)
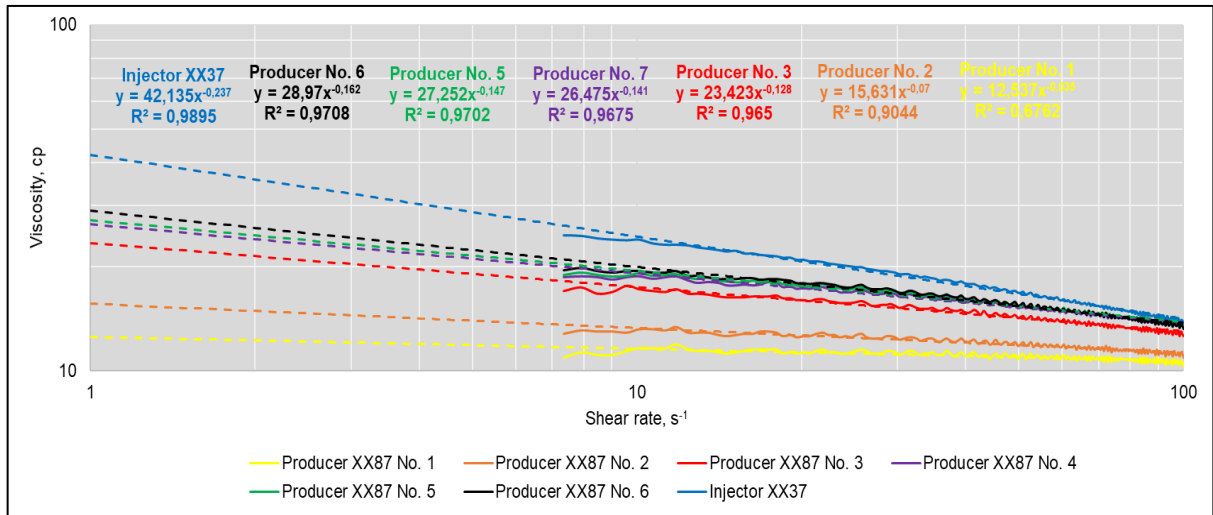

Figure 4.7 — Rheological curve analysis of injected (Well XX37) and produced (Well XX87) polymer solutions

Table 4.6 — Rheology measurements of the injected and produced polymer solution from Injector XX37 and Producer XX87

Well	Produced Volume, m^3	Dissolved O_2 concentration, ppm	The location of the collected sample	Viscosity at 7.34 s^{-1}, cp	The power law index (n), dimensionless[1]
Injector XX37		1.5	Injected	25.1	1-0.237 = 0.763
Producer XX87 No. 6	6.5	0	Formation	21.0	1-0.162 = 0.838
Producer XX87 No. 5	4.4	0	between tubing and perforation	21.3	1-0.147 = 0.853
Producer XX87 No. 4	3.6	0	between tubing and perforation	21.3	1-0.141 = 0.859
Producer XX87 No. 3	3.3	0.2	between tubing and perforation	19.2	1-0.128 = 0.872
Producer XX87 No. 2	2.9	N/A	between tubing and perforation	14.9	1-0.070 = 0.930
Producer XX87 No. 1	2.0	N/A	downhole tubing	13.1	1-0.035 = 0.965
[1](API RP 63 1990)					

4.4 Chapter Conclusions

As mentioned earlier, the very large investment associated with the polymer bank during a polymer flood necessitates a determination that the polymer is not substantially degraded during the process of preparation and injection. This chapter provides a methodology for assessing chemical degradation in the field, and the methodology is demonstrated for the field application at the Kalamkas. This study indicates the possibility of optimizing operational expenditure and increasing the economic efficiency of the polymer flood project operated by an eductor type unit. Consistent with [32], 200-400 ppb oxygen in polymer preparation and injection

process does not degrade polymer viscosity. In addition, this chapter provides additional field-based support that dissolved oxygen of the injected polymer solution is effectively consumed by surrounding rock and provides further chemical stability in the formation.

5. AN UNCONVENTIONAL APPROACH TO MODEL A POLYMER FLOOD

5.1 Introduction

During the operation of polymer projects, well monitoring, dedicated field studies, lab analysis, inter-well tracer tests, and well tests (step-rate and pressure fall-off tests) were conducted. The results of these studies were used to build a conceptual polymer flood model. An unconventional approach to model the polymer flood will be shown in the successful example of the West pilot. To date, we are working on the East polymer model, and the results are not yet complete.

5.2 Methodology

The overall approach to building the reservoir model is schematically shown in Figure 5.1.

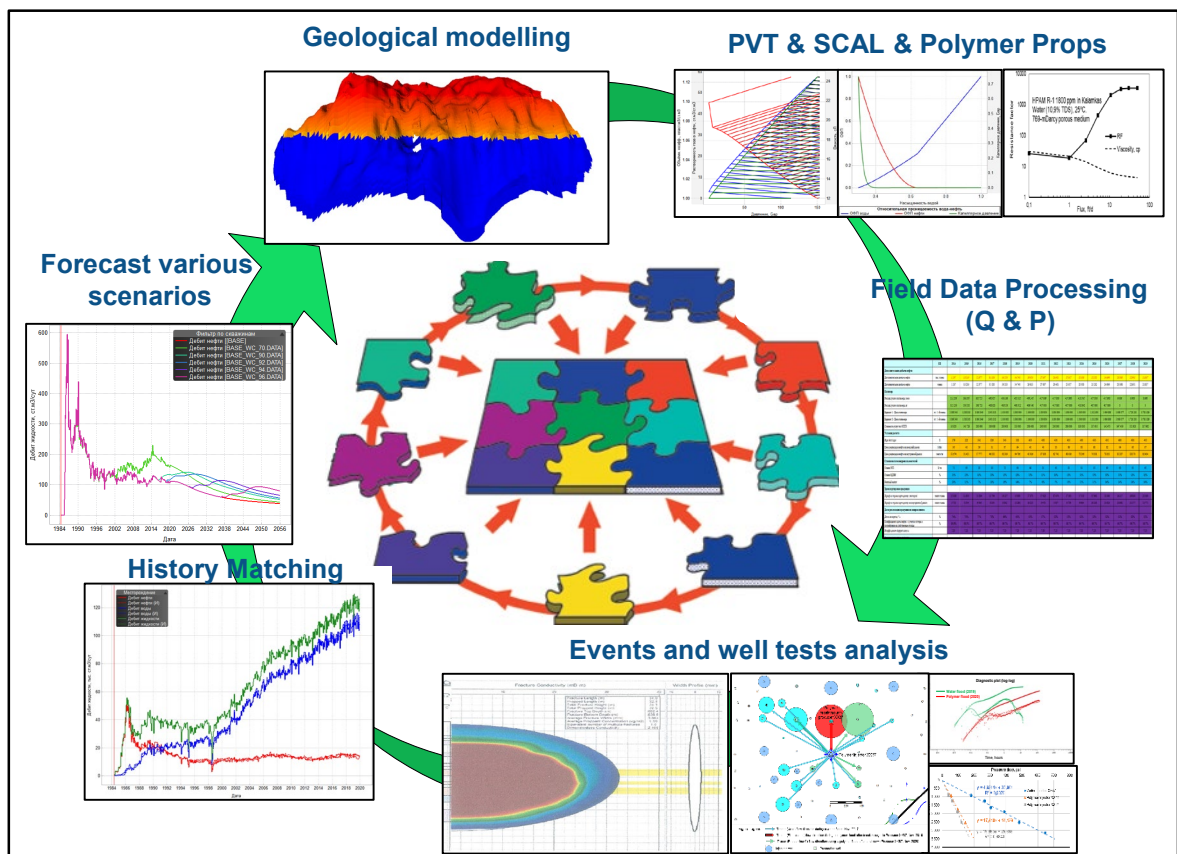Figure 5.1 — Overall approach to build a reservoir model for a polymer flood

1. Geological modeling consists of structural modeling, creating a 3D grid, lithology and facies modeling, petrophysical modeling, oil reserves estimation, and finally initialization of the reservoir model. Grid dimensions were 50 m length, 50 m width, and 0.2 m height. Block V sector model included 1 439 340 cells (149x69x140), illustrated in Figure 5.2.

2. Laboratory experimental (PVT, SCAL) results were systematically analyzed and existing models updated (Figure 5.3 and Figure 5.4).
3. Production and injection history were systematically investigated by analysis of production and injection logging tests (PLT&ILT). To accurately history-match reservoir performance, the upper reservoir was considered out-of-zone injection (Figure 5.5).
4. Special core flooding experiments were conducted to estimate polymer rheology, retention, and mechanical degradation - providing key properties for the polymer flood and considered during setting polymer properties in the ".data" file.
5. For characterizing the production wells, we extensively analyzed well stimulation history (including hydraulic fracturing), well tests (pressure fall-off & step-rate tests), and inter-well tracer test results to build fractures or fracture-like features with proper orientation and configuration.
6. Water and polymer flood history matching emphasizing bottom-hole pressures (BHP).
7. Sensitivity analysis and forecast of various scenarios were performed to study the impact of polymer properties (viscosity, slug size, injection rate) on net present value – NPV.
8. We developed a correlation equation to estimate incremental oil production based on geological properties (layering, effective formation height, net to gross – NTG) and reservoir dynamic parameters (productivity index variation, depletion intensity, water cut).

Figure legend :

- ▪ Wells   - - -   Polymer flood area
- ● Polymer injectors
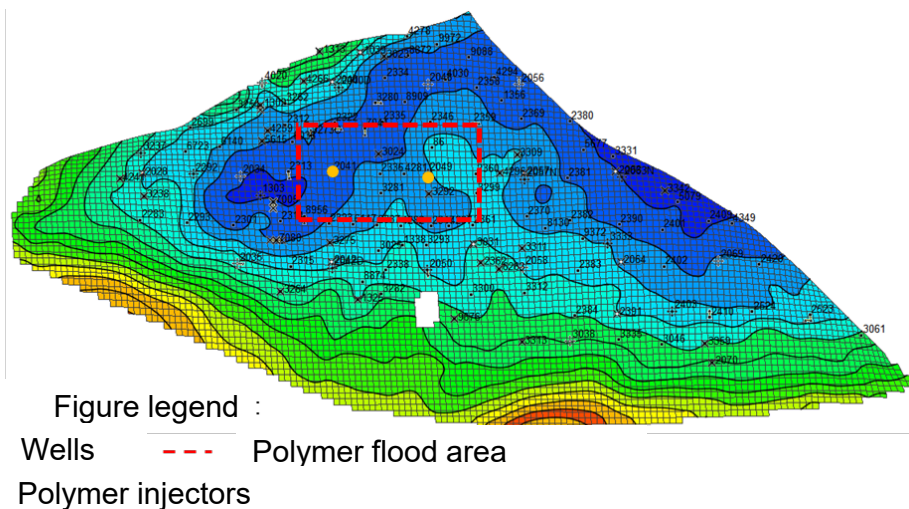
Figure 5.2 — Block V sector model which includes the West polymer flood pilot
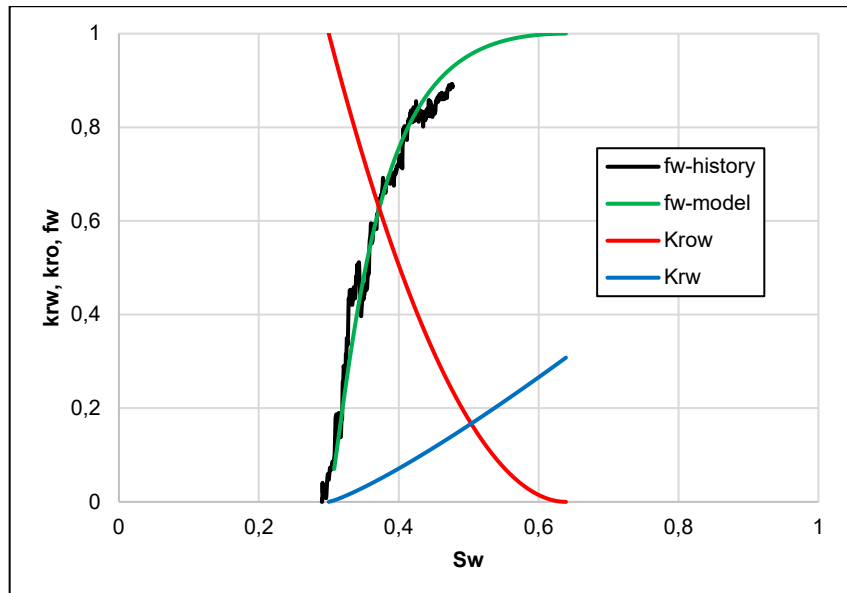
Figure 5.3 — Relative permeability curves matched with a historical watercut

Relative permeabilities analytically matched watercut history using a Buckley-Leverett function. As shown in Figure 5.3, the actual watercut (black curve) is approximated well using a theoretical fractional water function (green curve). This approach saved significant time and resources.
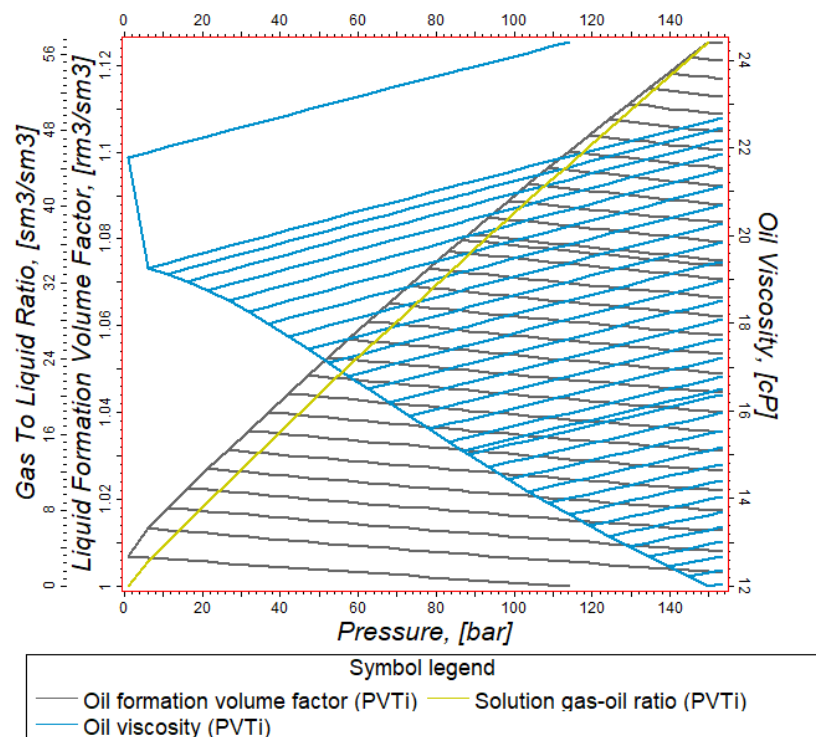
Figure 5.4 — Oil PVT properties used in the model

After a detailed analysis of all the formation samples for the reservoir, a PVT model was built in PVTi software using the oil and gas component compositions.
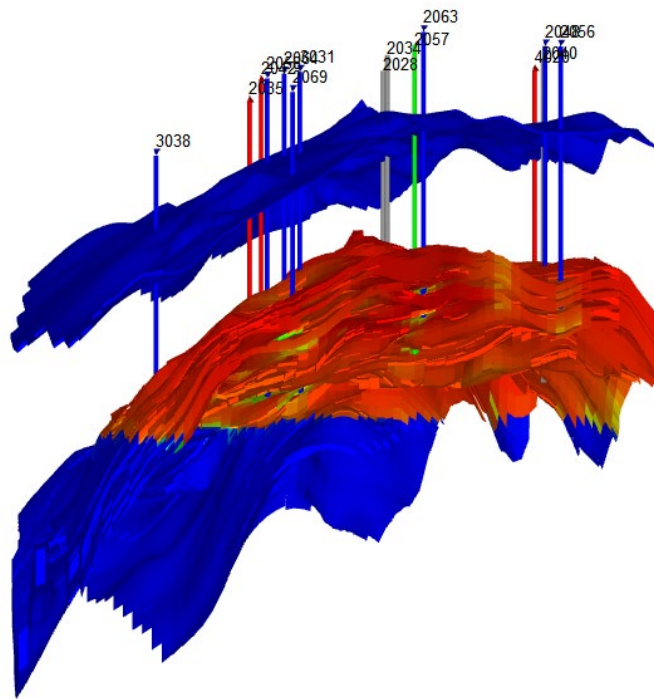
Figure 5.5 — Target reservoir and synthetic upper reservoir (considered out-of-zone injection)

The target reservoir model included 29 operated injection wells, with 15 of them registering out-of-zone injection at specific times. Total ineffective injection over 40 years was estimated at 1.5 million m^3 water. Our model considered these events to reproduce the real reservoir development history.

5.3 Polymer flood observed key aspects

Polymer Rheology in Porous Media or Resistance Factor. Resistance factor is defined as a ratio of injected water to polymer solution mobilities. Some researchers [150; 164; 165; 166] claimed that HPAM (the same type of polymer used in the Kalamkas project) solutions reduced mobility much more than expected from the solution viscosity. They suggested that the polymer substantially decreased permeability due to polymer adsorption and/or mechanical entrapment. This effect was often achieved during flooding experiments on short cores using freshly prepared HPAM solution. This permeability reduction behavior is considered in most modern simulators (e.g., Eclipse, tnavigator), including the model used for this study. In contrast, Seright et al. (2011) [141] demonstrated that this mechanism is not practically achievable in field applications because HPAM high molecular species (which were responsible for permeability reduction) are filtered or destroyed at the injection sandface and will not propagate far into the reservoir. Consequently, deep in the formation where permeability >100 md, polymer solution are expected to provide mobility reduction proportional to the low shear rate viscosity measured in a rheometer. Thus, in a high-permeability formation like the Kalamkas field, polymer solution resistance factor or apparent viscosity in porous media is best

represented by low-shear-rate viscosity measurements. In contrast, if polymer retention truly caused low mobility and permeability reduction, BHP values in polymer injectors would increase to high values. This effect has been demonstrated in our reservoir model, and the results show high BHP values were never observed in the Kalamkas field (Table 5.1). Thus, we excluded permeability reduction as a mechanism to provide more mobility reduction than expected from rheology measurements.

Table 5.1 — Analysis of the effect of permeability reduction on the polymer injector BHP

Case	Permeability reduction	Injector BHP, bar	History matching quality, +/- %
0 (history)		125.9	
1	1	123.6	-1.9
2	1.1	132.0	4.6
3	1.2	136.3	7.6
5	1.4	145.4	13.4
6	1.8	165.1	23.7
7	2	175.6	28.3
8	3	226.2	44.3
9	4	279.9	55.0

Residual Resistance Factor – RRF. Residual resistance factor is defined as a ratio of water mobility before versus after a polymer flood. As mentioned in the Introduction section, the original four East pilot polymer injectors were returned to water injection after a long period of polymer flooding. The pilot is an infilled 5-spot with an average well spacing of 200-250 m, including 9 producers (Figure 5.6a). The producers' post-polymer water injection performance has been extensively analyzed.

After the pilot started, liquid production of all producers were increased by changing downhole pumps. This action led to the first oil rate to increase, then stabilization, and later decline between March 2015 and February 2016. The polymer response started in August 2016 at 30% PV injected. This effect continued until the end of the project. As a result, the watercut decreased from 91% to 86%, and the oil rate increased by ~60%. When the polymer bank size reached 50% PV, injectors were returned to waterflooding. As shown in Figure 5.6b, water injection led to a sharp (during the first month) water-cut increase from 86% to 91%, and oil rate decreased by at least 60% - i.e., oil production returned to the previous level before the polymer response.

As demonstrated in this field case for the Kalamkas high permeability conditions (>500 md), residual resistance factor is not significantly different from unity. It supports our conservative view for polymer-flood design, which assumes that resistance factor was approximated well using low-shear-rate viscosity measurements and no permeability reduction. Thus, we suggest setting RRF in the simulator at 1. But even if the model assumes no permeability reduction, it could not reproduce the performance during post-polymer water injection—because of viscous fingering of the chase water through the polymer bank in the high permeable

path. This effect has been experimentally proved by Seright (2017) [52] and illustrated in Figure 5.7.

(a)

(b)
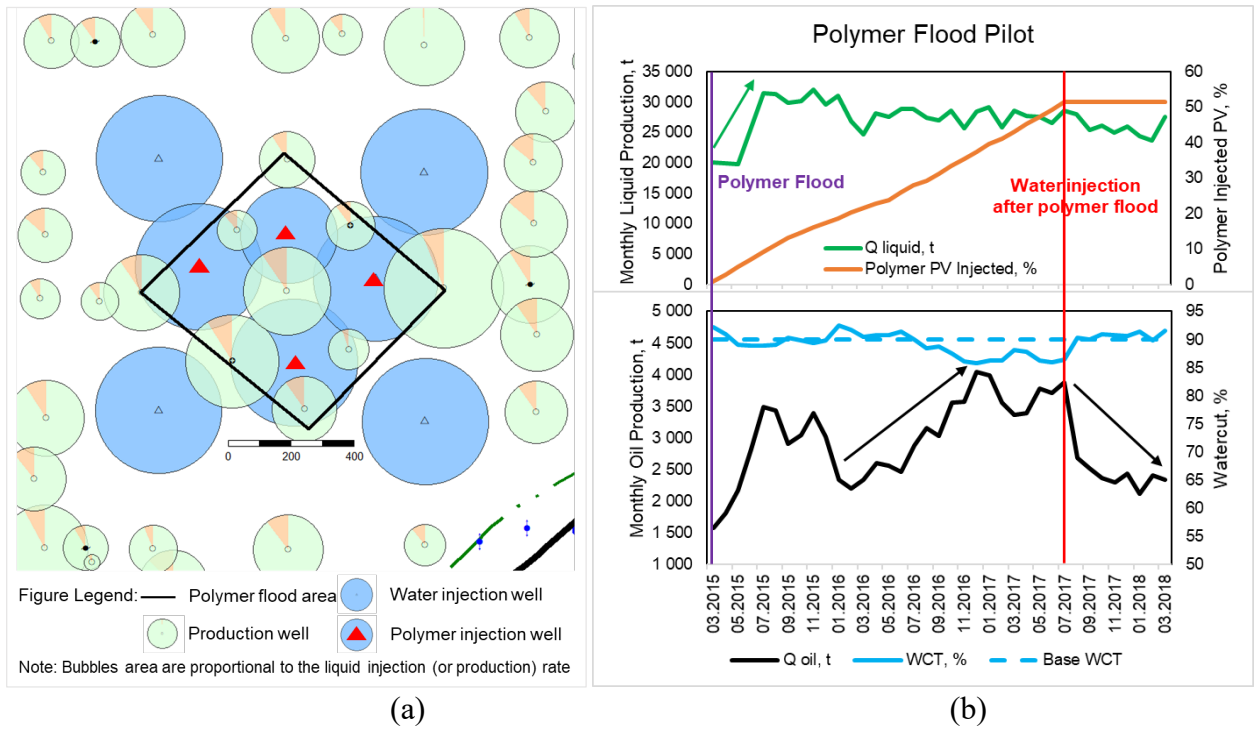
Figure 5.6 — Polymer flood pilot area (a) and production response (b)
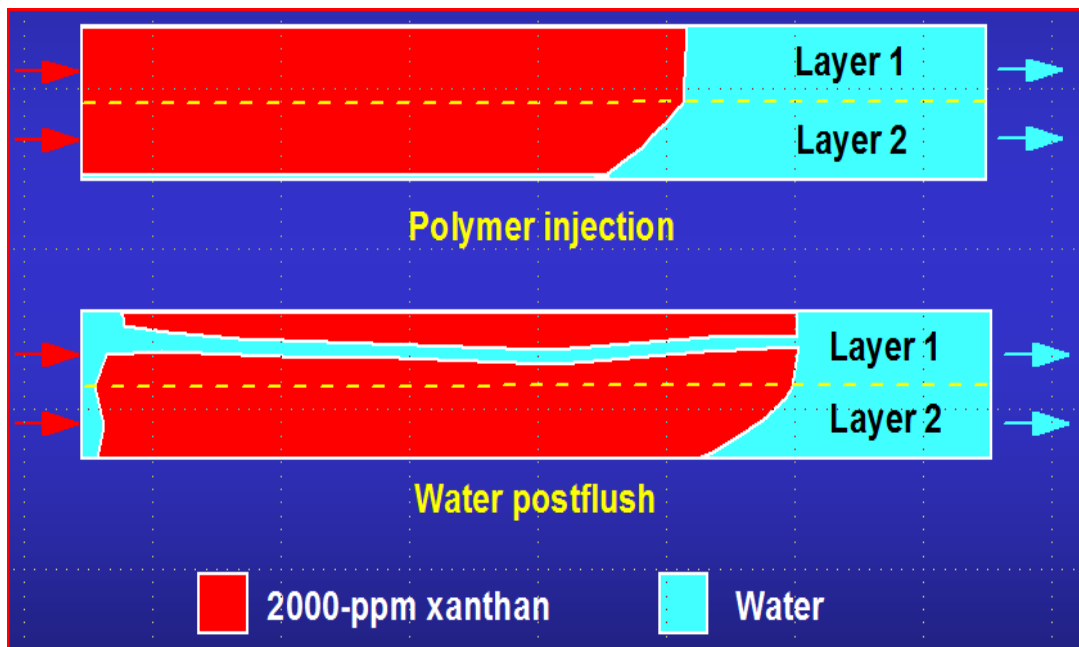
Figure 5.7 — Viscous fingering during water injection after polymer flood [52]

The simulation scenario associated with a post-polymer chase waterflood (WF) is shown in Figure 5.8. The blue curve show projections from the model during post-polymer chase water injection, while the green curve shows the projection for continued polymer injection. In this model, the switch from polymer to water injection began at the start of the blue curve (Feb. 2020). These projections suggest that a post-polymer waterflood will maintain oil rates and water cuts that are

76

significantly more desirable than associated with waterflooding alone (e.g., the red dashed curve). Additionally, the difference in oil production between continuing polymer flood (green curve) and returning to water injection (blue curve) is only 9.2%. Clearly, an economically rational scenario is a chase waterflood. However, as the East pilot demonstrated, oil rates are actually expected to return to the water flood base case after returning to water injection. Thus, considering the model's ability and real polymer flood physics, we suggest an accurate forecast for water chase flood rapidly returns to the waterflood base case line (red dashed curve).
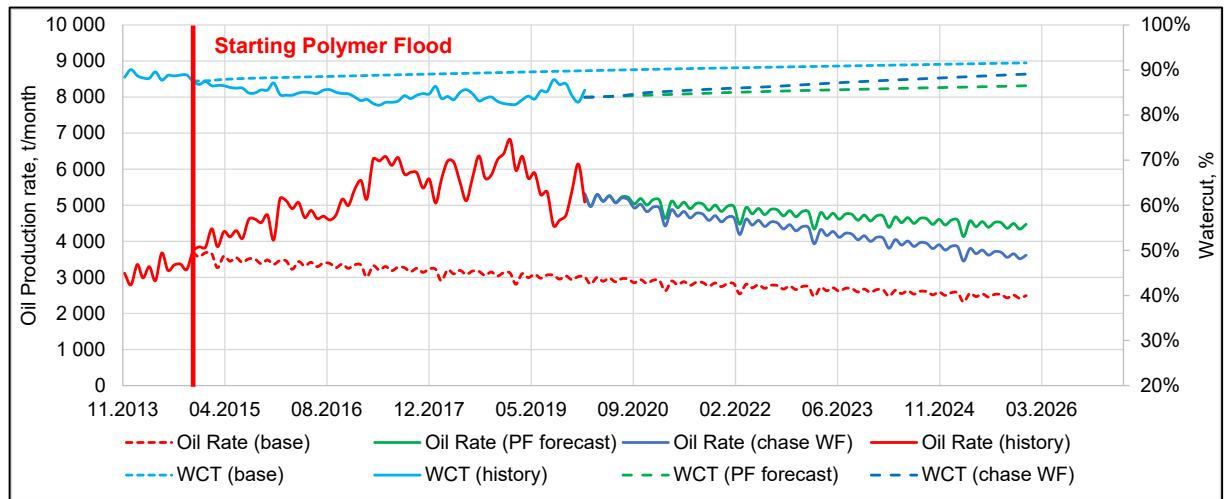
Figure 5.8 — Post polymer waterflood oil production response in the model

Inaccessible pore volume - IAPV. Considering uncertainties in laboratory studies to date and the high permeability condition of the Kalamkas field, we suggest IAPV should be set as zero during simulations. Previous works [167; 168] demonstrated that is approach is appropriately conservative, and also most likely is correct/true. Simulation studies revealed that BHP and watercut response are not sensitive to IAPV values from 5% to 30%.

Polymer retention. Laboratory measurements of polymer retention were performed using a core plug from the target polymer-flooded reservoir. The core plug was chosen to represent the average permeability of the target reservoir. The rock absolute permeability was 380 md and porosity was 31.3%. The plug sample was cleaned with toluene, then saturated with formation water from the target reservoir., (This water was cleaned/filtered to remove oxidized products and suspended solids). The Kalamkas formation water contains 4 600-ppm calcium, 2 200-ppm magnesium, and has a total salinity of 98 700-ppm TDS. This water was used to prepare polymer solutions during the field polymer flood. The polymer used in the field and in this lab test was SNF Superpusher K-129, which is a partially hydrolyzed polyacrylamide (HPAM) with a molecular weight of approximately 14 million g/mol and a hydrolysis degree of approximately 17%. We used 1000, 1500, 2000 ppm HPAM solutions in our retention test.

After preparation and saturation with brine, we measured residual oil saturation, and then injected polymer solutions at a fixed rate (1 ft/D) at the reservoir temperature of 40ºC. Polymer concentrations were measured using the bleach

method [139]. The retention of each polymer slug injected was calculated using Equation (5.1), as recommended in [139]:

$$R = \frac{W \times Ci - Y \times Cp}{M} \qquad (5.1)$$

where: R = retention, µg/g; W = weight of polymer injected, g; Ci = concentration of polymer solution injected, unit fraction; Y = weight of fluid produced and analyzed, g; Cp = concentration of polymer in the produced sample, unit fraction; M = bulk mass of the core, g. The retention test results are shown in Figure 5.9.
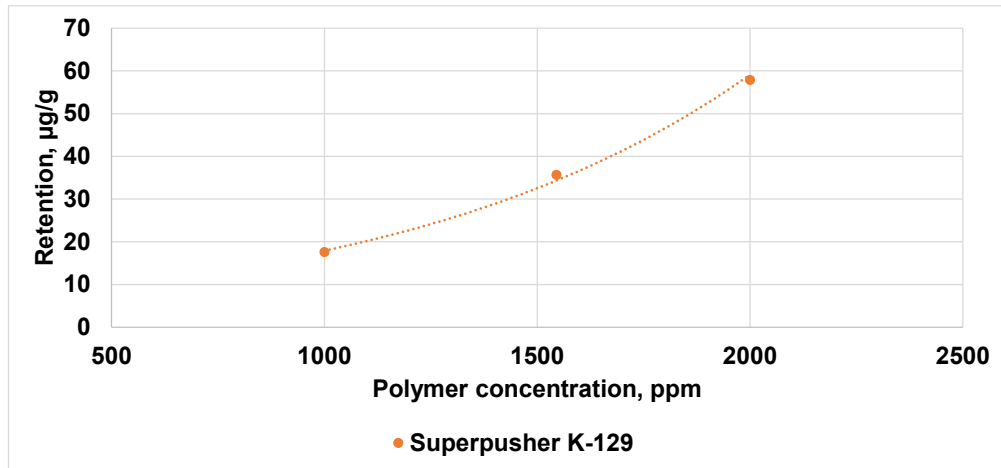
Figure 5.9 — Polymer retention test result

Polymer rheology. Polymer solution rheology was measured using a high-precision rheometer (Anton Paar MCR 502) at shear rates from 0-500 1/s, and reservoir temperature (40°C). As a solvent, we used formation water sampled from the field, which is used to prepare polymer solutions. Figure 5.10 plots rheology for 500-5000-ppm HPAM concentrations.
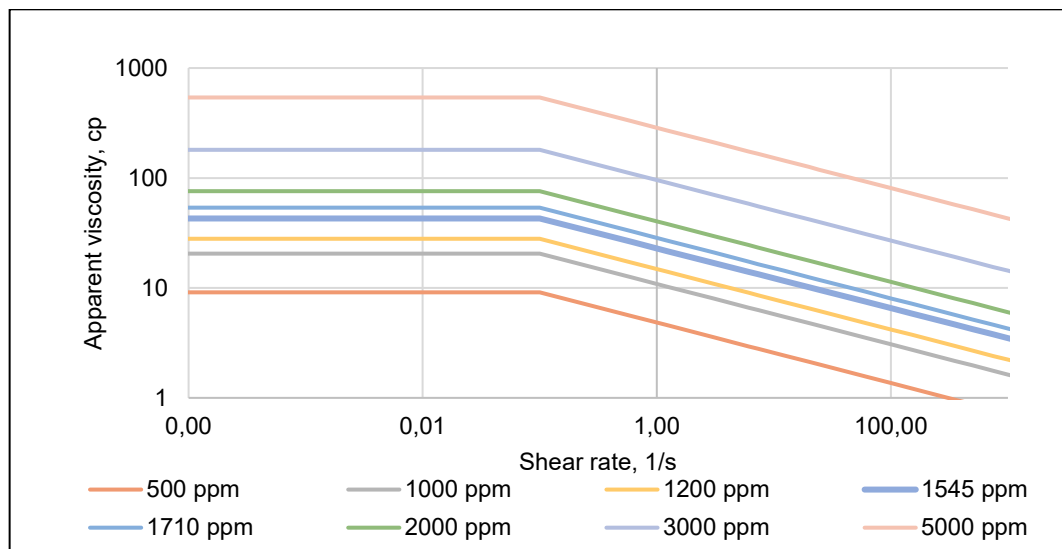
Figure 5.10 — Superpusher K-129 polymer rheology at reservoir conditions

Polymer induced fractures and their impact on the flood. Sagyndikov et al. (2022) [46] provided Kalamkas field evidence to clarify the utility of near-wellbore fractures to promote injectivity and mitigate mechanical degradation of HPAM solutions. Well tests (step rate and pressure fall-off test) indicated that fractures were not open during water injection before polymer injection. In contrast, open fractures were confirmed during polymer injection using well tests and comparison of actual injectivities versus those calculated using the Darcy radial flow equation coupled with laboratory measurements of HPAM rheology in Kalamkas cores. In addition, viscosity measurements of sampled solutions from polymer injectors showed the absence of mechanical degradation. This finding provided further confirmation that polymer injection occurred above the formation parting pressure and that the injection area associated with the fracture was large enough to ensure the stability of the solution. Thus our model assumed no mechanical degradation of polymer solutions and fracture flow near-wellbore. We used pressure fall-off test and inter-well test results to set fracture conductivity, half-length, (Figure 3.9, Table 3.7) and orientation (Figure 5.11, Figure 5.12).

Figure 5.11 — Setting fracture configuration to the model based on well tests, Injector XX41
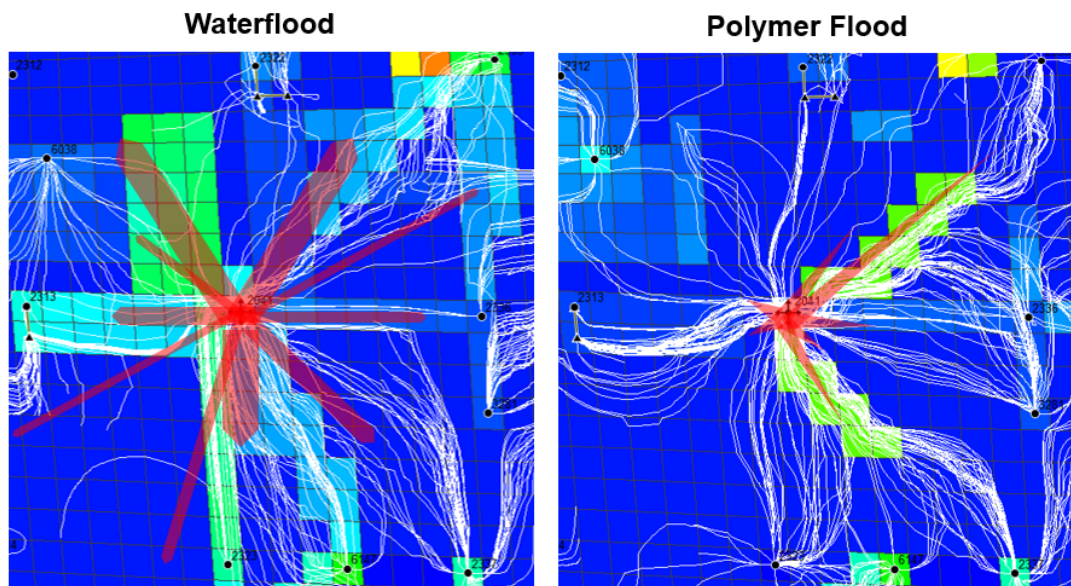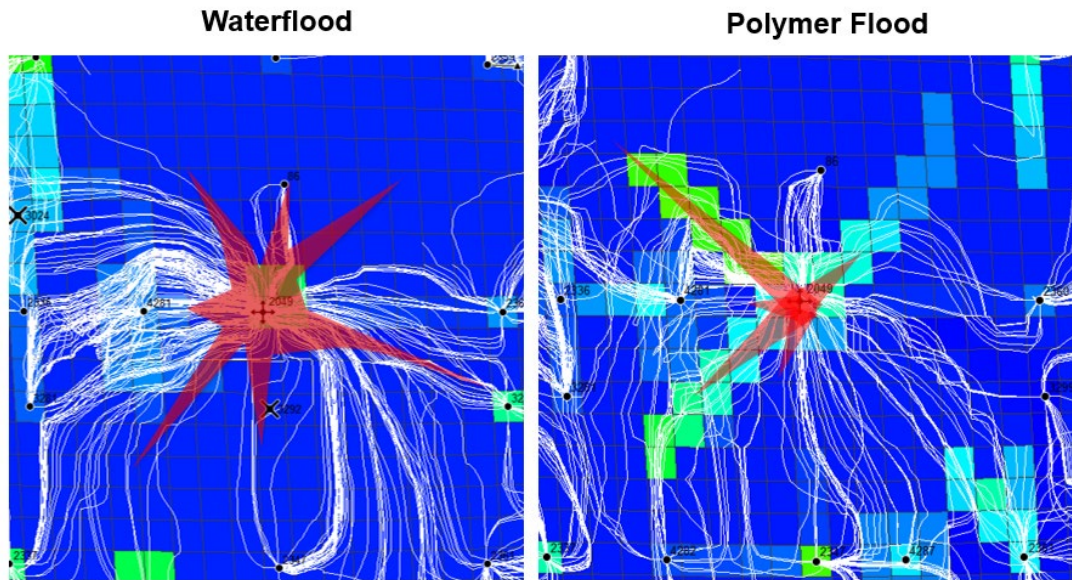
Figure 5.12 — Setting fracture configuration to the model based on well tests, Injector XX49

Injector Bottom-hole pressure (BHP) history matching. As shown on the left sides of Figure 5.13 and Figure 5.14, simulated BHP of the polymer injectors without fracture-like features shows a sharp increase, but this behavior is not observed in the field. In the previous section "Polymer induced fractures and their impact on the flooding", we demonstrated how to set fracture length and orientation. We used permeability as the main parameter to match the BHP. As a result, we obtained good history matching of BHP in polymer injectors, as shown on the right sides of Figure 5.13 and Figure 5.14.
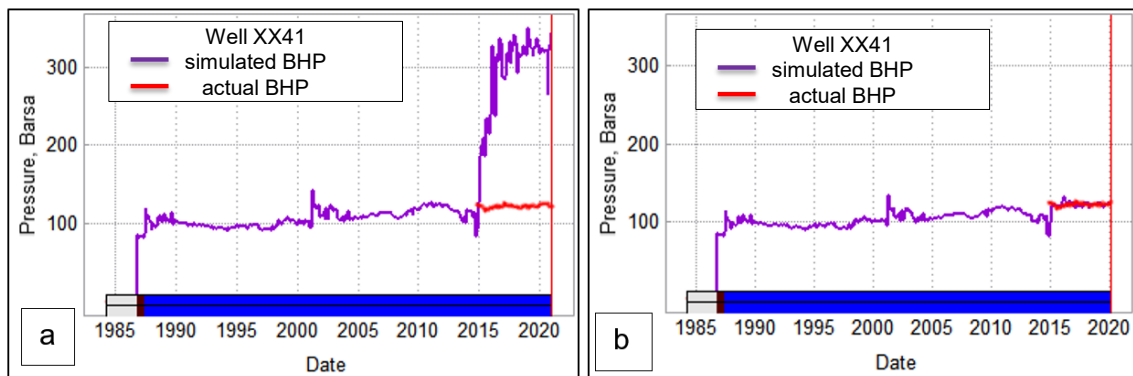
Figure 5.13 — BHP history matching for the Injector XX41 (left side: without fractures; right side: with fractures)
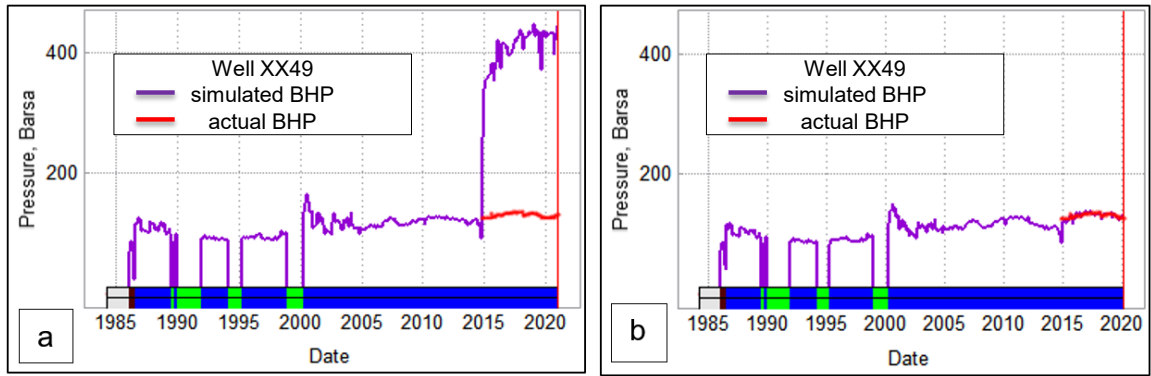
Figure 5.14 — BHP history matching for the Injector XX49 (left side: without fractures; right side: with fractures)

5.4 Results and discussions

Reservoir dynamic modeling shows satisfactory quality during the entire polymer flood period. Moreover, main parameters, such as liquid/oil rates and watercut, show minimum discrepancy. For example, at the end of the simulation period (Jan. 2020), the convergence on the oil rate was 99%, on the liquid rate – 98%, and watercut matches the actual 84% (Figure 5.15).
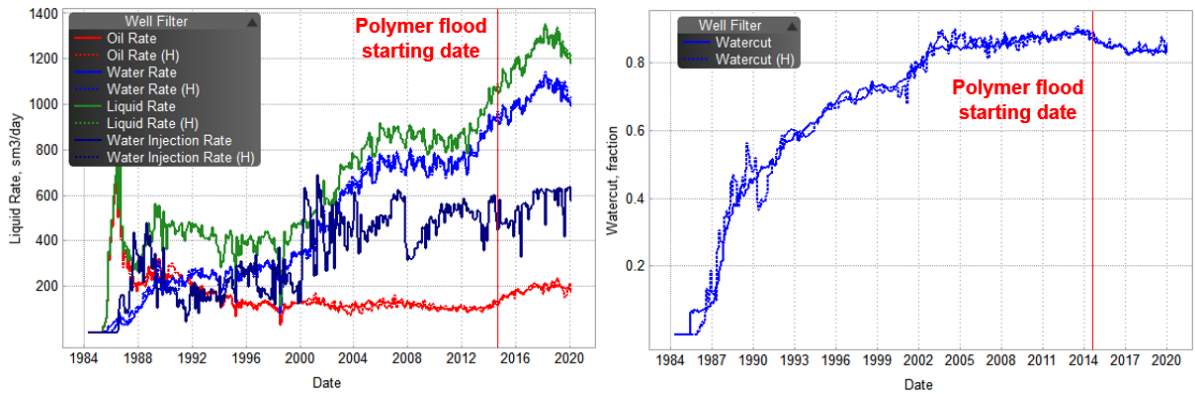
Figure 5.15 — Reservoir simulation history matching results

Model viability. We compared production forecast data and actual results for the 2020-2021 period to assess model viability (Figure 5.16). The forecast shows good convergence.
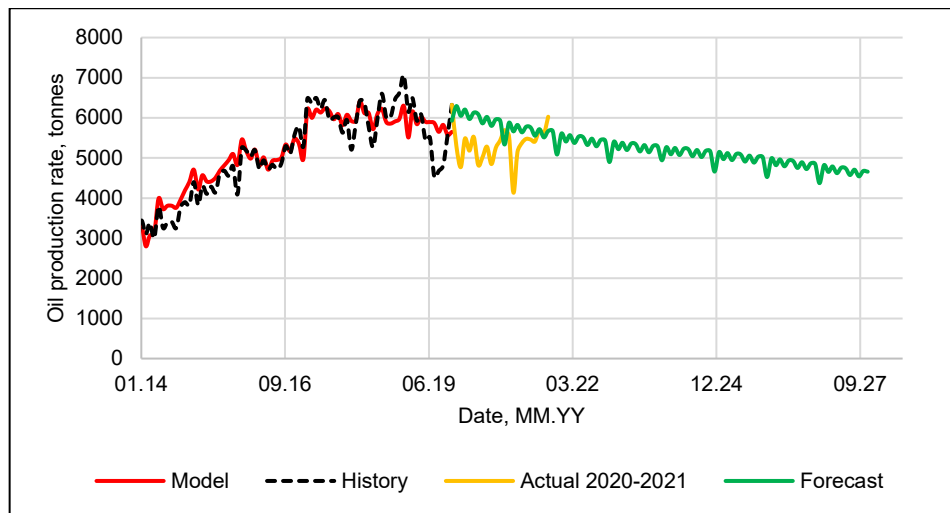
Figure 5.16 — Model forecast viability analysis

Optimization scenarios. After finishing the history matching work, we performed various simulation scenarios with different polymer concentrations, slug sizes, and injection rates. The forecast period was 10 years for all options, i.e., until 2029 (Figure 5.17, Figure 5.18, Figure 5.19). As shown in Figure 5.17, increasing polymer concentration (or viscosity) increases incremental oil production. However, extra expenditures related to additional polymer concentration lead to decreased net present value (NPV). In contrast, increasing the injection rate at a constant polymer concentration shows the same effect (Figure 5.18). In another case (Figure 5.19), assuming constant polymer consumption and making concentration & injection rate combination as variables, we can see that injection rate of 700-800 m^3/d and polymer concentration of 1.3-1.5 kg/sm^3 are the optimum ranges in terms of incremental oil production and NPV.

We also performed a simulation scenario with the optimum design (injection rate & polymer concentration) until ~110% pore volume (PV) was injected (Figure 5.20). This scenario aims to show an economically feasible project life, with at least 60% of PV injected when the oil price is 40$ USD per one barrel (the most pessimistic case). In contrast, the most optimistic view (90$/bbl) shows close to 70% of PV injected. Therefore, consistent with [116] and [52], our simulation studies reveal that polymer flood at oil price volatility is a long-term project that extends the field's economically feasible lifetime and enhances oil recovery.
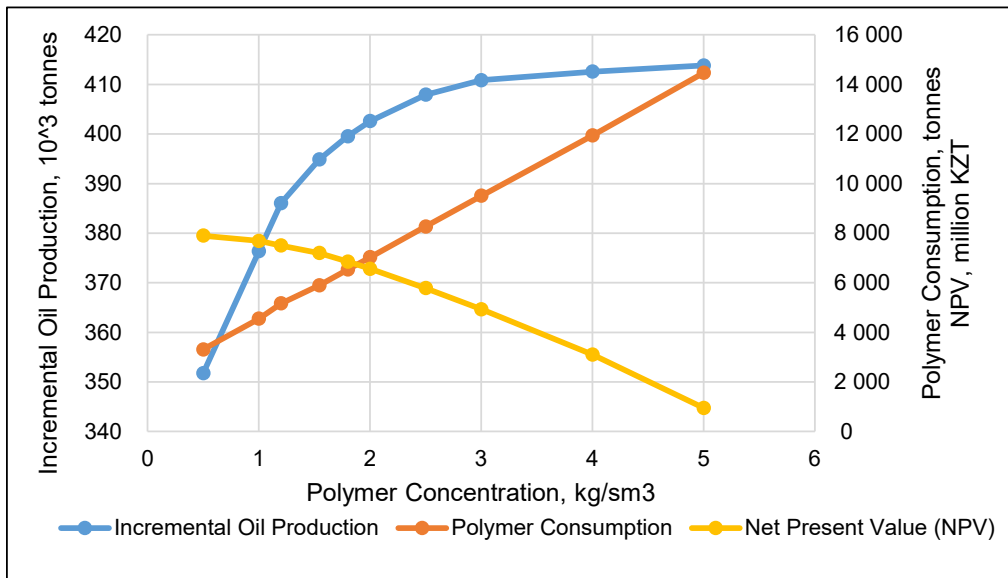
Figure 5.17 — Projected effect of polymer concentration
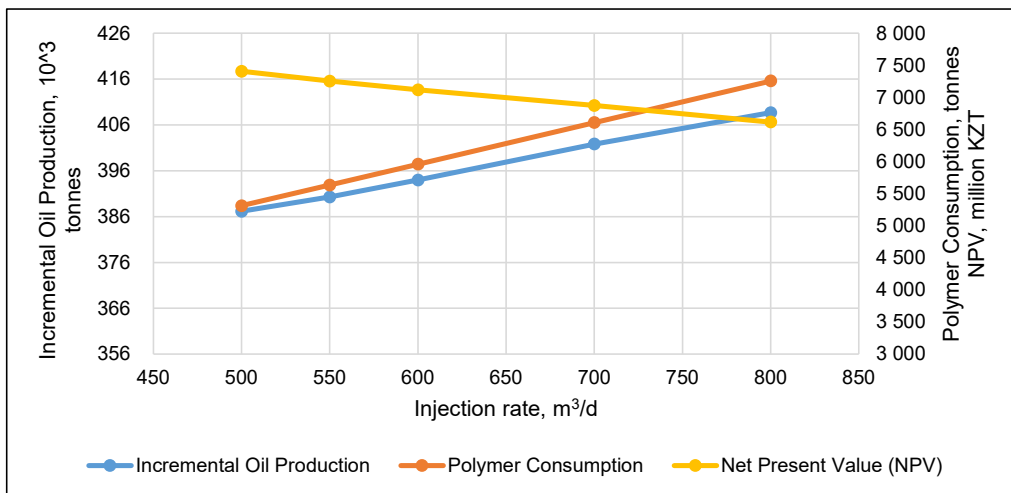
Figure 5.18 — Projected effect of injection rate
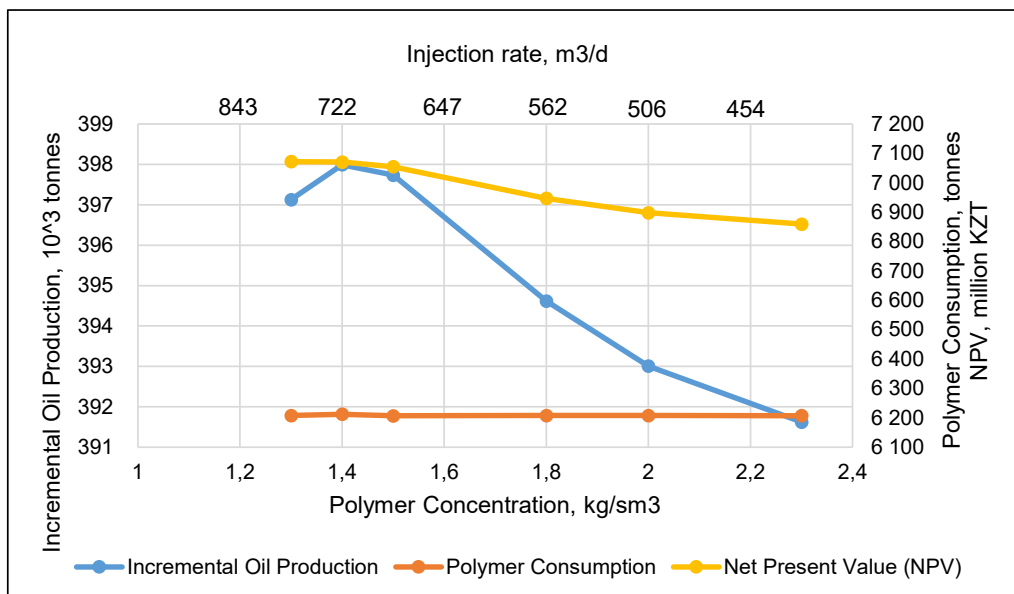
Figure 5.19 — Projected effect of polymer concentration and injection rate
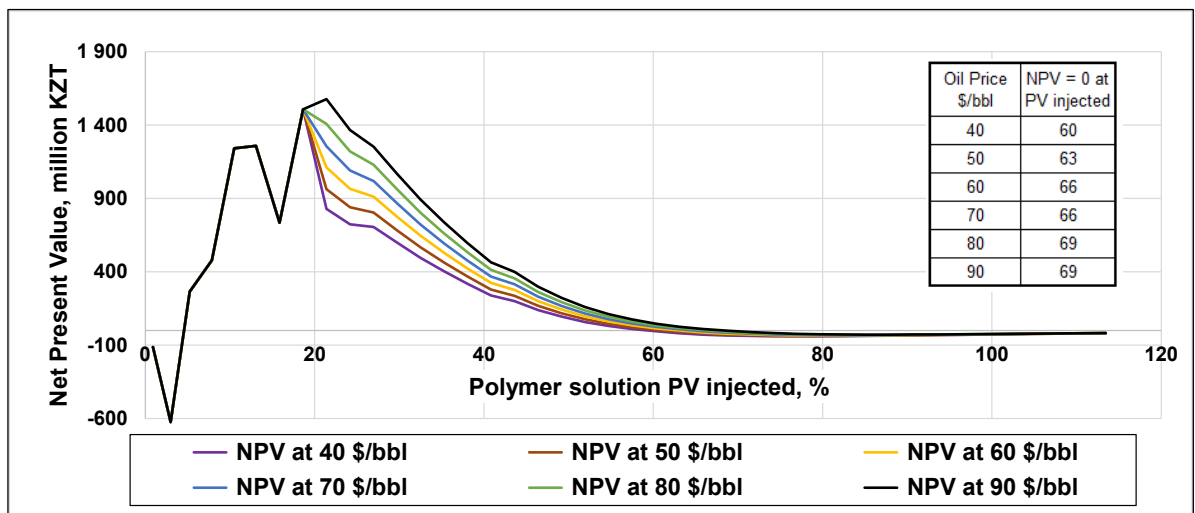
Figure 5.20 — Projected effect of oil price

Analytical equation to forecast a polymer flood. It is well known that the process of geological modeling and reservoir simulation requires enormous resources, including time, software, and electronic computing capacities. Additionally, the accuracy of the modeling depends on initial information and the quality of history matching. Therefore, to save time and accelerate the process of making a decision, we created five new synthetic areas (Figure 5.21) with different geological properties (net-to-gross, layering, formation height) and current reservoir conditions (productivity indexes variation, depletion intensity, watercut). The simulation results for six areas (existing pilot and 5 new) are shown in Figure 5.22, and the derived equation is shown in Equation (5.2). Equation (5.2) assumes that polymer concentration and injection rate are the same as in pilot wells pattern (XX41 and XX49).
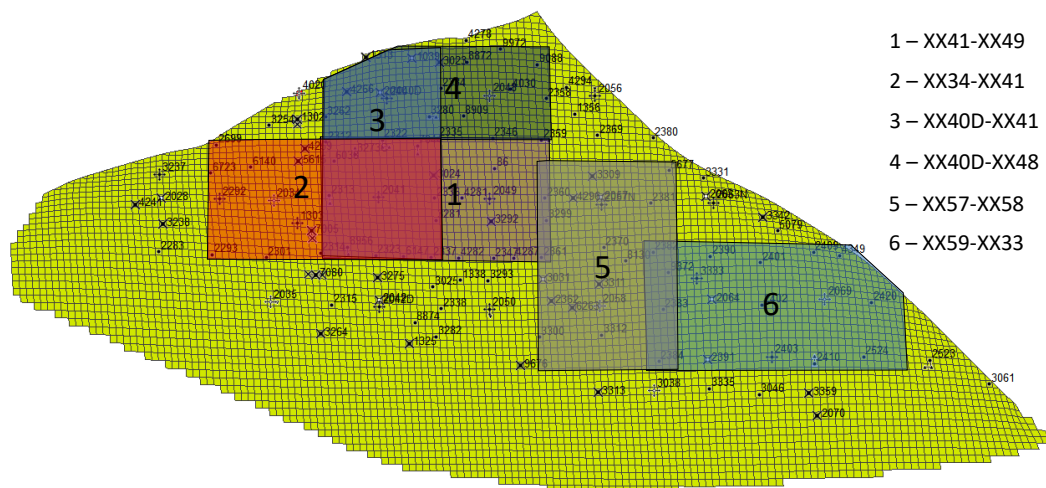
Figure 5.21 — Synthetic areas to simulate polymer flood at different geological and reservoir conditions
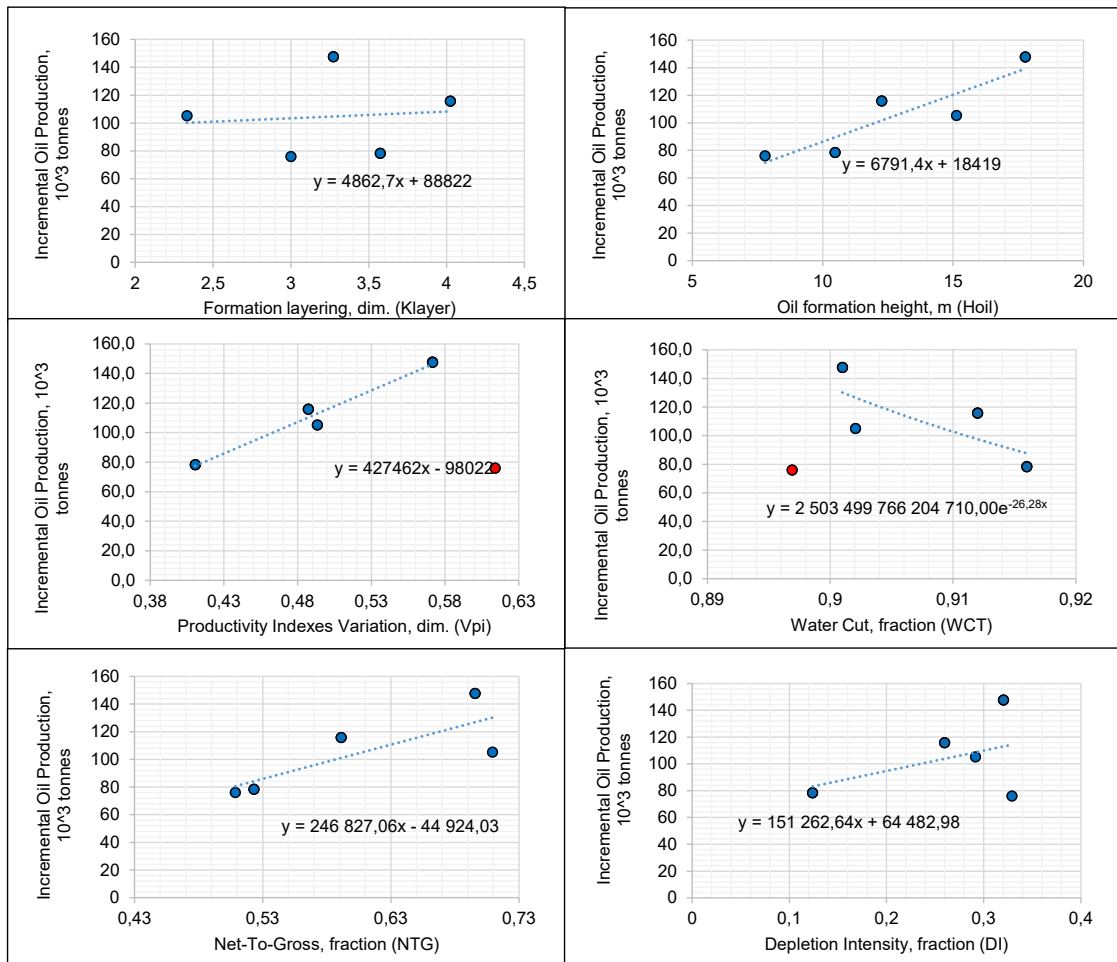
Figure 5.22 — Analytical equation to forecast polymer flooding

$$IOP = (4862.7 * K_{layer} + 6791 * H_{oil} - 246827 * NTG + 151262 * DI + 427462 * V_{PI} + 2.50E + 15 * exp(-2.63E + 01 * WCT)) + 28777 \div 6 \qquad (5.2)$$

where: IOP = incremental oil production for 5 years, thousand tonnes; K layer = formation layering or compartmentalization index, dim.; Hoil = oil formation height, m; NTG = net-to-gross, fraction; DI = depletion intensity (defined as a difference between depletion of recoverable reserves and watercut), fraction; V pi = productivity indexes variation, dim.; WCT = watercut, fraction.

Comparison of the actual (field-observed) oil production with predictions from Eq. 5.2 matched reasonably well for most wells (shown by the blue circles in Figure 5.22). In two wells (the red circles in Figure 5.22), the match was not as good. This equation allows easy predictions in place of the expense and effort required for simulation. Of course, the development of empirical relations like Eq. 5.2 must be obtained individually for different reservoirs.

5.5 Chapter Conclusions

1. An unconventional method for modeling a polymer flood was developed that accounts for more realistic conditions that occur during polymer injection into vertical wells. These conditions include (a) fractured injection wells, (b) no mechanical degradation of injected polymer solutions, (c) no significant permeability reduction caused by the injected polymer, and (d) no polymer inaccessible pore volume. This model was applied in the Kalamkas oil field.
2. The model focuses on history matching of bottom-hole injection pressures and forecasts far better than conventional models that assume no fractures are present.
3. The model correctly predicts very rapid deterioration of water cuts and oil production rates after switching from polymer back to water injection—better than conventional models that assume a significant permeability reduction by the polymer.
4. An empirical equation matched oil production reasonably well for most wells in six areas of the Kalamkas oil field. This equation allows easy predictions in place of the expense and effort required for simulation.
5. Given oil-price volatility, feasibility studies reveal that our polymer flood should be a long-term project that extends the field's economic lifetime and enhances oil recovery.

6. CONCLUSIONS

The goal of this Ph.D. thesis was to investigate polymer flood at the Kalamkas field to develop a systematic approach for improving technology. To achieve this, we analyzed Kalamkas oilfield development features and current stage of the polymer flood pilot, reviewed recent worldwide polymer EOR projects focusing on the Kalamkas field polymer flood aspects, assessed polyacrylamide solution chemical and mechanical stability, developed a novel method for the field assessment of polymer degradation, experimentally and numerically studied Kalamkas polymer flood implementation, and conducted project feasibility studies.

A field review shows that the Kalamkas oil reservoirs have a high layered permeability contrast and unfavorable water-oil mobility ratio, which jeopardizes uniform depletion and oil recovery. In view of the low reservoir temperature, elevated mobility ratio, and high formation permeability, it was recognized that the Kalamkas field has considerable potential for enhancing oil production by polymer flooding. Recent tertiary pilot results show positive performances. However, it still requires further investigation to provide improvements.

A comprehensive literature review shows that for the polymer flood project dissolved oxygen level should be as close to zero as practical – certainly less than 200 parts per billion. This technology can be applied in formations with any water salinity. However, practical considerations favor using the least saline water that is available. Field experience, as well as laboratory and theory, consistently reveal that the polymer bank size should be as large as practical (typically ~1 pore volume). Once the injection is switched from polymer back to water injection, water cuts will quickly rise to high values. Other chemical EOR such as ASP/SP flooding at the Kalamkas conditions will be too risky relative to polymer flood, especially in terms on-site production/injection problems and high cost of chemicals & water treatment. Using horizontal wells can greatly enhance polymer injectivity and control injection above the formation parting pressure.

Dedicated field polymer stability studies provides field evidence to clarify the utility of near wellbore fractures to promote injectivity and mitigate mechanical degradation of HPAM solutions. Also, we provided a new sampling methodology that demonstrated minimum mechanical and oxidative degradation under the Kalamkas field circumstances, whereas previous sampling methods may have provided overly pessimistic indications of HPAM stability. Also, the research provides additional field-based support that the dissolved oxygen of the injected polymer solution is effectively consumed by surrounding rock and provides further chemical stability in the Kalamkas formation. Based on field studies, we recommended modifying the East eductor injection unit to ensure an undetectable or acceptable oxygen level that will save 25% cost of chemicals.

An unconventional method for modeling a polymer flood was developed that accounts for more realistic conditions that occur during polymer injection into vertical wells. These conditions include (a) fractured injection wells, (b) no mechanical degradation of injected polymer solutions, (c) no significant

permeability reduction caused by the injected polymer, and (d) no polymer inaccessible pore volume. This model was applied in the Kalamkas oil field. Also, we developed an empirical equation for analytical forecasting of polymer flood performance based on geological parameters and reservoir dynamics. This analytical tool can be used for pattern selection and ranking during full field deployment.

Finally, feasibility studies show that at given oil-price volatility, the Kalamkas polymer flood should be a long-term project that extends the field's economic lifetime and enhances oil recovery.

REFERENCES

1. Alvarado, V., Manrique, E. (2010). Enhanced Oil Recovery: Field Planning and Development Strategies (1st ed.). Gulf Professional Publishing.
2. Sheng, J. (2010). Modern Chemical Enhanced Oil Recovery: Theory and Practice (1st ed.). Gulf Professional Publishing.
3. Lake, L. W. (1989). Enhanced Oil Recovery. Englewood Cliffs, New Jersey: Prentice-Hall Inc.
4. Kirkpatrick, R., Flanders, W., DePauw, R. (1985). Performance of the Twofreds CO2 Injection Project. SPE Annual Technical Conference and Exhibition, Las Vegas, Nevada, USA. SPE-14439-MS. https://doi.org/10.2118/14439-MS.
5. Pooladi-Darvish, M., Hong, H., Theys, S. O. P., Stocker, R., Bachu, S., Dashtgard, S. (2008). CO2 Injection for Enhanced Gas Recovery and Geological Storage of CO2 in the Long Coulee Glauconite F Pool, Alberta. SPE Annual Technical Conference and Exhibition, Denver, Colorado, USA. SPE-115789-MS. https://doi.org/10.2118/115789-MS.
6. Abou-Sayed, A. S., Zaki, K. S., Sarfare, M. D. (2005). An Assessment of Engineering, Economical and Environmental Drivers of Sour Gas Management by Injection. SPE International Improved Oil Recovery Conference in Asia Pacific, Kuala Lumpur, Malaysia. SPE-97628-MS. https://doi.org/10.2118/97628-MS.
7. Wilson, A. (2015). Tengiz Field Sector Model for IOR/EOR Process Evaluation. Journal of Petroleum Technology 67(01): 81–83. SPE-0115-0081-JPT. https://doi.org/10.2118/0115-0081-jpt.
8. Hao, H., Hou, J., Zhao, F., Huang, H., Wang, Z., Liu, H. (2019). Feasibility Study of Gas-EOR Using CO2 and N2 Mixture in a Heavy Oil Reservoir: Experiments and Pilot Test. Carbon Management Technology Conference, Houston, Texas, USA. CMTC-552521-MS. https://doi.org/10.7122/cmtc-552521-MS.
9. Wassmuth, F., Green, K., Arnold, W., Cameron, N. (2009). Polymer Flood Application to Improve Heavy Oil Recovery at East Bodo. Journal of Canadian Petroleum Technology 48(02): 55–61. PETSOC-09-02-55. https://doi.org/10.2118/09-02-55.
10. Delamaide, E., Bazin, B., Rousseau, D., Degre, G. (2014a). Chemical EOR for Heavy Oil: The Canadian Experience. SPE EOR Conference at Oil and Gas West Asia, Muscat, Oman. SPE-169715-MS. https://doi.org/10.2118/169715-MS.
11. Delamaide, E., Zaitoun, A., Renard, G., Tabary, R. (2014b). Pelican Lake Field: First Successful Application of Polymer Flooding In a Heavy-Oil Reservoir. SPE Reservoir Evaluation & Engineering 17(03): 340–354. SPE-165234-PA. https://doi.org/10.2118/165234-PA.

12. Jain, S., Prasad, D., Pandey, A., Koduru, N., Raj, R. (2020). Bhagyam ASP Pilot: Successful Formulation Development to Pilot Design and Planning. SPE Improved Oil Recovery Conference, Virtual. SPE-200408-MS. https://doi.org/10.2118/200408-MS.

13. Finol, J., Al-Harthy, S., Jaspers, H., Batrani, A., Al-Hadhrami, H., van Wunnik, J., Stoll, M., Faber, R., de Kruijf, A. (2012). Alkali-Surfactant-Polymer Flooding Pilot Test in Southern Oman. SPE EOR Conference at Oil and Gas West Asia, Muscat, Oman. SPE-155403-MS. https://doi.org/10.2118/155403-MS.

14. Volokitin, Y., Shuster, M., Karpan, V., Mikhaylenko, E., Koltsov, I., Rakitin, A., Tkachev, I., Salym, M. P. (2017). West Salym ASP Pilot: Surveillance Results and Operational Challenges. SPE Russian Petroleum Technology Conference, Moscow, Russia. SPE-187838-MS. https://doi.org/10.2118/187838-MS.

15. Guo, H., Li, Y., Li, Y., Kong, D., Li, B., Wang, F. (2017). Lessons Learned From ASP Flooding Tests in China. SPE Reservoir Characterisation and Simulation Conference and Exhibition, Abu Dhabi, UAE. SPE-186036-MS. https://doi.org/10.2118/186036-MS.

16. Sorbie, K. S. (1991). Polymer-Improved Oil Recovery (1991st ed.). Springer.

17. Willhite, P., Green, D. (2020). Enhanced Oil Recovery, Second Edition. Society of Petroleum Engineers.

18. Leibin, E.L., Ogay E.K. 1979. Technological scheme of the Kalamkas field development. KazNIPIneft report, Shevchenko (in Russian).

19. Wang, Dongmei, Han, Peihui, Shao, Zhenbo, Weihong, Hou, and Seright, R.S. 2008a. Sweep Improvement Options for the Daqing Oil Field. *SPE Res Eval & Eng* **11** (01): 18-26. SPE-99441-PA. https://doi.org/10.2118/99441-PA.

20. Wang, D., Seright, R., Shao, Z., and Wang, J. 2008b. Key Aspects of Project Design for Polymer Flooding at the Daqing Oil Field. *SPE Res Eval & Eng* **11**(6): 1117–1124. SPE-109682-PA. http://doi.org/10.2118/109682-PA.

21. Usachev, B.P., Sazonov, B.F., Shvetsov, I.A., Kukin V.V., Soliakov, U.V. 1985. Improving the method of polymer flooding in order to expand the area of its profitable use and increase efficiency. Research report #82.2525.85 Giprovostokneft (in Russian).

22. Svetsov, I.A. et al. 1985. Development and implementation of technology for the use of water-soluble polymers in the complicated geological and physical conditions of the Kalamkas oil field. Research report Girovostokneft (in Russian).

23. Abitova, A., Utkilbayev, N., Siziumova, V. et al. 2013. Development of treatment for conformance control of injection wells using thickened water at the Kalamkas field. Research report KazNIPImunaigas (in Russian).

24. Abitova, A., Utkilbayev, N., Siziumova, V. et al. 2014. Implementation of pilot testing of water flooding technology with increased viscosity of the displacing agent in the areas of the Kalamkas field. Research report KazNIPImunaigas (in Russian).

25. Sagyndikov, M., Mukhambetov, B., Orynbasar, Y., Nurbulatov, A., Aidarbayev, S. 2018. Evaluation of Polymer Flooding Efficiency at brownfield development stage of giant Kalamkas oilfield, Western Kazakhstan. Paper presented at the SPE Annual Caspian Technical Conference and Exhibition held in Astana, Kazakhstan, 31st October – 2nd November 2018. SPE-192555-MS. https://doi.org/10.2118/192555-MS.

26. Lotfollahi, Mohammad, Farajzadeh, Rouhi, Delshad, Mojdeh, Al-Abri, Al-Khalil, Wassing, Bart M., Al-Mjeni, Rifaat, Awan, Kamran, and Pavel Bedrikovetsky. 2016. Mechanistic Simulation of Polymer Injectivity in Field Tests. *SPE J.* **21**(3): 1178–1191. doi: https://doi.org/10.2118/174665-PA.

27. Skauge, T., Skauge, A., Salmo, I.C., Ormehaug, P.A., Al-Azri, N., Wassing, L.M., Glasbergen, G., Van Wunnik, J.N., and Masalmeh, S.K.. 2016. Radial and Linear Polymer Flow - Influence on Injectivity. Paper 179694-MS presented at the SPE Improved Oil Recovery Conference, Tulsa, Oklahoma, USA, 11-April. doi: https://doi.org/10.2118/179694-MS.

28. Asen, S.M., Stavland, A., Strand, D., Hiorth, A. 2019. An Experimental Investigation of Polymer Mechanical Degradation at the Centimeter and Meter Scale. *SPE J* **24** (4): 1700-1713. SPE-190225-PA. https://doi.org/10.2118/190225-PA.

29. Delamaide, E. 2019. How to Use Analytical Tools to Forecast Injectivity in Polymer Floods. Paper SPE-195513-MS Paper presented at the SPE Europec featured at 81st EAGE Conference and Exhibition, London, England, UK, June 2019. https://doi.org/10.2118/195513-MS.

30. Sagyndikov, M., Salimgarayev, I., Ogay, E., Seright, R.S., Kudaibergenov, S. (2022a). Assessing polyacrylamide solution chemical stability during a polymer flood in the Kalamkas field, Western Kazakhstan. Bulletin of the Karaganda University Chemistry Series 105(1). https://doi.org/10.31489/2022Ch1/99-112.

31. Seright, R. S., Campbell, A. R., Mozley, P. S., Han, P. (2010). Stability of Partially Hydrolyzed Polyacrylamides at Elevated Temperatures in the Absence of Divalent Cations. SPE Journal 15(02): 341–348. https://doi.org/10.2118/121460-PA.

32. Seright, R. S., Skjevrak, I. (2015). Effect of Dissolved Iron and Oxygen on Stability of Hydrolyzed Polyacrylamide Polymers. SPE Journal 20(03): 433–441. SPE-169030-PA. https://doi.org/10.2118/169030-PA.

33. Wilson, A. (2017). Challenges During Surface-Facility-Project Implementation for a Full-Field Polymer Flood. J Pet Technol 69 (6): 81-28. SPE-0617-0081-JPT. https://doi.org/10.2118/0617-0081-JPT.

34. Methodological guidelines for assessing the technological efficiency of application of enhanced oil recovery methods, RD-153-39.1-004 96. Moscow, 1996. (in Russian)

35. Sipachev, N. V., Posevich, A. G. 1981. On the characteristics of the displacement of oil by water. Izv. Vuzov Oil and gas. (in Russian)

36. Lysenko, V. D., Graifer, V. I. 2005. Rational Development of Oil Reservoirs. Moscow, NEDRA. (in Russian)

37. Boyko, V. S. 1990. Development and operation of oil fields. Nedra § 1.6 p. 29-32. (in Russian)

38. Program of pilot works on the testing of polymer flooding technology in areas of the Kalamkas field. 2017. Technical report of KazNIPImunaygas LLP, Aktau 2017, p. 105-119. (in Russian)

39. Ryles, R. G. (1988). Chemical Stability Limits of Water-Soluble Polymers Used in Oil Recovery Processes. SPE Reservoir Engineering 3(01): 23–34. SPE-13585-PA. https://doi.org/10.2118/13585-PA.

40. Moradi-Araghi, A., Doe, P. H. (1987). Hydrolysis and Precipitation of Polyacrylamides in Hard Brines at Elevated Temperatures. SPE Reservoir Engineering 2(02): 189–198. SPE-13033-PA. https://doi.org/10.2118/13033-PA.

41. Levitt, D., Pope, G. A. (2008). Selection and Screening of Polymers for Enhanced-Oil Recovery. SPE Symposium on Improved Oil Recovery, Tulsa, Oklahoma, USA. SPE-113845-MS. https://doi.org/10.2118/113845-MS.

42. Diab, W. N., Al-Shalabi, E. W. (2019). Recent Developments in Polymer Flooding for Carbonate Reservoirs under Harsh Conditions. Offshore Technology Conference Brasil, Rio de Janeiro, Brazil. OTC-29739-MS. https://doi.org/10.4043/29739-MS.

43. Gaillard, N., Giovannetti, B., Leblanc, T., Thomas, A., Braun, O., Favero, C. (2015). Selection of Customized Polymers to Enhance Oil Recovery from High Temperature Reservoirs. SPE Latin American and Caribbean Petroleum Engineering Conference, Quito, Ecuador. SPE-177073-MS. https://doi.org/10.2118/177073-MS.

44. Seright, R.S., Wavrik, K.E., Zhang, G., AlSofi, A.M. (2021). Stability and Behavior in Carbonate Cores for New EOR Polymers at Elevated Temperatures in Hard Saline Brines. SPE Reservoir Evaluation & Engineering 24(1): 1-18. SPE-200324-PA. https://doi:10.2118/200324-PA.

45. Ispanbetov, T. (2019). Polymer flooding in Zaburunje and Moldabek fields, Kazakhstan (in Russian).

46. Sagyndikov, M., Seright, R., Kudaibergenov, S., Ogay, E. (2022b). Field Demonstration of the Impact of Fractures on Hydrolyzed Polyacrylamide Injectivity, Propagation, and Degradation. SPE Journal 27(02): 999–1016. SPE-208611-PA. https://doi.org/10.2118/208611-PA.

47. Sagyndikov, M., Seright, R., Tuyakov, N. (2022c). An Unconventional Approach to Model a Polymer Flood in the Kalamkas Oilfield. SPE Improved Oil Recovery Conference, Virtual. SPE-209355-MS. https://doi.org/10.2118/209355-MS.

48. Chauveteau, G., Kohler, N. (1974). Polymer Flooding: The Essential Elements for Laboratory Evaluation. SPE Improved Oil Recovery Symposium, Tulsa, Oklahoma. SPE-4745-MS. https://doi.org/10.2118/4745-MS.

49. Wang, D., Dong, H., Lv, C., Fu, X., Nie, J. (2009). Review of Practical Experience by Polymer Flooding at Daqing. SPE Reservoir Evaluation & Engineering 12 (03): 470–476. SPE-114342-PA. https://doi.org/10.2118/114342-PA.

50. Song, H., Ghosh, P., Mejia, M., Mohanty K. Polymer Transport in Low-Permeability Carbonate Rocks. SPE Reservoir Evaluation & Engineering 14 (01). SPE-206024-PA. https://doi.org/10.2118/206024-PA.

51. Telkov, V. (2016). A new vision of polymer flooding as method of high-viscous oil displacement. International scientific conference "Geopetrol 2016", Krakow, Poland.

52. Seright, R. S. (2017). How Much Polymer Should Be Injected During a Polymer Flood? Review of Previous and Current Practices. SPE Journal 22(01): 1–18. SPE-179543-PA. https://doi.org/10.2118/179543-PA.

53. Thakuria, C., Al-Amri, M. S., Al-Saqri, K. A., Jaspers, H. F., Al-Hashmi, K. H., Zuhaimi, K. (2013). Performance Review of Polymer Flooding in a Major Brown Oil Field of Sultanate of Oman. SPE Enhanced Oil Recovery Conference, Kuala Lumpur, Malaysia. SPE-165262-MS. https://doi.org/10.2118/165262-MS.

54. Guntupalli, S., Kechichian, J., Al-Yaarubi, A., Al-Amri, A., Al-Amri, M., Al-Hinai, G., Al-Shuaili, K., Svec, Y., al Habsi, Y. (2018). A Successful ASP Sweep Evaluation in a Field Pilot. SPE EOR Conference at Oil and Gas West Asia, Muscat, Oman. SPE-190462-MS. https://doi.org/10.2118/190462-MS.

55. Choudhuri, B., Thakuria, C., Belushi, A. A., Nurzaman, Z., Hashmi, K. A., Batycky, R. (2015). Optimization of a Large Polymer Flood With Full-Field Streamline Simulation. SPE Reservoir Evaluation & Engineering 18(03): 318–328. SPE-169746-PA. https://doi.org/10.2118/169746-PA.

56. Ning, S., Barnes, J., Edwards, R., Dunford, K., Eastham, K., Dandekar, A., Zhang, Y., Cercone, D., Ciferno, J. (2019). First Ever Polymer Flood Field Pilot to Enhance the Recovery of Heavy Oils on Alaska's North Slope—Polymer Injection Performance. SPE/AAPG/SEG Unconventional Resources Technology Conference, Denver, Colorado, USA. URTEC-2019-643-MS. https://doi.org/10.15530/urtec-2019-643.

57. Dandekar, A., Bai, B., Barnes, J., Cercone, D., Ciferno, J., Ning, S., Seright, R., Sheets, B., Wang, D., Zhang, Y. (2019). First Ever Polymer Flood Field Pilot - A Game Changer to Enhance the Recovery of Heavy Oils on Alaska's North Slope. SPE Western Regional Meeting, San Jose, California, USA. SPE-195257-MS. https://doi.org/10.2118/195257-MS.

58. Zhao, Y., Yin, S., Seright, R. S., Ning, S., Zhang, Y., Bai, B. (2020). Performance of Low Salinity Polymer Flood in Enhancing Heavy Oil Recovery on the Alaska North Slope. SPE/AAPG/SEG Unconventional Resources Technology Conference, Virtual. URTEC-2020-1082-MS. https://doi.org/10.15530/urtec-2020-1082.

59. Poulsen, A., Shook, G. M., Jackson, A., Ruby, N., Charvin, K., Dwarakanath, V., Thach, S., Ellis, M. (2018). Results of the UK Captain Field Interwell EOR Pilot. SPE Improved Oil Recovery Conference, Tulsa, Oklahoma, USA. SPE-190175-MS. https://doi.org/10.2118/190175-MS.

60. Jones, C., Ross, M., Getliff, J., Fuller, M., Hiscox, I., Mandracchia, F. (2015). Captain Field Injector Performance, Historical Perspective and Recent Improvements. SPE European Formation Damage Conference and Exhibition, Budapest, Hungary. SPE-174183-MS. https://doi.org/10.2118/174183-MS.

61. Jackson, A. C., Dean, R. M., Lyon, J., Dwarakanath, V., Alexis, D., Poulsen, A., Espinosa, D. (2019). Surfactant Stimulation Results in Captain Field to Improve Polymer Injectivity for EOR. SPE Offshore Europe Conference and Exhibition, Aberdeen, UK. SPE-195747-MS. https://doi.org/10.2118/195747-MS.

62. Morel, D. C., Jouenne, S., VERT, M., Nahas, E. (2008). Polymer Injection in Deep Offshore Field: The Dalia Angola Case. SPE Annual Technical Conference and Exhibition, Denver, Colorado, USA. SPE-116672-MS. https://doi.org/10.2118/116672-MS.

63. Morel, D. C., Vert, M., Jouenne, S., Gauchet, R., Bouger, Y. (2012). First Polymer Injection in Deep Offshore Field Angola: Recent Advances in the Dalia/Camelia Field Case. Oil and Gas Facilities 1(02): 43–52. SPE-135735-PA. https://doi.org/10.2118/135735-PA.

64. Demin, W., Gang, W., Huifen, X. (2011). Large Scale High Viscous-Elastic Fluid Flooding in the Field Achieves High Recoveries. SPE Enhanced Oil Recovery Conference, Kuala Lumpur, Malaysia. SPE-144294-MS. https://doi.org/10.2118/144294-MS.

65. Gao, C. H. (2014). Experiences of Polymer Flooding Projects at Shengli Oilfield. SPE EOR Conference at Oil and Gas West Asia, Muscat, Oman. SPE-169652-MS. https://doi.org/10.2118/169652-MS.

66. He, J., Song, Z., Qiu, L., Xie, F., Tan, Z., Yue, Q., Li, X. (1998). High Temperature Polymer Flooding in Thick Reservoir in ShuangHe Oilfield. SPE International Oil and Gas Conference and Exhibition in China, Beijing, China. SPE-50933-MS. https://doi.org/10.2118/50933-MS.

67. Guo, Y., Zhang, J., Liu, Y., Liu, G., Xue, X., Luo, P., Ye, Z., Zhang, X., Liang, Y. (2020). Successful Scale Application of Associative Polymer Flooding for Offshore Heavy Oilfield in Bohai Bay of China. SPE/IATMI Asia Pacific Oil & Gas Conference and Exhibition, Bali, Indonesia. SPE-196467-MS. https://doi.org/10.2118/196467-MS.

68. Delamaide, E., Soe Let, K. M., Bhoendie, K., Jong-A-Pin, S., Paidin, W. R. (2016). Results of a Polymer Flooding Pilot in the Tambaredjo Heavy Oil Field, Suriname. SPE Canada Heavy Oil Technical Conference, Calgary, Alberta, Canada. SPE-180739-MS. https://doi.org/10.2118/180739-MS.

69. Ilyasov, I., Gudz, A., Podkorytov, A., Komarov, V., Glushchenko, N. (2020). Results of the First Polymer Flooding Pilot at East-Messoyakhskoe Oil Field. SPE Russian Petroleum Technology Conference, Virtual. SPE-201822-MS. https://doi.org/10.2118/201822-MS.

70. Clemens, T., Deckers, M., Kornberger, M., Gumpenberger, T., Zechner, M. (2013). Polymer Solution Injection – Near Wellbore Dynamics and Displacement Efficiency, Pilot Test Results, Matzen Field, Austria. EAGE Annual Conference & Exhibition incorporating SPE Europec, London, UK. SPE-164904-MS. https://doi.org/10.2118/164904-MS.

71. Lüftenegger, M., Kadnar, R., Puls, C., Clemens, T. (2015). Operational Challenges and Monitoring of a Polymer Pilot, Matzen Field, Austria. EUROPEC 2015, Madrid, Spain. SPE-174350-MS. https://doi.org/10.2118/174350-MS.

72. Chiotoroiu, M. M., Peisker, J., Clemens, T., Thiele, M. R. (2017). Forecasting Incremental Oil Production of a Polymer-Pilot Extension in the Matzen Field Including Quantitative Uncertainty Assessment. SPE Reservoir Evaluation & Engineering 20(04): 0894–0905. SPE-179546-PA. https://doi.org/10.2118/179546-PA.

73. Melo, M. A., Lins, A. G., Silva, I. P. (2017). Lessons Learned From Polymer Flooding Pilots in Brazil. SPE Latin America and Caribbean Mature Fields Symposium, Salvador, Bahia, Brazil. SPE-184941-MS. https://doi.org/10.2118/184941-MS.

74. Melo, M. A., Holleben, C. R., Silva, I. G., de Barros Correia, A., Silva, G. A., Rosa, A. J., Lins, A. G., & de Lima, J. C. (2005). Evaluation of Polymer-Injection Projects in Brazil. SPE Latin American and Caribbean Petroleum Engineering Conference, Rio de Janeiro, Brazil. SPE-94898-MS. https://doi.org/10.2118/94898-MS.

75. Buciak, J., Fondevila Sancet, G., del Pozo, L. (2014). Polymer-Flooding-Pilot Learning Curve: Five-Plus Years' Experience To Reduce Cost per Incremental Barrel of Oil. SPE Reservoir Evaluation & Engineering 18(01): 11–19. SPE-166255-PA. https://doi.org/10.2118/166255-PA.

76. Pozo, L. D., Daparo, W. D., Fernandez, G., Carbonetti, J. (2018). Implementing a Field Pilot Project for Selective Polymer Injection in Different Reservoirs. SPE Improved Oil Recovery Conference, Tulsa, Oklahoma, USA. SPE-190205-MS. https://doi.org/10.2118/190205-MS.

77. Hryc, A., Hochenfellner, F., Best, R. O., Maler, S., Freedman, P. (2018). Development of a Field Scale Polymer Project in Argentina. SPE Improved Oil Recovery Conference, Tulsa, Oklahoma, USA. SPE-190326-MS. https://doi.org/10.2118/190326-MS.

78. Hryc, A., Hochenfellner, F., Best, R. O., Maler, S., Puliti, R. (2016). Evaluation of a Polymer Injection Pilot in Argentina. SPE Latin America and Caribbean Heavy and Extra Heavy Oil Conference, Lima, Peru. SPE-181210-MS. https://doi.org/10.2118/181210-MS.

79. Ogezi, O., Strobel, J., Egbuniwe, D., Leonhardt, B. (2014). Operational Aspects of a Biopolymer Flood in a Mature Oilfield. SPE Improved Oil Recovery Symposium, Tulsa, Oklahoma, USA. SPE-169158-MS. https://doi.org/10.2118/169158-MS.

80. Watson, A., Trahan, G. A., Sorensen, W. (2014). An Interim Case Study of an Alkaline-Surfactant-Polymer Flood in the Mooney Field, Alberta, Canada. SPE Improved Oil Recovery Symposium, Tulsa, Oklahoma, USA. SPE-169154-MS. https://doi.org/10.2118/169154-MS.

81. Saboorian-Jooybari, H., Dejam, M., Chen, Z. (2015). Half-Century of Heavy Oil Polymer Flooding from Laboratory Core Floods to Pilot Tests and Field Applications. SPE Canada Heavy Oil Technical Conference, Calgary, Alberta, Canada. SPE-174402-MS. https://doi.org/10.2118/174402-MS.

82. Liu, J. Z., Adegbesan, K., Bai, J. J. (2012). Suffield Area, Alberta, Canada – Caen Polymer Flood Pilot Project. SPE Heavy Oil Conference Canada, Calgary, Alberta, Canada. SPE-157796-MS. https://doi.org/10.2118/157796-MS.

83. Irvine, R., Davidson, J., Edwards, S., Kingsbury, J., Hui-June, P., Tardiff, C. (2012). Case Study of Polymer Flood Pilot in a Low Permeability Mannville Sand of the Western Canadian Sedimentary Basin Using Produced Water for Blending. SPE Improved Oil Recovery Symposium, Tulsa, Oklahoma, USA. SPE-154050-MS. https://doi.org/10.2118/154050-MS.

84. Delaplace, P., Delamaide, E., Roggero, F., Renard, G. (2013). History Matching of a Successful Polymer Flood Pilot in the Pelican Lake Heavy Oil Field, Canada. SPE Annual Technical Conference and Exhibition, New Orleans, Louisiana, USA. SPE-166256-MS. https://doi.org/10.2118/166256-MS.

85. Prasad, D., Pandey, A., Kumar, M. S., Koduru, N. (2014). Pilot to Full-Field Polymer Application in One of the Largest Onshore Field in India. SPE Improved Oil Recovery Symposium, Tulsa, Oklahoma, USA. SPE-169146-MS. https://doi.org/10.2118/169146-MS.

86. Kumar, M. S., Pandey, A., Jha, M. K. (2012). Polymer Injectivity Test in Mangala Field - A Significant Step towards Field Wide Implementation. SPE Oil and Gas India Conference and Exhibition, Mumbai, India. SPE-155162-MS. https://doi.org/10.2118/155162-MS.

87. Kumar, P., Raj, R., Koduru, N., Kumar, S., Pandey, A. (2016). Field Implementation of Mangala Polymer Flood: Initial Challenges, Mitigation and Management. SPE EOR Conference at Oil and Gas West Asia, Muscat, Oman. SPE-179820-MS. https://doi.org/10.2118/179820-MS.

88. Baloch, S., Leon, J., Masalmeh, S., Chappell, D., Brodie, J., Romero, C., al Mazrouei, S., al Tenaiji, A., al Balooshi, M., Igogo, A., Azam, M., Maheshwar, Y., Dupuis, G. (2021). Expanding Polymer Injectivity Tests on a Second Giant Carbonate UAE Oil Reservoir at High Salinity & High Temperature Conditions. Abu Dhabi International Petroleum Exhibition & Conference, Abu Dhabi, UAE. SPE-207498-MS. https://doi.org/10.2118/207498-MS.

89. Gaillard, N., Giovannetti, B., Favero, C. (2010). Improved Oil Recovery using Thermally and Chemically Protected Compositions Based on co- and ter-polymers Containing Acrylamide. SPE Improved Oil Recovery Symposium, Tulsa, Oklahoma, USA. SPE-129756-MS. https://doi.org/10.2118/129756-MS.

90. Vermolen, E. C., van Haasterecht, M. J., Masalmeh, S. K., Faber, M. J., Boersma, D. M., Gruenenfelder, M. (2011). Pushing the Envelope for Polymer Flooding Towards High-temperature and High-salinity Reservoirs with Polyacrylamide Based Ter-polymers. SPE Middle East Oil and Gas Show and Conference, Manama, Bahrain. SPE-141497-MS. https://doi.org/10.2118/141497-MS.

91. Rodriguez, L., Antignard, S., Giovannetti, B., Dupuis, G., Gaillard, N., Jouenne, S., Bourdarot, G., Morel, D., Zaitoun, A., Grassl, B. (2018). A New Thermally Stable Synthetic Polymer for Harsh Conditions of Middle East Reservoirs: Part II. NMR and Size Exclusion Chromatography to Assess Chemical and Structural Changes During Thermal Stability Tests. SPE Improved Oil Recovery Conference, Tulsa, Oklahoma, USA. SPE-190200-MS. https://doi.org/10.2118/190200-MS.

92. Moore, J. K. (1969). "Reservoir Barrier and Polymer Waterflood: Northeast Hallsville Crane Unit," J. Pet. Tech.: 1130-1136.

93. Szabo, M. (1975). Laboratory Investigations of Factors Influencing Polymer Flood Performance. Society of Petroleum Engineers Journal 15(04): 338–346. SPE-4669-PA. https://doi.org/10.2118/4669-PA.

94. Kamal, M.S., Sultan, A.S., et al. (2015). Review on Polymer Flooding: Rheology, Adsorption, Stability, and Field Applications of Various Polymer Systems. Polymer Reviews, 55:3, 491-530. DOI: 10.1080/15583724.2014.982821

95. Jeanes, A., Pittsley, J. E. and Senti, F. R. (1961) J. Appl. Polym. Sci., 5: 519-526.

96. Lipton, D. (1974). Improved Injectability of Biopolymer Solutions. Fall Meeting of the Society of Petroleum Engineers of AIME, Houston, Texas. SPE-5099-MS. https://doi.org/10.2118/5099-MS.

97. Dominguez, J., Willhite, G. (1977). Retention and Flow Characteristics of Polymer Solutions in Porous Media. Society of Petroleum Engineers Journal 17(02): 111–121. SPE-5835-PA. https://doi.org/10.2118/5835-PA.

98. Yang, F., Wang, D., Yang, X., Sui, X., Chen, Q., Zhang, L. (2004). High Concentration Polymer Flooding is Successful. SPE Asia Pacific Oil and Gas Conference and Exhibition, Perth, Australia. SPE-88454-MS. https://doi.org/10.2118/88454-MS.

99. Clarke, A., Howe, A. M., Mitchell, J., Staniland, J., Hawkes, L. A. (2015). How Viscoelastic Polymer Flooding Enhances Displacement Efficiency. SPE Asia Pacific Enhanced Oil Recovery Conference, Kuala Lumpur, Malaysia. SPE-174654-MS. https://doi.org/10.2118/174654-MS.

100. Alagic, E., Dopffel, N., Bødtker, G., Hovland, B., Mukherjee, S., Kumar, P., Dillen, M. (2020). Biodegradation Mitigation and Protection Strategies for the Biopolymer Schizophyllan. SPE Europec, Virtual. SPE-200562-MS. https://doi.org/10.2118/200562-MS.

101. Elhossary, D. A., Sebastian, A., Alameri, W., Al-Shalabi, E. W. (2021). Bulk Rheology and Injectivity Assessments of Potential Biopolymer and Synthetic Polymer for Applications in Carbonates Under Harsh Conditions. Abu Dhabi International Petroleum Exhibition & Conference, Abu Dhabi, UAE. SPE-208105-MS. https://doi.org/10.2118/208105-MS.

102. Al-Murayri, M. T., Kamal, D. S., Garcia, J. G., Al-Tameemi, N., Driver, J., Hernandez, R., Fortenberry, R., Britton, C. (2018). Stability of Biopolymer and Partially Hydrolyzed Polyacrylamide in Presence of H2S and Oxygen. SPE Annual Technical Conference and Exhibition, Dallas, Texas, USA. SPE-191581-MS. https://doi.org/10.2118/191581-MS.

103. Abbas, S., Sanders, A. W., Donovan, J. C. (2013). Applicability of Hydroxyethylcellulose Polymers for Chemical EOR. SPE Enhanced Oil Recovery Conference, Kuala Lumpur, Malaysia. SPE-165311-MS. https://doi.org/10.2118/165311-MS.

104. Seright, R. S., Seheult, M., Talashek, T. (2009). Injectivity Characteristics of EOR Polymers. SPE Reservoir Evaluation & Engineering 12(05): 783–792. SPE-115142-PA. https://doi.org/10.2118/115142-PA.

105. Wang, Z., Zhang, J., Jiang, Y. (1988). Evaluation Of Polymer Flooding In Daqing Oil Field And Analysis Of Its Favourable Conditions. International Meeting on Petroleum Engineering, Tianjin, China. SPE-17848-MS. https://doi.org/10.2118/17848-MS.

106. Manichand, R. N., Moe Soe Let, K. P., Gil, L., Quillien, B., Seright, R. S. (2013). Effective Propagation of HPAM Solutions Through the Tambaredjo Reservoir During a Polymer Flood. SPE International Symposium on Oilfield Chemistry, The Woodlands, Texas, USA. SPE-164121-MS. https://doi.org/10.2118/164121-MS.

107. Zhao, Y., Yin, S.Z., Seright, R.S., Ning, S., Zhang, Y., Bai, B.J. (2020). Enhancing Heavy-Oil-Recovery Efficiency by Combining Low-Salinity-Water and Polymer Flooding. SPE J. 26 (3): 1535-1551. SPE-204220-PA. https://doi.org/10.2118/204220-PA.

108. Jouenne, S., Klimenko, A., Levitt, D. (2016). Polymer Flooding: Establishing Specifications for Dissolved Oxygen and Iron in Injection Water. SPE J. 22(2): 438-446. SPE-179614-PA. https://doi.org/10.2118/179614-PA.

109. Ma, Y., McClure, M. W. (2016). The Effect of Polymer Rheology and Induced Fracturing on Injectivity and Pressure-Transient Behavior. SPE Reservoir Evaluation & Engineering 20(02): 394–402. SPE-184389-PA. https://doi.org/10.2118/184389-PA.

110. Khodaverdian, M. F., Sorop, T., Postif, S. J., van den Hoek, P. J. (2009). Polymer Flooding in Unconsolidated Sand Formations: Fracturing and Geomechanical Considerations. EUROPEC/EAGE Conference and Exhibition, Amsterdam, The Netherlands. SPE-121840-MS. https://doi.org/10.2118/121840-MS.

111. Van den Hoek, P. J., Al-Masfry, R. A., Zwarts, D., Jansen, J. D., Hustedt, B., van Schijndel, L. (2009). Optimizing Recovery for Waterflooding Under Dynamic Induced Fracturing Conditions. SPE Reservoir Evaluation & Engineering 12(05): 671–682. SPE-110379-PA. https://doi.org/10.2118/110379-PA.

112. Van den Hoek, P. J., Mahani, H., Sorop, T. G., Brooks, A. D., Zwaan, M., Sen, S., Shuaili, K., Saadi, F. (2012). Application of Injection Fall-Off Analysis in Polymer flooding. SPE Europec/EAGE Annual Conference, Copenhagen, Denmark. SPE-154376-MS. https://doi.org/10.2118/154376-MS.

113. Thomas, A., Giddins, M., Wilton, R. (2019). Why is it so Difficult to Predict Polymer Injectivity in Chemical Oil Recovery Processes? IOR 2019 – 20th European Symposium on Improved Oil Recovery. https://doi.org/10.3997/2214-4609.201900114.

114. Volokitin, Y., Shuster, M., Karpan, V., et al. (2018). Results of Alkaline-Surfactant-Polymer Flooding Pilot at West Salym Field. Paper presented at the SPE EOR Conference at Oil and Gas West Asia, Muscat, Oman. SPE-190382-MS. https://doi.org/10.2118/190382-MS

115. Sorbie, K., Seright, R. (1992). Gel Placement in Heterogeneous Systems With Crossflow. SPE/DOE Enhanced Oil Recovery Symposium, Tulsa, Oklahoma. SPE-24192-MS. https://doi.org/10.2118/24192-MS.

116. Sheng, J. J., Leonhardt, B., Azri, N. (2015). Status of Polymer-Flooding Technology. Journal of Canadian Petroleum Technology 54(02): 116–126. SPE-174541-PA. https://doi.org/10.2118/174541-PA.

117. Taber, J., Martin, F., and Seright, R. 1997. EOR Screening Criteria Revisited Part 1: Introduction to Screening Criteria and Enhanced Recovery Field Projects. SPE Res Eng 12(3): 189-198. SPE-35385-PA. https://doi.org/10.2118/35385-PA.

118. Clark, S. R., Pitts, M. J., Smith, S. M. (1993). Design and Application of an Alkaline-Surfactant-Polymer Recovery System for the West Kiehl Field. SPE Advanced Technology Series 1(01): 172–179. SPE-17538-PA. https://doi.org/10.2118/17538-PA.

119. Wang, Z., Pang, R., Le, X., Peng, Z., Hu, Z., Wang, X. (2013). Survey on injection–production status and optimized surface process of ASP flooding in industrial pilot area. Journal of Petroleum Science and Engineering 111:178–183. https://doi.org/10.1016/j.petrol.2013.09.010.

120. Aitkulov, A., Dao, E., Mohanty, K. K. (2018). ASP Flood After a Polymer Flood vs. ASP Flood After a Water Flood. SPE Improved Oil Recovery Conference, Tulsa, Oklahoma, USA. SPE-190271-MS. https://doi.org/10.2118/190271-MS.

121. Healy, R., Reed, R., Stenmark, D. (1976). Multiphase Microemulsion SysteMS. Society of Petroleum Engineers Journal 16(03): 147–160. SPE-5565-PA. https://doi.org/10.2118/5565-PA.

122. Nelson, R., Pope, G. (1978). Phase Relationships in Chemical Flooding. Society of Petroleum Engineers Journal 18(05): 325–338. SPE-6773-PA. https://doi.org/10.2118/6773-PA.

123. Windsor, P. A. (1954). Solvent Properties of Amphiphillic Compounds. London: Butterworth Scientific Publication

124. He, L., Gang, C., Guochen, S. (2007). Technical Breakthrough in PCPs' Scaling Issue of ASP Flooding in Daqing Oilfield. SPE Annual Technical Conference and Exhibition, Anaheim, California, USA. SPE-109165-MS. https://doi.org/10.2118/109165-MS.

125. Pandey, A., Koduru, N., Stanley, M., Pope, G. A., Weerasooriya, U. P. (2016). Results of ASP Pilot in Mangala Field: A Success Story. SPE Improved Oil Recovery Conference, Tulsa, Oklahoma, USA. SPE-179700-MS. https://doi.org/10.2118/179700-MS.

126. Jiecheng, C., Wanfu, Z., Qingguo, W., Gang, C., Wenguang, B., Changming, Z., Meie, L. (2014). Technical Breakthrough in Production Engineering Ensures Economic Development of ASP Flooding in Daqing Oilfield. SPE Asia Pacific Oil & Gas Conference and Exhibition, Adelaide, Australia. SPE-171506-MS. https://doi.org/10.2118/171506-MS.

127. Dean, E., Pitts, M., Wyatt, K., James, D., Mills, K., Al-Murayri, M., Al-Kharji, A. (2020). Practical Chemical Formulation Design – Time to Break Away from Micellar Polymer Floods, Again. SPE Improved Oil Recovery Conference, Virtual. SPE-200385-MS. https://doi.org/10.2118/200385-MS.

128. Gao, S., He, Y., Zhu, Y., Han, P., Peng, S., Liu, X. (2020). Associated Polymer ASP Flooding Scheme Optimization Design and Field Test after Polymer Flooding in Daqing Oilfield. SPE Improved Oil Recovery Conference, Virtual. SPE-200443-MS. https://doi.org/10.2118/200443-MS.

129. Pandey, A., Beliveau, D., Corbishley, D. W., Suresh Kumar, M. (2008). Design of an ASP Pilot for the Mangala Field: Laboratory Evaluations and Simulation Studies. SPE Indian Oil and Gas Technical Conference and Exhibition, Mumbai, India. SPE-113131-MS. https://doi.org/10.2118/113131-MS.

130. Maerker, J.M. 1975. Shear Degradation of Partially Hydrolyzed Polyacrylamide Solutions. SPE J. 15 (4): 311-322. SPE-5101-PA. https://doi.org/10.2118/5101.

131. Seright, R.S. 1983. The Effects of Mechanical Degradation and Viscoelastic Behaviour on Injectivity of Polyacrylamide Solutions. SPE J. 23 (3): 475-485. SPE-9297-PA. https://doi.org/10.2118/9297-PA.

132. Zhang, J. 1995. The EOR Technology. Beijing: Petroleum Industry Publishing Company of China.

133. Shao, Z.B, Zhou, J.S., Sung, G., Niu, J.G, Liu, F.Q., Han, Z.R. 2005. Studies on Mechanical Degradation of Partially Hydrolyzed Polyacrylamide in Course of Polymer Flooding: Changes in Relative Molecular Mass, Viscosity and Related Parameters. Oilfield Chemistry. 22(1). 25th March 2005. 72-77.

134. You, Q., F.L., Wang, Y.F., and Mu, L.N. 2007. Comparison of the Properties of Injected and Released Polyacrylamide in Polymer Flooding. Journal of Beijing University of Chemical Technology. 34 (4) 2007.414-417.

135. Putz, A.G., Bazin, B, and Pedron, B.M. 1994. Commercial Polymer Injection in the Courtenay Field, 1994 Update. Paper presented at the 1994 Annual Technical Conference and Exhibition New Orleans, LA. 25-28 September. SPE-28601-MS. https://doi.org/10.2118/28601-MS.

136. Shupe, R.D. 1981. Chemical Stability of Polyacrylamide Polymers. J Pet Technol 33(8): 1513–1529. SPE-9299-PA. https://doi.org/10.2118/9299-PA.

137. Yang, S.H. and Treiber, L.E. 1985. Chemical Stability of Polyacrylamide Under Simulated Field Conditions. Paper presented at the SPE Annual Technical Conference and Exhibition, Las Vegas, Nevada, 22–25 September. SPE-14232-MS. https://doi.org/10.2118/14232-MS.

138. Morris, C.W., Jakson, K.M. 1978. Mechanical Degradation of Polyacrylamide Solutions in Porous Media. Paper presented at the 5th Symposium on Improved Methods for Oil Recovery of the SPE of AIME held in Tulsa, Oklahoma, USA, 16 – 19 April 1978. SPE-7064-MS. https://doi.org/10.2118/7064-MS.

139. American Petroleum Institute RECOMMENDED PRACTICE 63 (API RP 63), 1990. Recommended Practices for Evaluation of Polymers Used in Enhanced Oil Recovery Operations.

140. Noik, Ch., Delaplace, Ph., Muller, G. 1995. Physico-Chemical Characteristics of Polyacrylamide Solutions after Mechanical Degradation through a Porous Medium. Paper presented at the SPE International Symposium on Oilfield Chemistry held in San Antonio, Texas, USA, 14 – 17 February 1995. SPE-28954. https://doi.org/10.2118/28954-MS.

141. Seright, R.S., Fan, T., Wavrik, K., and Balaban, R.C. 2011. New Insights into Polymer Rheology in Porous Media. SPE J. 16 (1): 35-42. SPE-129200-PA. https://doi.org/10.2118/129200-PA.

142. Puls, C., Clemens, T., Sledz, C., Kadnar, R., Gumpenberger, T. 2016. Mechanical Degradation of Polymers During Injection, Reservoir Propagation and Production – Field Test Results 8 TH Reservoir, Austria. Paper presented at the SPE Europec featured at 78th EAGE Conference & Exhibition held in Vienna, Austria, 30th May – 2nd June 2016. SPE-180144-MS. https://doi.org/10.2118/180144-MS.

143. Garrepally, S., Jouenne, S., Leuqeux, F., Olmsted, P.D. 2020. Polymer Flooding – Towards a Better Control of Polymer Mechanical Degradation at the Near Wellbore. Paper presented at the SPE Improved Oil Recovery Conference originally scheduled to be held in Tulsa, OK, USA, 18 - 22 April 2020. Due to COVID-19 the physical event was postponed until 31st August – 4th September 2020 and was changed to a virtual event. SPE-200373-MS. https://doi.org/10.2118/200373-MS.

144. Xue, X., Han M., Zhang L., Gao, J., Liu, Y., Zhang, J. 2012. The down hole sampling investigation of polymer solutions in Bohai oilfield. China Offshore Oil and Gas J. 24 (5): 37-39.

145. Morel, D.C., Zaugg, E., Jouenne, J.A., Danquigny, J.A., Cordelier, P.R. 2015. Dalia/Camelia Polymer Injection in Deep Offshore Field Angola Learnings and In Situ Polymer Sampling Results. Paper presented at the SPE Enhanced Oil Recovery Conference held in Kuala Lumpur, Malaysia, 11 - 13 August 2015. SPE-174699-MS. https://doi.org/10.2118/174699-MS.

146. Xue, X., Han M., Zhang L., Gao, J., Liu, Y., Zhang, J. 2012. The down hole sampling investigation of polymer solutions in Bohai oilfield. China Offshore Oil and Gas J. 24 (5): 37-39.

147. Dandekar, A., Bai, B., Barnes, J., Cercone, D., Ciferno, J., Edwards, R., Ning, S., Schulpen, W., Seright., R., Sheets, B., Wang, D., Zhang, Y. 2021. First Ever Polymer Flood Field To Enhance The Recovery Of Heavy Oils On Alaska's North Slope - Pushing Ahead One Year Later. Paper SPE 200814 presented at the SPE Western Regional Meeting. Bakersfield, California. 20-22 April. https://doi.org/10.2118/195257-MS.

148. Seright, R. & Brattekas, B. 2021. Water Shutoff and Conformance Improvement: An Introduction. Petroleum Science (4th February) 1-29. doi: 10.1007/s12182-021-00546-1

149. Dauben, D.L., and Menzie,D.E. 1967. Flow of Polymer Solutions Through Porous Media. J Pet Technol 19 (8): 1065–1073. https://doi.org/10.2118/1688-PA.

150. Hirasaki, G.J. and Pope, G.A. 1974. Analysis of Factors Influencing Mobility and Adsorption in the Flow of Polymer Solution Through Porous Media. SPE J. 14 (4): 337-346. SPE-4026-PA. https://doi.org/10.2118/4026-PA.

151. Heemskerk, J., Rosmalen, R, Janssen-van, R., Holtslag, R.J., and Teeuw, D. 1984. Quantification of Viscoelastic Effects of Polyacrylamide Solutions. Paper presented at the SPE Enhanced Oil Recovery Symposium, Tulsa, Oklahoma, 15th April 1984. https://doi.org/10.2118/12652-MS.

152. Lotfollahi, M., Farajzadeh, R., and Delshad, M. 2016. Mechanistic Simulation of Polymer Injectivity in Field Tests. SPE J. 21 (4): 1178–1191. SPE-174665-PA. https:// doi. org/ 10. 2118/ 174665- PA.

153. Tai, I., Giddins, M.A., Muggeridge, A. 2021. Improved Calculation of Wellblock Pressures for Numerical Simulation of Non-Newtonian Polymer Injection. SPE J. 22(5): 2352-2363. SPE-205339-PA. https://doi.org/10.2118/205339-PA.

154. Horne, R. A. and Johnson, D. S. 2002. The Viscosity of Water Under Pressure. J Phys Chem 70 (7): 2182–2190. https:// doi. org/ 10. 1021/ j100879a018.

155. Moe Soe Let, K. P., Manichand, R. N., and Seright, R. S. 2012. Polymer Flooding a ~500-Cp Oil. Paper presented at the Eighteenth SPE Improved Oil Recovery Symposium, Tulsa, Oklahoma, USA, 14–18 April. SPE-154567-MS. https:// doi. org/ 10. 2118/ 154567- MS.

156. Houze, O., Viturat, D., Fjaere, O.S. et al. 2020. Dynamic Data Analysis. v5.30.01. KAPPA.

157. Dyes, A. B., Kemp, C.E. and Caudle, B.H. 1958. Effect of Fractures on Sweep-Out Pattern. In Petroleum Transactions, AIME, Vol. 213, 245-249, SPE-1071-G. Richardson, Texas: SPE.

158. Vitor, H. S. Ferreira & Rosangela, B. Moreno, Z. L. (2017). Polyacrylamide Mechanical Degradation and Stability in the Presence of Iron. Offshore Technology Conference, Rio de Janeiro, Brazil. OTC-27953-MS. https://doi.org/10.4043/27953-MS.

159. Jouenne, S., Chakibi, H., Levitt, D. (2017). Polymer Stability After Successive Mechanical-Degradation Events. SPE J 23 (1): 18-33. SPE-186103-PA. https://doi.org/10.2118/186103-PA.

160. Xu, T., White, S.P., Pruess, K., & Brimhall, G. (2000). Modeling Pyrite Oxidation in Saturated and Unsaturated Subsurface Flow Systems. Transport in Porous Media 39: 25–5S6.

161. Sulin, V.A. (1946). Waters of Petroleum Formations in the System of Nature Waters. Gostoptekhizdat, Moscow, 96. (in Russian).

162. Levitt, D.B., Slaughter, W., Pope, G.A. et al. (2011). The Effect of Redox Potential and Metal Solubility on Oxidative Polymer Degradation. SPE Res Eval & Eng 14 (3): 287-298. SPE-129890-PA. http://dx.doi.org/10.2118/129890-PA.

163. Wellington, S.L. (1983). Biopolymer Solution Viscosity Stabilization—Polymer Degradation and Antioxidant Use. SPE J. 23 (6): 901-912. SPE-9296-PA. http://dx.doi.org/10.2118/9296-PA.

164. Pye, D. J. (1964). Improved Secondary Recovery by Control of Water Mobility. J Pet Technol 16 (8): 911-916. SPE-845-PA. http://dx.doi.org/10.2118/845-PA.

165. Smith, F. W. (1970). The Behavior of Partially Hydrolyzed Polyacrylamide Solutions in Porous Media. J Pet Technol 22 (2): 148-156. SPE-2422-PA. http://dx.doi.org/! 0.2118/2422-PA.

166. Jennings, R. R., Rogers, J. H. and West, T. J. (1971). Factors Influencing Mobility Control by Polymer Solutions. J Pet Technol 23 (3): 391-401. SPE-2867-PA. http://dx.doi.org/10.2118/2867-PA.

167. Manichand, R.N., and Seright, R.S. (2014). Field vs Laboratory Polymer Retention Values for a Polymer Flood in the Tambaredjo Field. SPE Res Eval & Eng. 17(3): 314-325. doi.org/10.2118/169027-PA.

168. Wang, D., Li, C., & Seright, R.S. (2020). Laboratory Evaluation of Polymer Retention in a Heavy Oil Sand for a Polymer Flooding Application on Alaska's North Slope. SPE Journal 25(4) 1842-1856. doi:10.2118/200428-PA.

APPENDICES

APPENDIX A

КАЗАҚСТАН РЕСПУБЛИКАСЫ   РЕСПУБЛИКА КАЗАХСТАН

REPUBLIC OF KAZAKHSTAN

ПАТЕНТ
PATENT

№ 7054

ПАЙДАЛЫ МОДЕЛЬГЕ / НА ПОЛЕЗНУЮ МОДЕЛЬ / FOR UTILITY MODEL

(21) 2021/1103.2

(22) 06.12.2021

(45) 29.04.2022

(54) Мұнай кенорнында полимерлік суландыру кезіндегі полимердің деструкциясын кәсіптік зерттеу тәсілі
Способ промыслового исследования деструкции полимера при полимерном заводнении нефтяной залежи
Method for the field assessment of polymer degradation during a polymer flood of oil reservoir

(73) Сагындиков Марат Серикович (KZ)
Sagyndikov Marat Serikovich (KZ)

(72) Сагындиков Марат Серикович (KZ)   Sagyndikov Marat Serikovich (KZ)
Иманбаев Бакыт Алтаевич (KZ)   Imanbayev Bakyt Altayevich (KZ)
Байпаков Саттибек Шаймурзаевич (KZ)   Baipakov Sattibek Shaimurzaevich (KZ)
Салимгараев Ильшат Искандарович (KZ)   Salimgaraev Ilshat Iskandarovich (KZ)

ЭЦҚ қол қойылды   А. Естаев
Подписано ЭЦП   А. Естаев
Signed with EDS   A. Yestayev

«Ұлттық зияткерлік меншік институты» РМК директорының м.а.
И.о. директора РГП «Национальный институт интеллектуальной собственности»
Executive director of RSE «National institute of intellectual property»

Согласовано:
Директор департамента геологии и
разработки месторождений
АО «Мангистаумунайгаз»
_____ Байпаков С.

Заместитель директора департамента
геологии и разработки месторождений
АО «Мангистаумунайгаз»
_____ Цао Кэчуань

Начальник ПУ «КМГ»
_____ Сарсенбай Н.М./
                     Нургабылов М.К.

Главный геолог ПУ «КМГ»
_____ Койшыбаев Б.Т./
  29.05.2020   Цюй Яньмин

Директор департамента повышения
нефтеотдачи пластов и перспективных
проектов «КазНИПИмунайгаз»
_____ Мухамбетов Б.Т.

УТВЕРЖДАЮ:
И.о. заместителя генерального директора
по геологии и разработке
_____ Лю Дунчжоу
«_____» _____ 2020 г.

ПЛАН
проведения отбора глубинных проб
жидкости из нагнетательной скважины №1124
месторождение Каламкас (участок ПЗ Восток Расширение)

Цель работ: Определение степени механической деструкции полимерного раствора, нагнетательной скважины 1124, методом замера реологических характеристик отбираемой закаченной жидкости в процессе плановой технологической остановки скважины и реверсивным само подъёмом жидкости на устье.

Задачи работ:
- Расчет возможности реверсивного подъема закачиваемой жидкости из пласта на устье скважины.
- Проведение обвязки скважины с насосным агрегатом и по интервальный отбор проб жидкости в специализированные герметичные пробоотборники производства SNF.
- Проведение реологических исследований отобранных проб полимерного раствора с целью определения степени механической деструкции.
- Отчет по результатам проведенных работ.

Основные результаты работы:
- Определение степени механической деструкции полимерного раствора скважины 1124.

Компания: АО «Мангистаумунайгаз»

Производственный объект: месторождение «Каламкас».

Основание: НИР «Концепция расширения технологии полимерного заводнения по месторождению Каламкас» (Заказ-наряд №25, Приложение №4-25).

Номер и дата договора: № 279-14 от «19» марта 2020г.

Акт
о проведенных отборах глубинных проб
жидкости из нагнетательной скважины №1124
месторождение Каламкас (участок ПЗ Восток Расширение)

(на двух листах)

от «_12_» _августа_ 2020г.

Составлен представителями:

от ПУ «Каламкасмунайгаз»:

Нач. ОГ и АРМ   Спанов А.К.
(должность, Ф.И.О., Подпись)

Зам. нач-ка ЦППД   Сарсенбайұлы С.
(должность, Ф.И.О., Подпись)

от Филиала ТОО «КМГ Инжиниринг»«КазНИПимунайгаз»:

инженер лаборатории Тленов А.С.
(должность, Ф.И.О., Подпись)

в том, что «_12_» _августа_ 2020г. проведен и в 10:45 закончен отбор глубинных проб жидкости из нагнетательной скважины №1124 месторождения Каламкас (участок ПЗ Восток Расширение). Отбор выполнен на самоизливе со скважины в количестве _7_ проб с целью оценки механической деструкции полимера при плановой остановке скважины. Работы выполнены на основании документа «**План проведения отбора глубинных проб жидкости из нагнетательной скважины №1124 месторождение Каламкас (участок ПЗ Восток Расширение)**» от 29.05.2020г.

Хронометраж отборов:

п/п пробоотборника	Достигнутый объем слитой жидкости в мерник, м³	Время завершения отбора	Комментарий
1	1,2	9:30	
2	2,4	9:50	
3	2,5	10:00	
4	2,9	10:10	
5	3,2	11:20	
6	3,6	10:35	
7	4	10:45	

Давление до начала отборов на остановленной скважине составило 48 атм. Давление после излива 4 м³ жидкости и завершения отборов достигло 10 атм.

Страница **1** из **2**

107

Отклонения при отборе проб:

Скорость изливаемого объема жидкости под давлением в скважине превышала возможности планового отбора проб. Попытка частичного перекрытия комплектной задвижки на агрегате насосном вызвала её отказ напором жидкости. Частичное же перекрытие задвижек до отбора проб может вызвать деструкцию полимера, что нарушит чистоту эксперимента. По этим причинам на месте принято согласованное решение вести отбор периодически с полным открытием задвижки на фонтанной арматуре (ФА) и крана в установленном пробоотборнике, изливом до нужного объема, закрытием крана на пробоотборнике, закрытием задвижки на ФА с последующей заменой пробоотборника и повторением цикла.

Подписи:
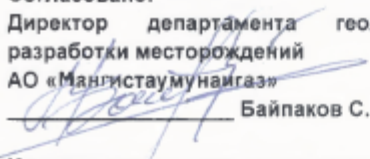от ПУ «Каламкасмунайгаз»: / _____ Спанов А.К.

/ _____ Сарсенбаулы С.

от Филиала ТОО «КМГ Инжиниринг»«КазНИПимунайгаз»:

/ Плеков А. / _____

Согласовано:
Директор департамента геологии и
разработки месторождений
АО «Мангистаумунайгаз»
_____ Байпаков С.

УТВЕРЖДАЮ:
Заместитель генерального директора
по геологии и разработке
_____ Цао Кэчуань
«____» _____ 2020 г.

И.о. заместителя директора департамента
геологии и разработки месторождений
АО «Мангистаумунайгаз»
_____ Хань Сяофэн

Начальник ПУ «КМГ»
_____ Сарсенбай Н.М./
Ян Лисинь
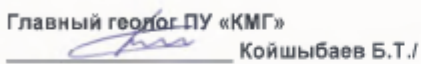
Главный геолог ПУ «КМГ»
_____ Койшыбаев Б.Т./
14. 10. 2020   Цюй Яньмин

Эксперт по ПНП Департамента по
разработке «КазНИПИмунайгаз»
_____ Сагындиков М.С.

ПЛАН
проведения отбора глубинных проб
жидкости из нагнетательной скважины №1141
месторождение Каламкас (участок ПЗ Восток Расширение)

Цель работ: Определение степени механической деструкции полимерного раствора, нагнетательной скважины 1141, методом замера реологических характеристик отбираемой закаченной жидкости в процессе плановой технологической остановки скважины и реверсивным само подъёмом жидкости на устье.

Задачи работ:

- Расчет возможности реверсивного подъема закачиваемой жидкости из пласта на устье скважины.

- Проведение обвязки скважины с насосным агрегатом и по интервальный отбор проб жидкости в специализированные герметичные пробоотборники производства SNF.

- Проведение реологических исследований отобранных проб полимерного раствора с целью определения степени механической деструкции.

- Отчет по результатам проведенных работ.

Основные результаты работы:

- Определение степени механической деструкции полимерного раствора скважины 1141.

1

Компания: АО «Мангистаумунайгаз»

Производственный объект: месторождение «Каламкас».

Основание: НИР «Концепция расширения технологии полимерного заводнения по месторождению Каламкас» (Заказ-наряд №25, Приложение №4-25).

Номер и дата договора: № 279-14 от «19» марта 2020г.

Акт
о проведенных отборах глубинных проб
жидкости из нагнетательной скважины №1141
месторождение Каламкас (участок ПЗ Восток Расширение)

(на двух листах)

от «_16_» _октября_ 2020г.

Составлен представителями:

от ПУ «Каламкасмунайгаз»:

Зам. нач. УПНД Соберсенов С.Р / сабтогол

(должность, Ф.И.О., Подпись)

от Филиала ТОО «КМГ Инжиниринг»«КазНИПимунайгаз»:

ведущий инженер Салимгараев И.И. /

(должность, Ф.И.О., Подпись)

в том, что «_16_» _октября_ 2020г. проведен отбор глубинных проб жидкости из нагнетательной скважины №1141 месторождения Каламкас (участок ПЗ Восток Расширение). Отбор выполнен на самоизливе со скважины в количестве _7_ проб с целью оценки механической деструкции полимера при вне плановой остановки скважины. Работы выполнены на основании документа «**План проведения отбора глубинных проб жидкости из нагнетательной скважины №1141 месторождение Каламкас (участок ПЗ Восток Расширение)**» от 16.10.2020г.

Хронометраж отборов:

п/п пробоотборника	Достигнутый объем слитой жидкости в мерник, м³	Время завершения отбора	Комментарий
1	0	10:45	
2	0,80	11:20	
3	1,62	11:24	
4	1,86	11:27	
5	2,15	11:29	
6	5,0	11:36	Увеличение целевого отбора до 5 м³
7	7,2	12:00	Увеличение целевого отб. до 7,2 м³

Давление до начала отборов на остановленной скважине составило 39 атм. Давление после излива 7,2 м³ жидкости и завершения отборов составило. 27 атм

Отклонения при отборе проб:

Нет.

Подписи:

от ПУ «Каламкасмунайгаз»: /_____

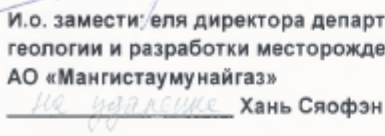**от Филиала ТОО «КМГ Инжиниринг» «КазНИПимунайгаз»:** Салимгараев ИИ /

Страница 1 из 1

Согласовано:
Директор департамента геологии и разработки месторождений АО «Мангистаумунайгаз»

_____ Байпаков С.Ш.

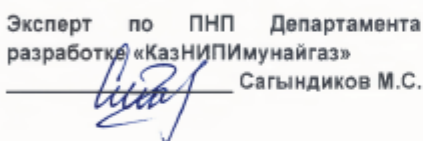Заместитель директора департамента геологии и разработки месторождений АО «Мангистаумунайгаз»

_____ Ван Юншань

Эксперт службы повышения нефтеотдачи пластов Филиала ТОО «КМГ Инжиниринг» «КазНИПИмунайгаз»

_____ Сагындиков М.С.

Директор ТОО «Атриум Актобе»
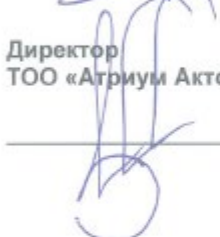
_____ Равнюшкин Д.В.

УТВЕРЖДАЮ:
И.о. заместителя генерального директора по геологии и разработке

_____ Лю Дунчжоу

«____» _____2021 г.

ПЛАН
проведения отбора глубинных проб жидкости из нагнетательных скважин №№2041 и 2049 месторождение Каламкас (участок ПЗ Запад)

Цель работ: Определение степени механической деструкции полимерного раствора, нагнетательных скважин №№2041 и 2049, методом замера реологических характеристик и содержания свободного кислорода в отбираемой закаченной жидкости в процессе остановки скважины и реверсивным само подъёмом жидкости на устье.

Задачи работ:
- Проведение обвязки скважины с агрегатом (типа ЦА-320), по интервальный отбор проб жидкости в специализированные герметичные пробоотборники производства SNF с замером содержания свободного кислорода (с использованием экспресс тестов CHEMets®).
- Проведение реологических исследований отобранных проб полимерного раствора с целью определения степени механической деструкции (на реометре Anton Paar марки MCR 502).
- Отчет по результатам проведенных работ.

Основные результаты работы:
- Определение степени механической деструкции полимерного раствора скважин №№2041 и 2049.

1

Компания: АО «Мангистаумунайгаз»

Производственный объект: месторождение «Каламкас».

Основание: НИР «Инженерно-техническое сопровождение ОПР по полимерному заводнению на месторождении Каламкас (Авторский надзор, технико-экономическая оценка за реализацией проекта ОПР по полимерному заводнению, проводимых на опытных участках месторождения Каламкас)» - Заказ-наряд №9, Приложение №4-9.

Номер и дата договора: № 207-14 от «19» марта 2021г.

Акт
о проведенных отборах глубинных проб жидкости из нагнетательной скважины №2041 месторождение Каламкас (участок ПЗ Запад)
(на двух листах)

от «24» _августа_ 2021г.

Составлен представителями:

от ПУ «Каламкасмунайгаз»:

техник геолог ЦППД Сатанбаев М.У.   /
<div align="right">(должность, Ф.И.О., Подпись)</div>

от Филиала ТОО «КМГ Инжиниринг»«КазНИПимунайгаз»:

эксперт СПНП Сагындиков М.С.   /
<div align="right">(должность, Ф.И.О., Подпись)</div>

ведущий инженер СПНП Салимгараев И.И.   /
<div align="right">(должность, Ф.И.О., Подпись)</div>

от ТОО «Атриум Актобе»:

руководитель технологической службы Елубаев Н.Б.   /
<div align="right">(должность, Ф.И.О., Подпись)</div>

в том, что «24» _августа_ 2021г. проведен и в 12:30 закончен отбор глубинных проб жидкости из нагнетательной скважины №2041 месторождения Каламкас (участок ПЗ Запад). Отбор выполнен на самоизливе со скважины в количестве 7 проб с целью оценки механической деструкции полимера и содержания в нем свободного кислорода (O_2). Работы выполнены на основании документа «**План проведения отбора глубинных проб жидкости из нагнетательных скважин №№2041 и 2049 месторождение Каламкас (участок ПЗ Запад)**» от 19.08.2021г.

Хронометраж отборов:

п/п пробоотборника	Достигнутый объем слитой жидкости в мерник, м³	Время завершения отбора	Комментарий
1	0 (устьевая при работе установки ПЗ)	9:05	O_2=0.2-0.3 ppm
2	2.2	9:25	замер кислорода не проведен из за высокого расхода
3	4	9:30	
4	8	9:54	O_2=0 ppm
5	12	10:15	O_2=0 ppm
6	16	11:40	O_2=0 ppm
7	20	12:05	O_2=0 ppm
8	24	12:25	O_2=0 ppm

Давление до начала отборов на остановленной скважине составило 44 атм. Давление после излива 24 м³ жидкости и завершения отборов 11 атм.

Компания: АО «Мангистаумунайгаз»

Производственный объект: месторождение «Каламкас».

Основание: НИР «Инженерно-техническое сопровождение ОПР по полимерному заводнению на м/р Каламкас».

Номер и дата договора: №207-14//24/2021АК от 19.03.2021г.

Акт
исследования прорыва полимера в добывающую скважину 1587 от нагнетательной
скважины 1137 (участок ПЗ Восток-2)

(на трех листах)

от «_28_» _апреля_ 2021г.

Составлен представителями:

от ПУ «Каламкасмунайгаз»:

геолог ОГ чАРМ Айдарбаев К.А. _(подпись)_
(должность, Ф.И.О., Подпись)

от Филиала ТОО «КМГ Инжиниринг» «КазНИПИмунайгаз»:

Эксперт по ПНП	Сагындиков М.С.	_(подпись)_
Ведущий инженер	Салимгарев П.П.	_(подпись)_
	(должность, Ф.И.О., Подпись)	

Мы, представители ПУ «Каламкасмунайгаз» и филиала ТОО «КМГ Инжиниринг» «КазНИПИмунайгаз» составили настоящий Акт о том, что:

28.04.2021 г.:

1. В 10:00 закачка на участке Восток-2 (наг. скважины 1131, 1132, 1137, 1138) остановлена на плановый ремонт.
2. До 16:00 проведены подготовительные работы на добывающей скважине 1587 по установке манометра, расходомера и специального герметичного пробоотборника (далее – бомба).
3. В 16:00 запустили добывающую скважину 1587 с начальным расходом 19 м3/час при 21 атм устьевого давления.
4. Проведен отбор 5-ти проб добываемого полимера в бомбы и проведен замер растворенного кислорода в последних 3-х пробах, окончание отбора 5-й пробы в 16:41.
5. В 16:59 запуск участка Восток-2, в т.ч. нагнетательную скважину 1137 с общим расходом 11 м3/час.
6. Ожидание отклика закачки 1137 на добывающей скважине 1587 до 18:10, дебит вырос с 1,3 до 1,75 м3/час, отбор последней 6-й пробы добываемого полимера в бомбу без замера кислорода.
7. В 18:12 закрытие скважины 1587 и транспортировка 6-ти бомб в лабораторию «КазНИПИмунайгаз» для реологических исследований.
8. Замер вязкостных свойств полимерного раствора проведен на реометре Anton Paar марки MCR 502 при скорости сдвига 7,34с-1 и комнатной температуре (~22°C). Замер растворенного кислорода проведен с использованием экспресс тестов CHEMets®. Результаты замеров представлены в сводной таблице ниже.

Сводная таблица замеров при исследовании прорыва полимера в доб. скважину 1587

Время	Расход, м3/ч	Расход, м3/сут	Нак. объем, м3	Руст, атм	Примечание
16:00	19,00	456	0,317	21	
16:01	17,80	427	0,613	20	
16:02	16,70	401	0,092	18	
16:03	15,50	372	1,150	17	
16:04	14,50	348	1,392	16	
16:05	13,40	322	1,615	14,5	
16:06	12,40	298	1,822	13	
16:07	11,40	274	2,012	11,5	Бомба №1 - 1141 µ=13,3сП
16:08	10,50	252	2,187	10	
16:09	9,70	233	2,348	9	
16:10	8,60	206	2,492	8,5	
16:11	7,60	182	2,618	8	
16:12	7,10	170	2,737	7,5	
16:13	6,70	161	2,848	7	Бомба №2 - 1142 µ=14,7сП
16:14	6,20	149	2,952		
16:15	5,60	134	3,045		
16:16	5,10	122	3,130		
16:17	5,00	120	3,213		
16:18	4,70	113	3,292		Бомба №3 - 1136 О2=0,2 µ=19,1сП
16:19	4,30	103	3,363		
16:20	4,00	96	3,430		
16:21	3,80	91	3,493		
16:22	3,70	89	3,555		Бомба №4 - 8360 О2=0 µ=21,3сП
16:23	3,70	89	3,617		
16:24	3,50	84	3,675		
16:25	3,10	74	3,727		
16:26	3,20	77	3,780		
16:27	3,00	72	3,830		
16:28	2,90	70	3,878		
16:29	2,75	68	3,924		
16:30	2,75	66	3,970		
16:31	2,62	63	4,014		
16:32	2,46	59	4,055		
16:33	2,30	55	4,093		
16:34	2,20	53	4,130		
16:35	2,10	50	4,165		
16:36	1,90	46	4,196		
16:37	1,90	46	4,228		
16:38	1,88	45	4,259		
16:39	1,83	44	4,290		
16:40	1,82	44	4,320		
16:41	1,77	42	4,350		Бомба №5 - 1130 О2=0 µ=21,3сП
16:42	1,76	42	4,379		
16:43	1,77	42	4,409		
16:44	1,78	43	4,438		
16:45	1,72	41	4,582		
16:50	1,62	39	4,717		
16:55	1,44	35	4,813		
16:59	1,30	31	4,834		Запуск скважины 1137 (11м3/ч)
17:00	1,28	31	4,898		
17:03	1,31	31	4,986		
17:07	1,31	31	5,007		
17:08	1,65	40	5,282		
17:18	1,22	29	5,445		
17:26	1,15	28	5,637		
17:36	1,21	29	5,879		
17:48	1,30	31	5,922		
17:50	1,34	32	5,944		
17:51	1,36	33	5,967		
17:52	1,40	34	6,014		
17:54	1,38	33	6,083		
17:57	1,42	34	6,106		
17:58	1,45	35	6,203		
18:02	1,53	37	6,280		
18:05	1,65	40	6,417		
18:10	1,75	42	6,446		Бомба №6 - 1141 µ=21,0сП
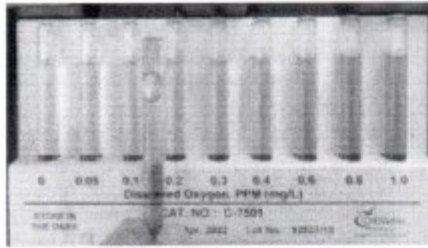
Скважина 1587 бомба №3 O2=0.2мг/л
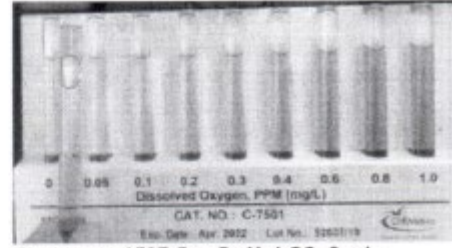
Скважина 1587 бомба №4 O2=0мг/л
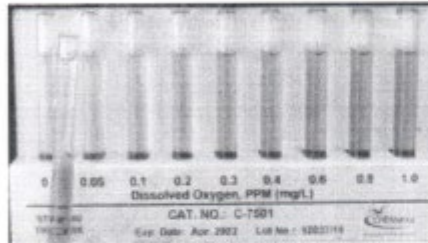
Скважина 1587 бомба №5 O2=0мг/л

115

| ҚАЗАҚСТАН РЕСПУБЛИКАСЫ
БІЛІМ ЖӘНЕ ҒЫЛЫМ МИНИСТРЛІГІ

«Қ. И. СӘТБАЕВ АТЫНДАҒЫ
ҚАЗАҚ ҰЛТТЫҚ ТЕХНИКАЛЫҚ ЗЕРТТЕУ
УНИВЕРСИТЕТІ» КОММЕРЦИЯЛЫҚ ЕМЕС
АКЦИОНЕРЛІК ҚОҒАМЫ | СӘТБАЕВ
УНИВЕРСИТЕТІ | МИНИСТЕРСТВО ОБРАЗОВАНИЯ И НАУКИ
РЕСПУБЛИКИ КАЗАХСТАН

НЕКОММЕРЧЕСКОЕ АКЦИОНЕРНОЕ ОБЩЕСТВО
«КАЗАХСКИЙ НАЦИОНАЛЬНЫЙ
ИССЛЕДОВАТЕЛЬСКИЙ ТЕХНИЧЕСКИЙ
УНИВЕРСИТЕТ ИМЕНИ К.И. САТПАЕВА» |

БҰЙРЫҚ	ПРИКАЗ
« _01_ » _03_ 20_22_ж/г. Алматы қаласы	№ _369-ө_ город Алматы

PhD докторантын
ғылыми-зерттеу тағылымдамаға
жіберу туралы

2018 жылғы 31 қазандағы № 604 ҚР БҒМ бұйрығымен бекітілген Жоғары оқу орнынан кейінгі білім берудің мемлекеттік жалпыға міндетті стандартына сәйкес **БҰЙЫРАМЫН:**

1. Қ. Тұрысов атындағы Геология және мұнай-газ ісі институтының 8D07202 – «Мұнай-газ ісі» мамандығы бойынша мемлекеттік білім гранты негізінде оқитын 3 курс докторанты Сагындиков Марат Серикович 2022 жылдың 3 мамырдан 4 шілде аралығында Назарбаев Университетінің "National Laboratory Astana" жеке мекемесінің материалдарды түрлендіру және қолданбалы физика зертханасына (Нұр-сұлтан қ., Қазақстан) ғылыми-зерттеу тағылымдамасын өтуге жіберілсін.

2. Қаржы және есеп департаменті (Токжигитова Г.Б.) іс-сапар шығындарын смета бойынша мемлекеттік тапсырыс есебінен төлесін.

3. Сагындиков М.С. тағылымдамадан келгеннен кейін жеті жұмыс күні ішінде «Мұнай-газ ісі» кафедрасына тәжірибеден өту туралы есептерін тапсырсын.

4. Осы бұйрықтың орындалуына бақылау Қ. Тұрысов атындағы Геология және мұнай-газ ісі институтының директоры А.Х. Сыздыковке жүктелсін.

Негіздеме: М.С.Сагындиковтың өтініші, Қ. Тұрысов атындағы Геология және мұнай-газ ісі институтының директоры А.Х.Сыздыковтың және «Мұнай-газ ісі» кафедра меңгерушісі Г.Ж.Еликбаеваның ұсынысы.

Басқарма мүшесі –
Корпоративтік даму және стратегиялық
жоспарлау жөніндегі проректор _____ Е.Кульдеев

066635